JUNE 2019

**HASAN KALYONCU UNIVERSITY**
**GRADUATE SCHOOL OF**
**NATURAL & APPLIED SCIENCES**

# USE OF GEOGRAPHIC INFORMATION SYSTEM FOR EVALUATING THE SOME GEOTECHNICAL PROPERTIES IN MALATYA, TURKEY

M.Sc. in Civil Engineering

**M.Sc. THESIS**
**IN**
**CIVIL ENGINEERING**

**by**
**Bahadır KARABAŞ**
**2019**

BAHADIR KARABAŞ

# Use of Geographic Information System for Evaluating the Some Geotechnical Properties in Malatya, Turkey

**M.Sc. Thesis**

**In**

**Civil Engineering**

**Hasan Kalyoncu University**

**Supervisor**

**Assist. Prof. Dr. Volkan İŞBUĞA**

**Co-Supervisor**

**Prof. Dr. Ali Fırat ÇABALAR**

**by**

**Bahadır KARABAŞ**

**June 2019**

## GRADUATE SCHOOL OF NATURAL & APPLIED SCIENCES INSTITUTE
## M.Sc. ACCEPTANCE AND APPROVAL FROM

Civil Engineering Department, Civil Engineering Master programme student **Bahadır KARABAŞ** prepared and submitted the thesis titled **"Use of Geographic Information System for Evaluating the Some Geotechnical Properties in Malatya, Turkey"** defended successfully at the VIVA on the date of 25/06/2019 and accepted by the jury as a M.Sc. thesis.

**PositionTitle, Name and SurnameSignature:**

**Department/University**

| | |
|---|---|
| **Supervisor** | Assist. Prof. Dr. Volkan İŞBUĞA<br>Civil Engineering Department<br>Hasan Kalyoncu University |
| **Jury Member** | Assist. Prof. Dr. M. Tolga GÖĞÜŞ<br>Civil Engineering Department<br>University of Gaziantep |
| **Jury Member** | Assist. Prof. Dr. Mehmet Eren GÜLŞAN<br>Civil Engineering Department<br>University of Gaziantep |

**This thesis is accepted by the jury members selected by institute management board and approved by institute management board.**

**Prof. Dr. Mehmet KARPUZCU**
**Director**

**I hereby declare that all information in this document has been obtained and presented in accordance with academic rules and ethical conduct. I also declare that, as required by these rules and conduct, I have fully cited and referenced all materials and results that are not original to this work.**

**Bahadır KARABAŞ**

## ABSTRACT

## USE OF GEOGRAPHIC INFORMATION SYSTEM FOR EVALUATING THE SOME GEOTECHNICAL PROPERTIES IN MALATYA, TURKEY

KARABAŞ, Bahadır

M.Sc. In Civil Engineering

Supervisor: Assist. Prof. Dr. Volkan İŞBUĞA

Co-Supervisor: Prof. Dr. Ali Fırat ÇABALAR

June 2019

86 Pages

In this study, soil investigation reports, field and laboratory test results in the archive of Malatya Metropolitan Municipality, Directorate of Reconstruction and Urban Planning Department are used. Data obtained from 192 borings are analyzed by using geographical information system.

Within the scope of the study, SPT-N calculation analyses, bearing capacity calculation analyses, ground water level and water content analyses, liquefaction calculation analyses, shear wave velocity calculation analyses, shear wave velocity calculation analyses 30 m, soil classification analyses according to NEHRP (USA) earthquake regulation and Eurocode 8 , earthquake hazard level analyses according to soil amplification calculation, local soil class analyses according to dominant vibration period are made and maps for these analyses are produced with Geographic Information System (GIS) based software. In this context, it is aimed to use geotechnical data more efficiently and productively in engineering studies.



**Keywords:** GIS, Malatya, geotechnical properties, SPT, NEHRP, Eurocode 8, local soil class.

# ÖZET

## MALATYA' DAKI ZEMINLERIN BAZI GEOTEKNIK ÖZELLIKLERININ COĞRAFI BILGI SISTEMI ILE DEĞERLENDIRILMESI

KARABAŞ, Bahadır

Yüksek Lisans Tezi, İnşaat Mühendisliği Bölümü

Tez Yöneticisi: Dr.Öğ.Üyesi Volkan İŞBUĞA

Yardımcı Tez Yöneticisi: Prof. Dr. Ali Fırat ÇABALAR

Haziran 2019

86 sayfa

Bu çalışmada, Malatya Büyükşehir Belediyesi İmar ve Şehircilik Daire Başkanlığı Müdürlüğü arşivindeki zemin etüt raporları, arazi ve laboratuvar deney sonuçları kullanılmıştır. 192 sondaj noktasında elde edilen veriler coğrafi bilgi sistemi yöntemi kullanılarak analiz edilmiştir.

Çalışma kapsamında SPT-N hesap analizleri, taşima gücü hesap analizleri, yeraltı suyu seviyesi ve su içeriği analizleri, sıvılaşma hesabı analizleri, kayma dalga hizi hesabı analizleri, kayma dalga hızı analizi 30 m, NEHRP (A.B.D.) deprem yönetmeliği ve Eurocode 8 göre zemin sınıflandırma analizleri, zemin büyütmesi hesabına göre deprem tehlike düzeyi analizleri, hakim titreşim periyoduna göre yerel zemin sınıfı analizleri yapılmış, analizlere yönelik haritalar Coğrafi Bilgi Sistemi (CBS) temelli yazılımlarla üretilmiştir. Bu bağlamda mühendislik çalışmalarında geoteknik verilerin daha etkin ve daha verimli kullanılması amaçlanmıştır.



**Anahtar Kelimeler:** CBS, Malatya, Geoteknik Özellikler, SPT, NEHRP, Eurocode 8, Yerel Zemin Sınıfı.

***My precious family …..***

**ACKNOWLEDGEMENTS**

I would like to express my appreciation to my academic advisers Prof. Dr. Ali Fırat ÇABALAR, Assist. Prof. Dr. Volkan İŞBUĞA and Instructor Nurullah AKBULUT for both their generous efforts leading me, my study as a graduate student and huge support during the thesis preparation period.

Thank you to the Malatya Metropolitan Municipality, Directorate of Reconstruction and Urban Planning Department within Malatya Metropolitan Municipality and its staff for providing us to use the necessary resources in order to create the database.

I am always grateful to my wife Güneş KARABAŞ and my daughters, Ayşe Begüm KARABAŞ and Zeynep Özge KARABAŞ, who have always been with me, my superiors and my colleagues who have always supported me during the preparation of this thesis.

## TABLE OF CONTENTS

**Page No**

## LIST OF TABLES

**Page No**

## LIST OF FIGURES

Page No

## ABBREVIATIONS OR SYMBOLS LIST

| | |
|---|---|
| $a_{maks}$ | Peak ground acceleration |
| ASTM | American society for testing and materials |
| BS | British standard |
| $C_N$ | Overburden correction in SPT test |
| $C_E$ | Stem bar energy ratio correction in SPT test |
| $C_B$ | Borehole diameter correction in SPT test |
| $C_R$ | Stem bar(rod) length correction in SPT test |
| $C_S$ | Inner tube(sampler) correction in SPT test |
| CRR | Cyclic resistance ratio |
| CSR | Cyclic stress ratio |
| D | Disturbed sample |
| Er | Stem bar energy ratio for SPT test |
| FS | Factor of safety |
| FEMA | Federal emergency management agency |
| FC | Fines content |
| g | Gravity acceleration ($cm/s^2$) |
| NCEER | National center for earthquake engineering research |
| NEHRP | National earthquake hazard reduction program |
| Pa | Atmospheric pressure 100 kPa |
| $q_a$ | Allowable bearing capacity ($kg/cm^2$) |
| R | Radius of earth epicenter (km) |
| $r_d$ | Stress reduction factor |
| UD | Undisturbed sample |
| SPT | Standard penetration test |
| Vp | Compression wave velocity (m/sec) |
| Vs | Shear wave velocity (m/sec) |
| Wn | Water content (%) |
| Z | The depth of middle level from ground surface (m) |

| | |
|---|---|
| $Z_1$, $Z_2$, $Z_3$, Z4 | Local soil classes |
| $\sigma_{vo}$ | Vertical total stress (kPa) |
| $\sigma'_{vo}$ | Vertical effective stress (kPa) |
| $\alpha$, $\beta$ | The coefficients to correct $(N_1)_{60}$ based on fine content values |
| $\tau_{av}$ | Average horizontal shear as a result of earthquake |
| To | Soil dominant vibration period (sec) |
| $\gamma$ | Unit weight ($kN/m^3$) |

# CHAPTER 1

# INTRODUCTION

## 1.1. General

Recently, larger buildings, larger roads and larger structures have been built to meet social needs. The developments in construction technology have increased the importance of researchs in soil mechanics. Determination of soil properties is the most important stage of project of construction works. The fact is that laboratory tests, field tests and geophysical methods are the most common methods used to determine the behavior of soils under static and dynamic loads.

Studies are carried out with the aim of examining the data obtained with developing technology and improving easy access. In this respect, the use of Geographical Information Systems (GIS) provides great convenience in the efficient use of the soil properties data obtained from the above methods (laboratory tests, field tests, geophysical methods). Actually, creating a visual map specific to a predetermined subject from the data obtained and transferring it to the digital platform provides great advantages. Thus, the soil properties of the desired point in a study area can be examined easily. Additional information can be easily incorporated into the studies. In the present study, it is aimed to create a database by editing the parameters of soil properties by using GIS system.

## 1.2. Objective of the Study

In this study, bearing capacity, liquefaction potential, shear wave velocity ($Vs_{30}$), Standard Penetration Tests (SPT), groundwater table values have been examined using the data obtained from the studies conducted by Malatya Municipality. It was aimed to create a database for the study area by transferring Standard Penetration Test (SPT) values obtained from boring data and other geotechnical data to digital medium. By using the created database, it was aimed to create maps in digital environment for different practical purposes. In this context, ArcGIS software was

used to apply geographic information system in geotechnical applications. The SPT-N, bearing capacity, liquefaction potential, groundwater level, water content and shear wave velocity ($Vs_{30}$), maps were produced by GIS based software.

### 1.3. Outline of the thesis

Chapter 1- Introduction: In this section, the importance of using the methods used to determine soil properties and the convenience provided by transferring the results taken from the methods to the GIS system are discussed.

Chapter 2- Literature review: In this section, previous studies with GIS system, general properties of the study area, its geology and seismicity are mentioned. In addition, information is given about the GIS.

Chapter 3- Materials and Methods: In this section, the methods used in this study are mentioned. Standard Penetration Test (SPT), bearing capacity analysis, liquefaction potential analysis, shear wave velocity analysis, soil amplification calculations, soil dominant vibration period, water content and ground water levels are included.

Chapter 4- Results and Discussion: In this section, the maps and figures created within the scope of the research and relevant evaluations and discussions are included.

Chapter 5- Conclusions and Recommendations: The results and recommendations of the thesis are given.

# CHAPTER 2

# LITERATURE REVIEW

## 2.1. General

In this section, previous studies on the GIS applications are introduced. In addition, general properties of the study area, its geology, and seismicity are given.

## 2.2 Previous Studies on GIS

There have been many studies in different areas using GIS applications. For example, a study of the use of GIS and field use for planning and adjustment of earthquake damage maps was conducted by Marx (1992) for Seattle. The GIS was used to create damage maps in India to mitigate the earthquake risk (Anand, 2000). Multimedia GIS database was created for tourism industry in Nigeria (Ayeni et al., 2004). The GIS database was used for the implementation of environmental emergency action plans (Spearin, 2004). Baysal and Tecim (2006) used GIS to conduct a suitability analysis of solid waste landfills in the field of Solid Waste Management. Demirci et al. (2006) channeled the field use changes of İstanbul Kucukcekmece water basin between 1963-2005 by using GIS with the comparison of water samples. These alterations of usage try to determine the water quality of water basin of Kucukcekmece Lake. Kargı and Sarı (2006) cited maps of the area by satellite the area for a mining search in Denizli region. Another application area of GIS was health geography made by Ergun and Sarac (2006). The spatial situation of spatial analysis health services was examined by GIS in this area. Another use of GIS was to determine the noise pollution (Kumbur, 2006). The noise pollution map was consisted by entering measurements into Mersin University Ciftlikkoy Campus numerical map. The GIS was also used to draw SPT map, SPT-N map, bearing capacity map, liquefaction map and earthquake map in an area (Undul and Gurpinar, 2003). Actually, the GIS allows us to examine very large geotechnical data and provides both visual and numerical information that is useful by extracting the soil map, SPT-N map, gravity map, liquefaction map and damage distribution maps.

Alparslan et al. (2006) studied the permeability, geology, tendency of soils for liquefaction, ground waters, hydrology and old landslide areas, land cover, vegetation index and surface temperature for the area between Buyukcekmece and Kucukcekmece Lakes using GIS approach. Şen (2004) examined the distribution of the potential of the liquefaction using the GIS approach over the area of Gumusler Municipality in Denizli province as an example. The study by Kıncal (2006) in İzmir can be another example for the studies of mapping the field side slope and geological data layers with the help of GIS. Sert et al. (2006) complied the bearing capacity map, liquefaction maps and damage maps are prepared in a study over Adapazarı area. Ayday et al. (2008) prepared the soil liquefaction potential, ground water and soil properties of the places within the borders of Tepebasi municipality in Eskisehir using a GIS software.

## 2.3 General Properties of the Study Area

### 2.3.1. Location and Geographical Position of the Study Area

Malatya is located in the Upper Euphrates basin of Eastern Anatolia Region and at the southwest edge of Adıyaman, Malatya, Elazığ, Bingöl, Mus, Van collapse area. It is surrounded by Elazığ and Diyarbakır in the east, Adıyaman in the south, Kahramanmaraş in the west, Sivas and Erzincan in the north. The surface area of the province's territory is 12.313.1 $km^2$, between 35 34` and 39 03` north latitudes and between 38 45` and 39 08`east longitudes. The spurs of the South-Eastern Taurus, formed during the Alpine folding of the 3$^{rd}$ geological period constitutes a large part of the province's territory and occupies the entire south-east-west direction. (ÇŞB, 2011). The part of the urban area, especially between the highway and the railway, has a varying slope from 0 to 5% (MMDD, 2009). To the south of the city, there are the Beydağları (Mountains) extending the current situation map in the east-west direction. The slopes of Beydağları vary between 10-20% and 20-30% in some places (MMDD, 2009).

In the east of the city, the slope on the top of Yıkıkhan hill was found to be 20-30% and +30. The north and west of the city is composed of slightly wavy plains which is nearly plain, and the slope varies between 0-5% and 5-10%. In the Malatya-Elazığ highway section of the study area, the northern and middle parts were found to be flat, less slope, the slope is between 10-20%, and towards the south the slope is

moderate and high. The slope is 20-30% and on the hills it is greater than 30% (MMDD, 2009). The study area covers approximately 100 km$^2$ of the settlement area of Malatya Municipality (Figure 2.1).

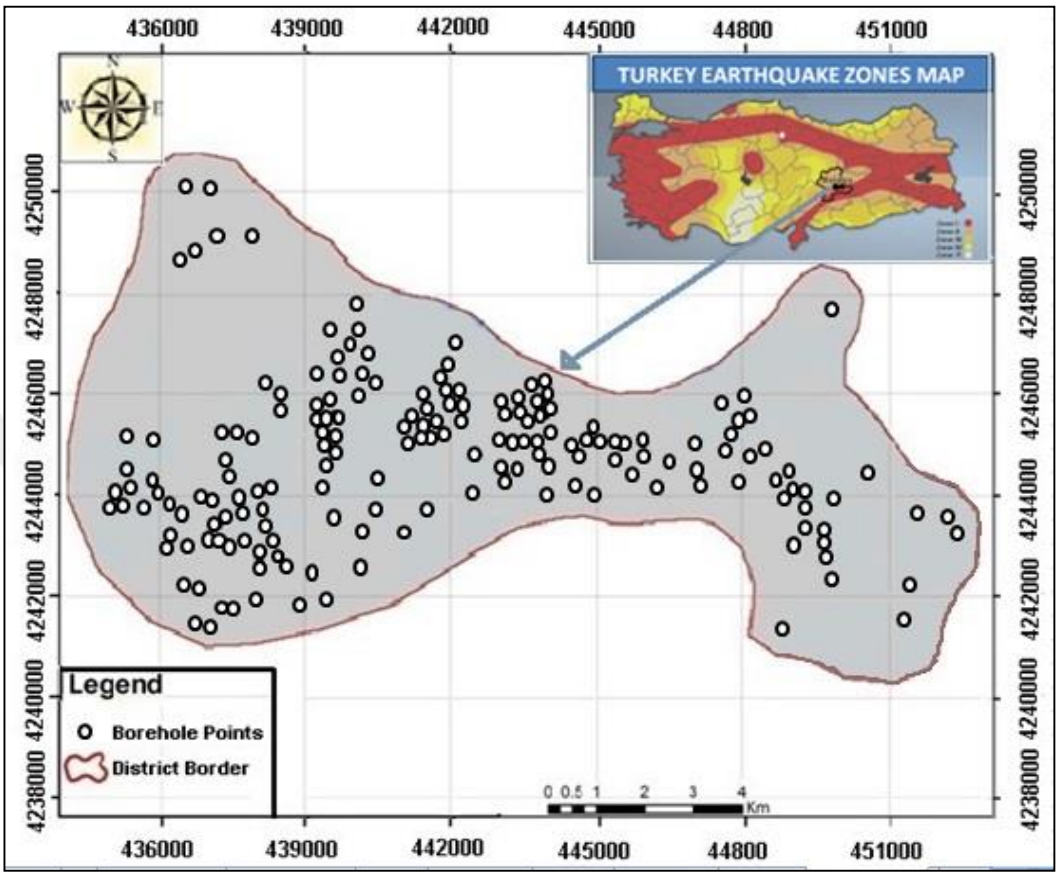


**Figure 2.1.** The map of the study area

### 2.3.2. General Geological Properties of the Area

Geological information of the study area is created by utilizing "Geotechnical Report Based on the Construction Plan of the Malatya Municipal Settlement Site" prepared by the Malatya Municipality in 2009 and the "Malatya Province Environmental Status Report" prepared by the Ministry of Environment and Urban Planning in 2011 (Figure 2.2).

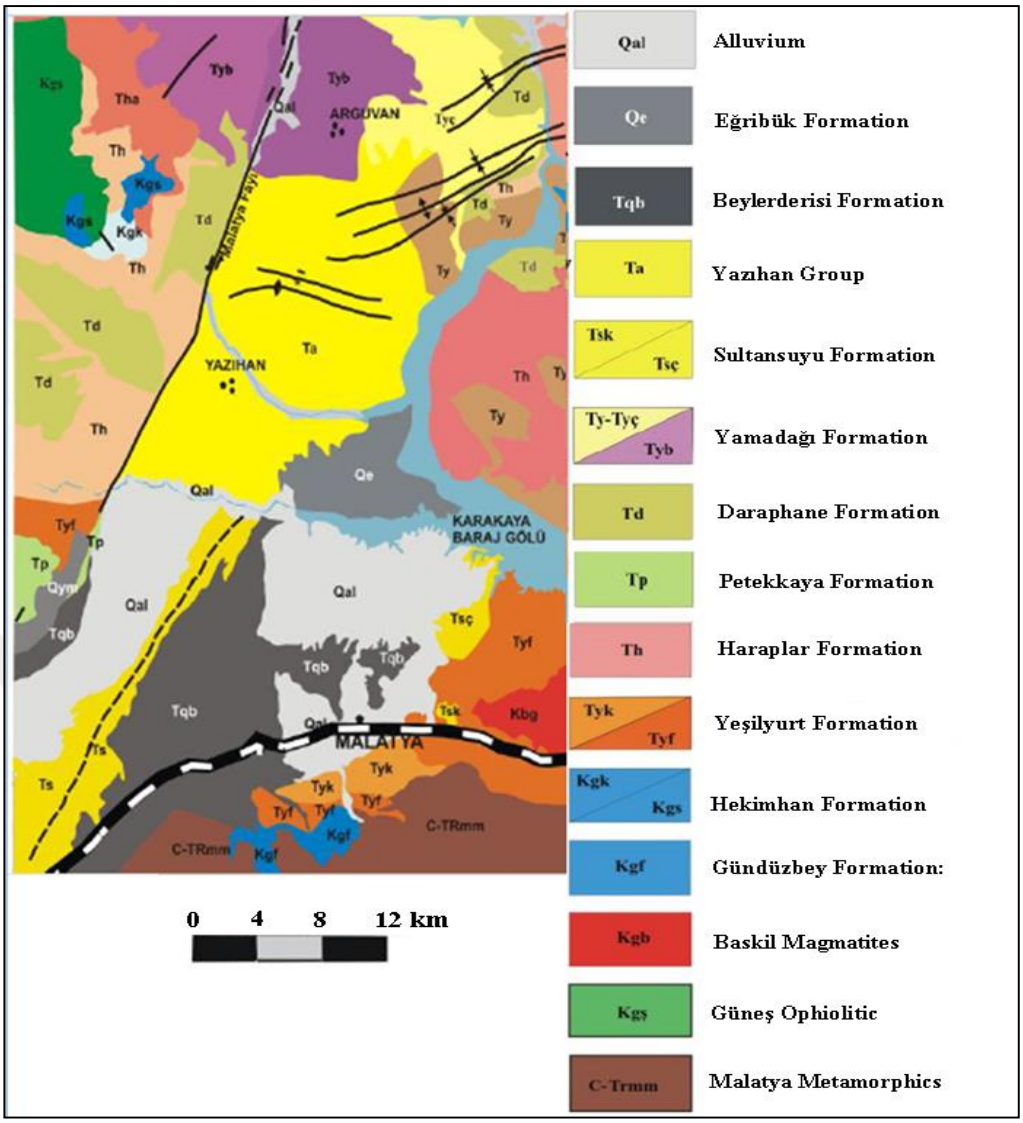


**Figure 2.2.** Geological map of Malatya (ÇSB, 2011)

### 2.3.2.1. Geology of the Study Area

In the study area, formations are presented as below (MMDD, 2009).

#### 2.3.2.1.1. Schists

It is the oldest unit of the study area and gives a view to the south of the Malatya-Elazığ Highway. It has a fairly curved, broken structure (Figure 2.3). It is impossible to see an orderly stack from the foundation to the ceiling (MMDD, 2009).

**Figure 2.3.** Schist in the study area (MMDD, 2009)

#### 2.3.2.1.2. Crystalline Limestones

Stratigraphically at the highest level, thin-medium bedded crystallized limestones of Metamorphics of Malatya and among these, intercalated metasandstone, calcschist and quartz-albite-chlorite shales based unit were found to be at permian age by lithological comparison (Figure 2.4). This forms high land surveyors in the southern part of Malatya-Elazığ highway. In general, it is NW-SE direction and $20^0$-$25^0$ NW slope (MMDD, 2009).

**Figure 2.4.** Crystalline limestone in the study area (MMDD, 2009)

#### 2.3.2.1.3. Granodiorites

Tavşan Tepe located in west of Inönü University in the area of survey is entirely composed of granodiorites (Figure 2.5). Granodiorites are massive and coarse grained (MMDD, 2009).

**Figure 2.5.** Granodiorites in Tavşantepe (MMDD, 2009)

#### 2.3.2.1.4. Volcano- Sediments

This formation tectonically overlying the Malatya Metamorphic Massif begins with ixel solutions basal conglomerates, sandstone and sandy limestone. This formation develops under increasingly changing conditions such as sandy micrite, biomicrite, pelitic cemented sandy limestones and clay stones and follows simultaneous intense submarine volcanic activity with the collapse of claystones, and tile red micrite showing enrichment in terms of oxide, iron that determines the beginning of volcanism. Baskil magmatic rocks consist of gabbro, diorite, monzonodiorite, quartz diorite, quartz, monzonite, granodiorite type iron and rocks and semi-depth dykes and cover rock in the type of volcanic-sedimentary rocks of these rocks (MMDD, 2009).

#### 2.3.2.1.5. Yeşilyurt Formation

The places are observed in region with a topography that are not too high and soft. In the south of Malatya large areas are common. The flysch levels and limestone levels identified in the formation are also distinguished by their symbol (MMDD, 2009).

It is observed in the basal flysch character as intercalation shape with conglomerates, sandstones, siltstones, claystones and marls. The conglomerates are very poorly sorted, the coarse Nümmulites fossiliferous rocks of which stratification partly observable and it is composed of the Malatya Metamorphics and Upper Cretaceous aged limestones,. The sandstones on them are gray black colored and very crumbly and cracked structure (MMDD, 2009).

Upon the flysch levels, very crumbly limestones including yellow-beige colored thin-medium bedded, cracked, coarse Nümmulites fossils are overlaid. The layers are NE-SW directional and $15^0$-$25^0$ NW slope. The unit covers large areas south of the study area. It is incompatible with the formation. On the Yeşilyurt Formation, the Beylerderesi Formation is transitional. Yeşilyurt Formation has very abundant microfossil (MMDD, 2009).

#### 2.3.2.1.6. Sultansuyu Formation

In general, the unit consisting of claystone, mudstone, marl, sandstone and conglomerates consists of similar sedimentary levels. The unit's rock type does not show a significant change at the regional scale. The claystone is brown-green, medium-stiffened white, stiffened thin-medium-thick layered (20 cm-3 m) thins and thickens in a general way. The mudstone is red-brown, medium stiffened , thick and very thick (2-4 m) terrestrial planar lamina. The sandstone is brown-colored, medium-well- stiffened and thin-too thick layered. (30-230 cm) Conglomerate is red-brown, medium well-stiffened , very thick layered (1.5-4.5 m) pebbles of varying size and ten or more 25 cm rounded and less angled and poorly sorted . It is located under the Beylerderesi Conglomerate. It covers large areas to the north of the highway in the north of the Malatya City Center. It is generally interpreted as horizontally layered or $5^0$-$10^0$ slope with alluvial fan sediment and braided stream sediments (MMDD, 2009).

#### 2.3.2.1.7. Beylerderesi Formation

The unit blockstone covering large areas to the west and north-west of Malatya City Center is conglomerate, terrestrial sandstone and mudstone inter bedded, the conglomerates of the unit are predominantly dark red, poorly sorted, and medium and very thick, disorderly layered. The components are usually composed of marble

and schists from the Malatya Metamorphics. Mudstone and clay matrix are cemented alluvial fan deposits. The granules are within the boundary between the pebbles and the block and are generally rounded, hemispherical. The interbeds and block levels of coarse sandstones and mudstones are observed locally. This unit is a view that covers all the units described until now in the stratigraphic sequence. There is no folding and tectonic effect, nor is it horizontal or $5^0$-$10^0$ slope. There is no age indicator in the unit. However, it is considered to be elderly because it is under alluvial and slope debris deposits. (MMDD, 2009).

#### 2.3.2.1.8. Soils in the Study Area

It is an unbalanced unit composed of unrounded, angled pebble, sand, shield and clay and due to topographical slope, it is stored in the northern skirts of Beydağı and E-W- directional Çöşnük Fault, which passes through the south of Malatya City Center. The spread of Slope debris expands somewhat down to the northern Highway. Loose or slightly stiffened, without layer thickness of slope debris varies from 1 to 80 m. In addition, slope debris of which thickness becomes thin from north to south is observed in Inonu University campus area and its vicinity. It occurs with the accumulation of material coming from the high mountain slopes in the south on the plains (MMDD, 2009).

**Figure 2.6.** Slope debris (MMDD, 2009)

#### 2.3.2.1.9. Alluvions

It is an alluvial unit composed of unbalanced pepple gravel, sand, silt and clay formed by Mercimek Horata, Hasanmandalı, Karanlıkdere and their tributaries which have seasonal flows in the direction of SN in Malatya City Center, Kuzu, Taşbağ, Kilis, Balık, Kenirik, Horşo, Çamurlu brooks which have a flow in the direction of SN in Malatya-Elazığ Highway Region and Bulgurlu Small Stream, Halo's Lake and their tributaries which have a flow in the direction of SE-NW. Depending on the size of the buildings, it is observed in the thickness between 1-5 m (MMDD, 2009).

**Figure 2.7.** Alluvion (MMDD, 2009)

### 2.3.2.2 Tectonics of the Study Area

The tectonics of the Eastern Mediterranean was explained within the frame of plate tectonics models proposed by McKenzie (1972). A large part of Turkey is located on Eurasia in the north and on the Anatolian plate between Africa and Arabia in the south. In this model, the collisions of Eurasia and African plates in Eastern Anatolia cause the Anatolian plate to escape to the west. The strike-slip faults developed during this escape constitute the tectonics that are still active in the region. The main tectonic lines in the McKenzie (1972) model are the North Anatolian Fault (NAF) with the right-lateral strike slip, Oludeniz fault (ODF) with left-lateral and Eastern Anatolian Fault (EAF) and Aegean Graben System (AGS) in the N-S direction (MMDD, 2009).

Eastern Anatolian Fault (EAF); The EAF zone separating the Anatolian Plate of the Plate of Arabia starts from Karlıova and extends towards Antakya for a length of 580 km. The EAF consists of seven distinct segments. EAF is left lateral strike depending on ODF system. The compression created by the Arabic plate moving to the S-SE throughout the ODF caused the Anatolian plate bounded by the NAF and EAF to escape to the west (MMDD, 2009).

#### 2.3.2.3. Groundwater

The Malatya Metamorphics and Baskil Magmatics are scarce in terms of groundwater. Limestones, which have generally good aquiferous properties, are scarce both in the hilly areas and in terms of groundwater in the region due to the fact that they are not thick (MMDD, 2009). The conglomerate sandstone layers in the Flysch have an aquifer property. For this reason, water from the borings to be opened in this formation is possible. Beylerderisi Conglomerate is boring porous and has an aquifer property in terms of groundwater. There are many water borings opened in this formation in the region. The ground level varies between 40-60 m depending on the topography. In ground drilling opened in the above-mentioned formations, no groundwater is found (MMDD, 2009). Sultansuyu Formation where marls and claystones are concentrated (Taştepe, Melekbaba Mah), there is no groundwater. To the east of Malatya City Center, on the plains north of the highway where conglomerates and sandstones are close to the surface, it is possible to see low flow groundwater sporadically due to the impermeable claystone and marls below (MMDD, 2009). Slope Debris is scarce in terms of groundwater in the west of Malatya City Center and in the western parts and in its foundation where Beylerderi Conglomerate situated. To the east of the city center, the groundwater is rich in the regions where Sultansuyu Formation and the flisches are located at the foundation. The ground level varies between 2-20 m depending on the topography (MMDD, 2009). Alluviums are observed in narrow areas in the study area. Their thickness is not much. For this reason it is insignificant in terms of groundwater (MMDD, 2009). Especially from the south of the city center, there are many small and very small spring waters in the foothills of the Çöşnük Fault. These sources are not evaluated because the city of Malatya has no drinking and potable water problems (MMDD, 2009).

#### 2.3.2.4. Surface Water

In the city center of Malatya, there are Water Spot Brook, Mercimek Brook, Horata Brook, Hasan Mandalı Brook and tributary rivers connected to these brooks. In the Malatya-Elazığ Highway Region, there are Karanlık Brook, Kuzu Brook, Toşbağ Brook, Kilis Brook, Toptaş Brook, Kenirik Brook, Horşo Brook, Çamurlu Brook and tributary rivers connected to these brooks (MMDD, 2009). All these brooks are in the direction of S-E and they are small streams in brook size as their name implies. Generally, these are brooks with low seasonal flows (MMDD, 2009).

### 2.3.3. Seismicity of the Region

In the Turkish Earthquake Region Map, Turkey is divided into 5 zones in terms of seismicity. The map shows soil acceleration values in Turkey with 90% probability for non-exceedance over the next 50 years (Figure 2.8)

In terms of Seismicity ;

I. Region, the most dangerous region, the regions where the soil acceleration is 0.4g and bigger,are red colored areas marked on the map.

II. Region, regions where the soil acceleration is expected to be between 0.3-0.4g

III. Region, regions where the soil acceleration is between 0.2-0.3g,

IV. Region, regions where the earth's acceleration is between 0.1-0.2g,

V. region, it is defined as places where soil acceleration is expected to be 0.1g or less (AFAD, 2018).

The study area is under the influence of Eastern Anatolian Fault Zone (EAF). The study area is located in the 1st Degree Hazardous Earthquake Region in Turkey Earthquake Zones Map. (Figure 2.9)

With in the frame of this conducted study, in the database of headship of management of disaster ans state of emergency, it is determined that in Malatya and its surroundings there has been 142 earthquakes between 1900 and 2018 higher than $M \geq 4.0$ and in Figure 2.10 it is shown these earthquake distrubiton. The number and magnitude of these earthquakes are presented in Figure 2.11 The earthquakes occurring In Malatya and its surroundings and in the years between 1900 and 2018 are presented in Table 2.1 (AFAD, 2018)

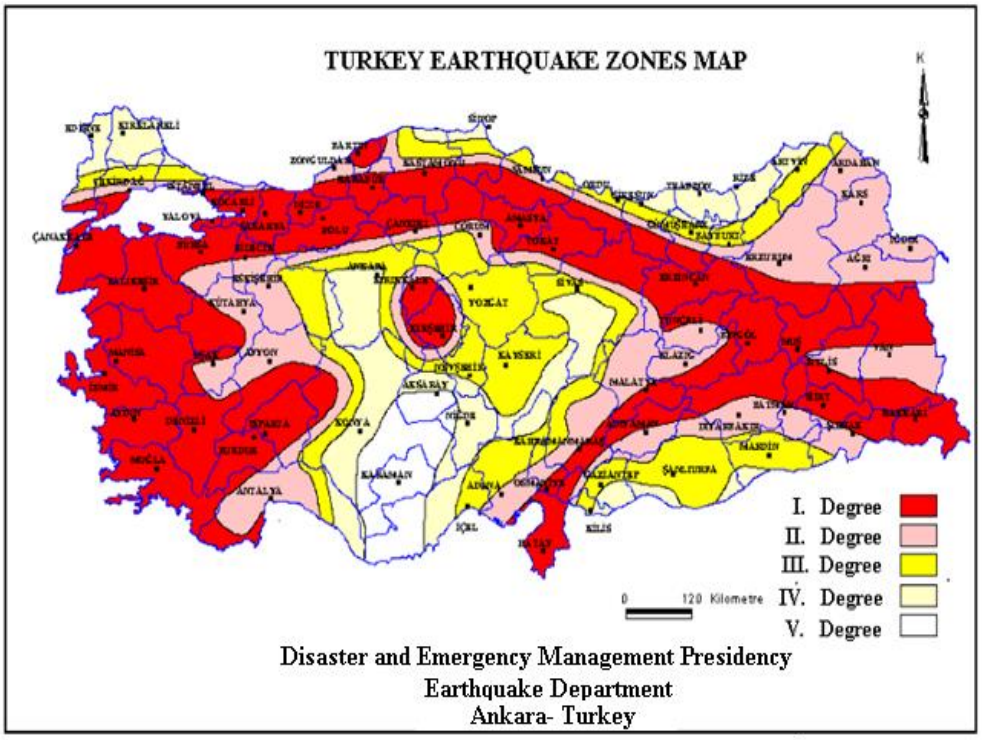


**Figure 2.8.** Turkey's eartquake zone maps and active fault map (AFAD, 2018)

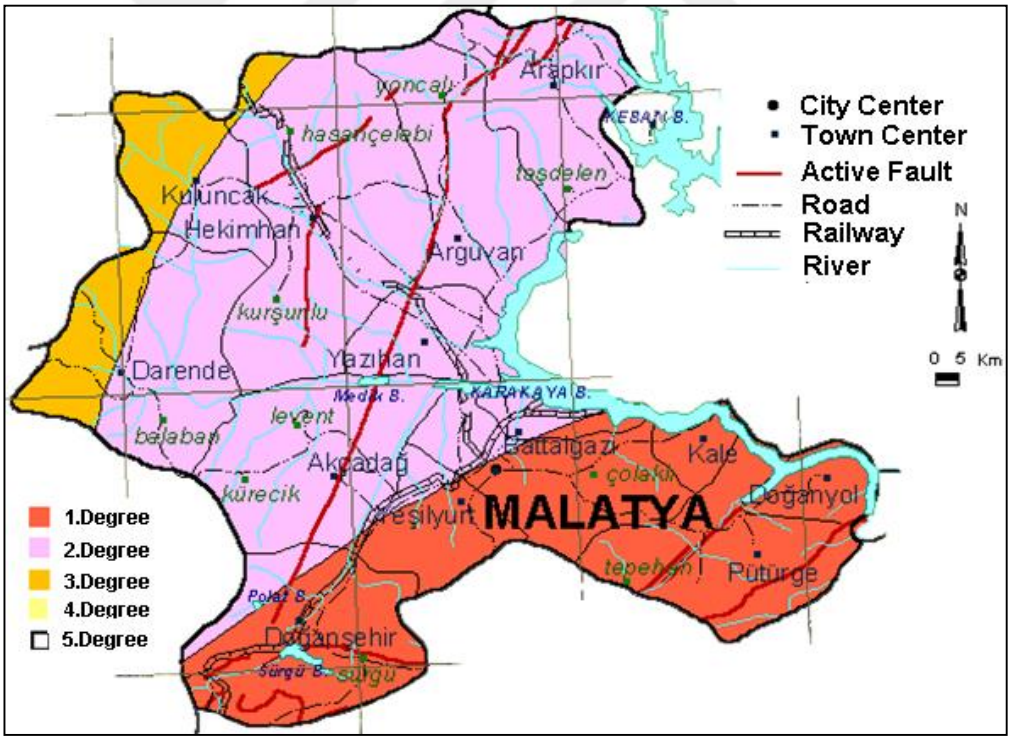


**Figure 2.9.** The city of Malatya earthquake region zones and active fault map (AFAD, 2018)

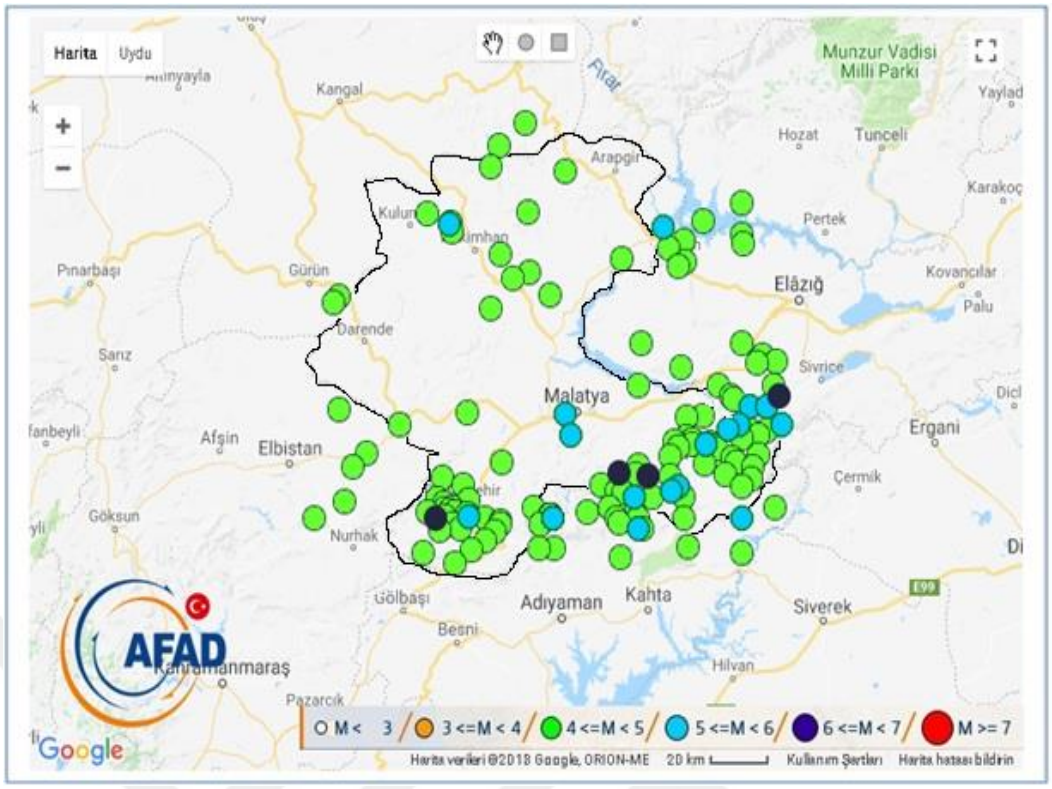


**Figure 2.10.** Distribution of M ≥ 4.0 earthquakes between 1900-2018 ın Malatya and surroundings (AFAD, 2018)

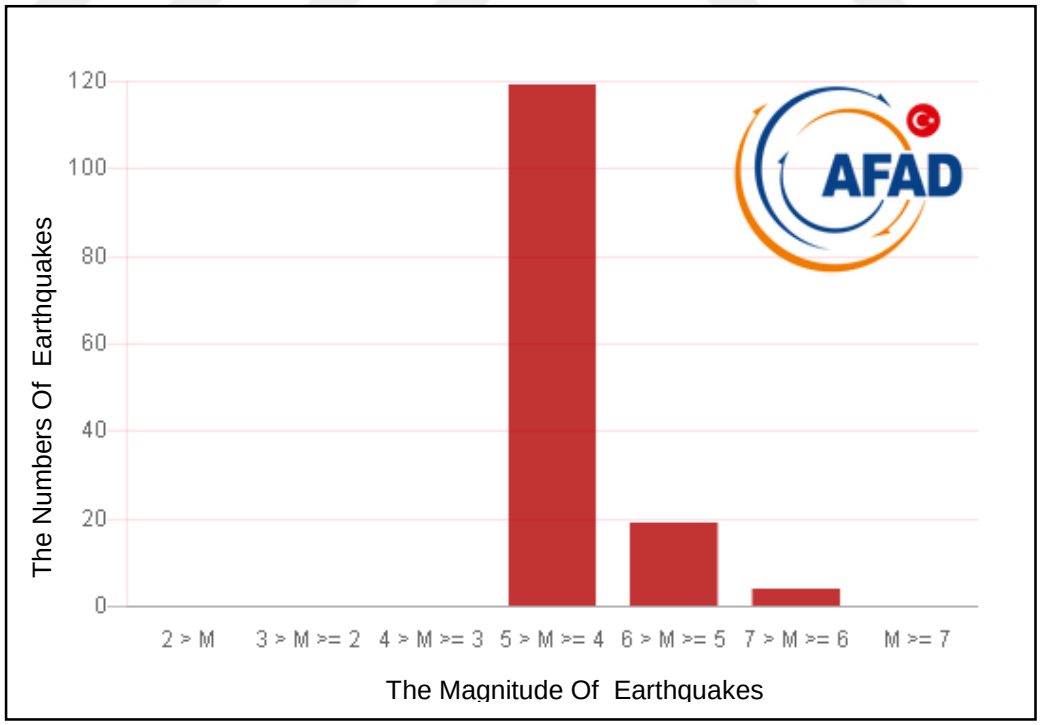


**Figure 2.11.** The numbers of earthquakes and the magnitude of earthquakes between 1900-2018 in Malatya and surroundings (AFAD, 2018)

**Table 2.1.** The ımportant earthquakes occured ın Malatya and ıts surroundings between the years of 1900-2018 (AFAD, 2018)

| Nu | Date | Time | Lat.-Log. | D | M | Location |
|---|---|---|---|---|---|---|
| 1 | 04.12.1905 | 07.04 | 38.12 – 38.63 | 10 | 6.8 | Pütürge - Malatya |
| 2 | 28.09.1908 | 06.27 | 38.35 – 39.15 | 10 | 6.1 | Malatya-Elazığ B. |
| 3 | 20.12.1940 | 05:18 | 38.30 – 38.30 | 10 | 5.8 | Yeşilyurt-Malatya |
| 4 | 14.06.1964 | 12:15 | 38.13 – 38.51 | 3.0 | 6,0 | Malatya-Adıyaman B. |
| 5 | 05.05.1986 | 03.35 | 38.00 – 37.78 | 4.1 | 6.0 | Doğanşehir-Malatya |
| 6 | 06.06.1986 | 10.39 | 38.00 – 37.91 | 21.9 | 5.8 | Doğanşehir-Malatya |
| 7 | 09.05.1998 | 15.38 | 38.25 – 38.94 | 17.2 | 5.8 | Pütürge - Malatya |
| 8 | 13.07.2003 | 01.48 | 38.32 – 39.03 | 10 | 5.5 | Doğanyol - Malatya |
| 9 | 09.02.2007 | 02.22 | 38.32 – 39.10 | 9.7 | 5.5 | Doğanyol - Malatya |
| 10 | 29.11.2015 | 00.28 | 38.84 – 37.84 | 22.4 | 5.0 | Hekimhan - Malatya |

D=Deepth (km), M:Magnitude B:Border

## 2.4 Geographic Information Systems (GIS)

Geographic Information System (GIS) is a computer system that allows the collection, storage, updating, control, analysis and display of geographical features (Yomralıoğlu, 2000). It is very important to use the information in a meaningful way. Using the information obtained in this respect with the help of GIS provides time, labor and easy access. Thematic maps with certain features are used in this process. In addition, the layered structure of this program allows many features to be displayed together. In terms of geotechnical engineering, it provides convenience and visual advantages in examining the geotechnical properties together. It provides the opportunity to update the studies. Maps containing geotechnical features prepared for specific regions help institutions to plan.

# CHAPTER 3

# ANALYSIS OF FIELD AND LABORATORY TESTS

## 3.1 Introduction

Within the scope of the thesis, approximately 100 $km^2$ of the settlement area (city center) of Malatya Municipality was investigated by means of 192 geotechnical boring data. In this study, for 1.5 m, 3 m, 4.5 m, 7.5 m, 15 m depths, standard penetration tests, liquefaction, water content values, bearing capacity, shear wave velocity were studied. Moreover, groundwater table depth values and shear wave velocity ($Vs_{30}$), soil classification according to the NEHRP and Eurocode 8, earthquake hazard level by soil amplification, local soil class by dominant vibration period were investigated, and illustrated by using GIS based maps.

## 3.2. Standard Penetration Test (SPT)

Standard penetration test is one of the most widely used field tests in the world. The test is based on hitting the split spoon sampler (having standard dimensions) to the soil with adopted dynamic energy resulting from freely dropping 63.5 kg weight of a tilt hammer from 76.2 cm. The first 15 cm of penetration is not taken into consideration. The number of blows necessary for penetration of the second and third 15 cm is collected then this value is recorded as SPT-N value. The test is usually repeated once at 1.5 m. If the 15 cm penetration does not take place with 50 blows, the test is stopped. At the end of the test, the thesis drilling report is prepared with the help of other geotechnical features. An example of SPT boring report prepared in Figure 3.1 is presented (Erol and Çekinmez, 2014).

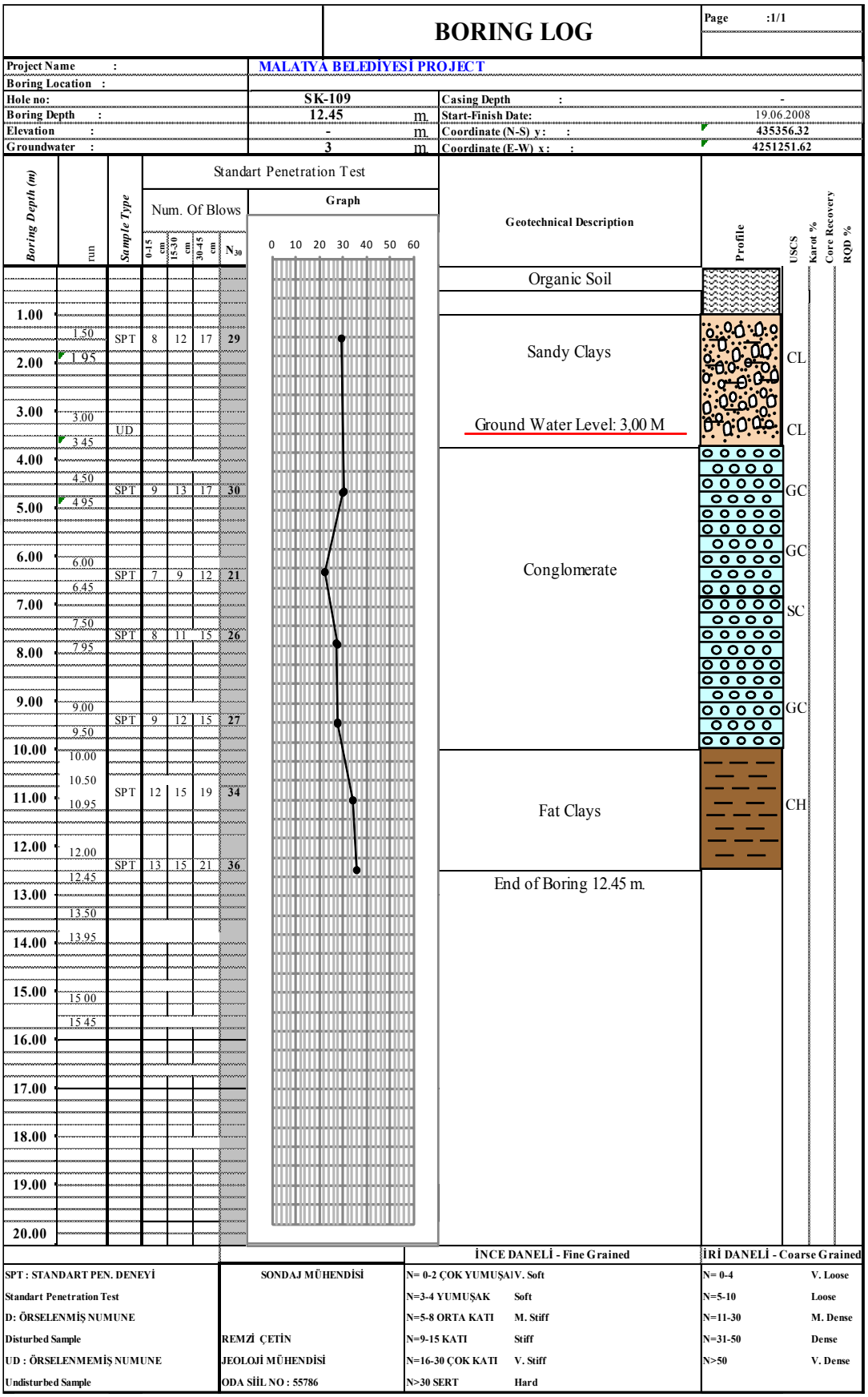


**Figure 3.1.** An example of SPT boring report (MMDD, 2009)

### 3.3. Bearing Capacity Calculations

The bearing capacity represents the load that the ground grain can carry in a unit area without deteriorating. In our studies, the bearing capacity obtained using field tests (based on SPT-N) and geophysical methods (based on Vs and Vp) were compared.

#### 3.3.1. Terzaghi and Peck (1967) Bearing Capacity Method

The method developed by Terzaghi and Peck'e determines the bearing capacity according to the base width and SPT-N values. Figure 3.2 was used to determine the bearing capacity (Bowles, 1996). The foundation width was chosen as 3 m.

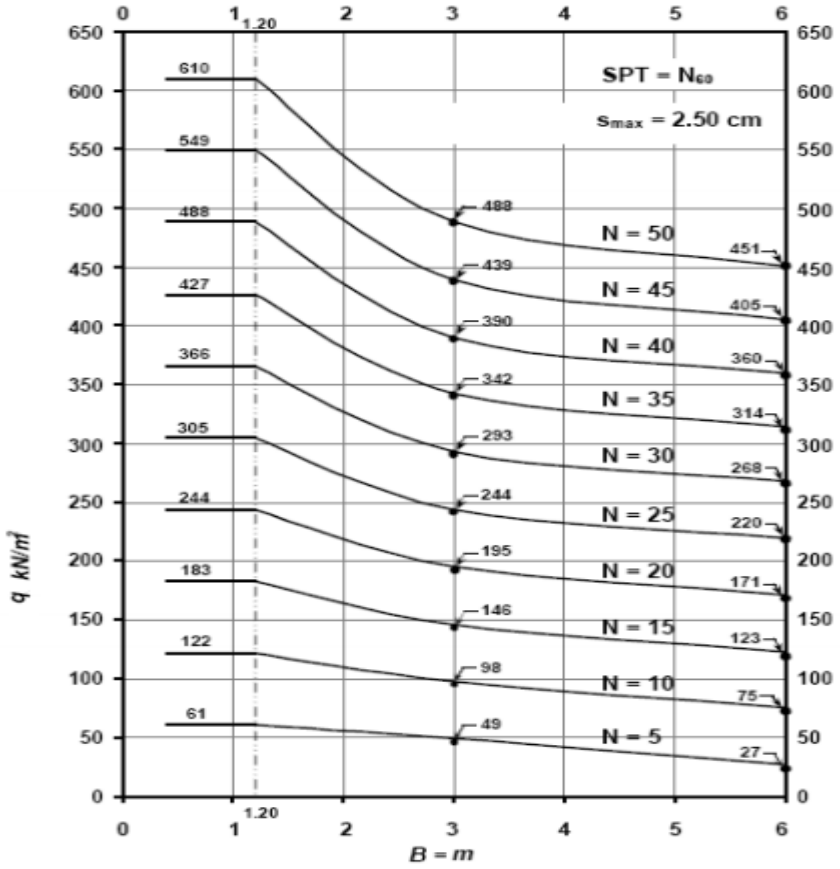


**Figure 3.2.** Change of allowable bearing capacity according to foundation width and SPT-N (Bowles, 1996).

#### 3.3.2. Meyerhof (1974) Bearing Capacity Method

Meyerhof developed bearing capacity formulas based on SPT-N values. Similar to the work done by Terzaghi and Peck, Meyerhof also limits the settlement at to 25

millimeters. Accordingly, the bearing capacity is calculated by using the following formulas (Bowles, 1996). The foundation width was chosen as 3 m.

$$q = 12 * N * Kd \quad (3.1)$$

$$q = 8 * N * ((B + 0{,}3505) / B)^2 \quad (3.2)$$

$$Kd = 1 + 0{,}33 * D / B \leq 1{,}33 \quad (3.3)$$

Here; abbreviations are used as:

q : Bearing capacity (kN / $m^2$)

N : SPT blow number

D : Foundation depth (m)

B : Foundation width (m)

### 3.3.3. Keceli (1990) Bearing Capacity Calculation

Keceli (1990) gives the following formula for the bearing capacity calculation using geophysical mehods, assuming that the soil exhibits elastic behavior (Keçeli, 1990). Accordingly, the bearing capacity is calculated by using the following formulas.

$$q = \frac{T * Vp * \gamma}{40} \quad (3.4)$$

Here;

q : Bearing capacity (kN / $m^2$)

T : Soil dominant vibration period (sec)

Vp : Compression Wave Velocity (m / sec)

$\gamma$ : The soil shows the unit weight. (kN / $m^3$)

### 3.3.4. Tezcan et al.(2010) Bearing Capacity Calculation

The foundation width- soil safety stress relationship in the calculation of the bearing capacity with the SPT test is taken into consideration by Terzaghi and Peck (1967), and this is also adopted by Tezcan et al. (2010). For this reason, in cases where the foundation width changes between 0 and 12 meters, the bearing capacity is calculated by using geophysical mehods via $\beta$ reduction factor (Tezcan et al., 2010). The foundation width was chosen as 3 m.

$$q = 0{,}1 * \gamma * Vs * \beta \quad (3.5)$$

Here;

q : Bearing capacity (kN / $m^2$)

Vs : Shaer wave velocity (m / sec)

$\gamma$ : The soil shows the unit weight. (kN / $m^3$)

$\beta$ : Reduction factor

B : Foundation width (m)

Relation of $\beta$ reduction factor and B foundation width

$\beta = 1$ $0 \leq B \leq 1.2$ m (3.6)

$\beta = 1.13 - 0.11B$ $1.2 \text{ m} \leq B \leq 3.00$ m (3.7)

$\beta = 0.83 - 0.01B$ $3.00 \text{ m} \leq B \leq 12$ m (3.8)

### 3.4. Liquefaction Potential

The word liquefaction, first introduced by Japanese researchers Mogami and Kubo in 1953. Liquefaction, under conditions where water can not be removed from the soil environment, soil deformation caused by the disturbance of water-saturated cohesionless soils (Ulusay, 2000). The soil that begins to lose its strength by liquefaction becomes unable to carry the loads transferred by the construction and consequently the constructions on the soil are laid down or deviated in different directions (Şen, 2004). During liquefaction, loss of bearing capacity is observed due to the aggregation and removal of soil particles. For this reason, there are settlements on the surface of the soil and overturning in the buildings (Aydan et al., 2000). Lateral propagation can be defined as the separation of the soil layers over soil level into large blocks and lateral movement of the separated blocks. Lateral propagation develops along surfaces with 3-5% of the slope (Şen, 2004). Flow liquefaction occurs along surfaces with a slope greater than 5%. During movement, very large soil masses can move quickly, in tens of kilometers, in a very short time (Ulusay, 2000).

#### 3.4.1 Calculations

Many methods of analysis related to field and laboratory tests are available in the literature for determining liquefaction sensitivity. The fact that the tests in the lab are time consuming and costly, field tests are widely preferred in the research of

liquefaction potential. Within the scope of this thesis, SPT blow numbers obtained in the field are used in determining the liquefaction sensitivity of the study area. It used T. L. Youd and I. M. Idriss (2001) metod in this thesis. This method is based on H.B. Seed and I. M. Idriss (1971) metod. The determination of the liquefaction potential is based on the determination of the safety coefficient against liquefaction of the soil. The safety coefficient is found by dividing the Cyclic Resistance Ratio (CRR) required for liquefaction of the soil to the Cyclic Stress Ratio (CSR) generated by earthquake. The CSR, which is the correlation of repeated stresses occurring during the earthquake, is calculated by the relation 3.9 (Youd et al., 2001).

$$CSR = (\tau_{av} / \sigma'_{vo}) = 0.65 * (a_{maks} / g)*(\sigma_{vo} / \sigma'_{vo})*r_d \quad (3.9)$$

CSR : Cyclic Stress Ratio generated by average horizontal shear as a result of earthquake

$a_{maks}$ : Peak Ground Acceleration ($cm/sec^2$)

g : Ground Acceleration ($cm/sec^2$)

$\sigma_{vo}$ : Vertical Total stress (kPa)

$\sigma'_{vo}$ : Vertical effective stress (kPa)

$r_d$ : Stress Reduction Factor

rd is a factor changing with the depth and is calculated by the relation 3.10 up to9.15 m. depth and between 9.15 m. and 23 m. depths it is calculated by the relation 3.11

$$z \leq 9.15 \text{ m for } r_d = 1.0 - 0.00765z \quad (3.10)$$

$$9.15 < z \leq 23 \text{ m for } r_d = 1.174 - 0.00267z \quad (3.11)$$

In calculating the cyclic resistance ratio(CRR) of the soil to liquefaction, the SPT blow counts are used, as mentioned in the previous paragraphs. The blow numbers (N) obtained from the SPT test are subjected to a series of corrections, as is known, to determine the corrected SPT Number of blows (N1) 60. These corrections are; ($C_N$) Overburden correction, ($C_E$) Stem bar energy ratio correction, ($C_B$) Borehole Diameter Correction, ($C_R$) Stem bar length correction , and ($C_S$) inner tube correction. The correction coefficients of SPT proposed by Youd et al., (2001) are given in Table 3.1. The formula (3.12) proposed by Youd et al., (2001) is used for Overburden correction($C_N$).

$C_N=2.2 / (1.2 + (\sigma'_{vo} / Pa))$ (3.12)

Pa : Atmospheric pressure 100 kPa

$\sigma'_{vo}$ : Effective cover stress (kPa)

The energy rate (Er) of donut type tilt hammer used in Turkey is 45%. The Stem bar energy ratio correction ($C_E$) is calculated by the relation 3.13.

$C_E = Er / 60$ (3.13)

The following expression is used to find the Corrected blow number considering all ($(N_1)_{60}$) for each level where the SPT test is performed (Youd et al., 2001).

$(N_1)_{60} = N.C_N.C_E.C_B.C_R.C_S$ (3.14)

**Table 3.1.** Coefficients used in the corrected spt number of blows (Youd et al., 2001)

| | | Coefficient |
|---|---|---|
| Well diameter ($C_B$ ) | 65-115 mm | 1.0 |
| | 150 mm | 1.05 |
| | 200 mm | 1.15 |
| Stem bar length (CR) | < 3 m | 0.75 |
| | 3-4 m | 0.8 |
| | 4-6 m | 0.85 |
| | 6-10 m | 0.95 |
| | 10-30 m | 1.0 |
| Inner tube use ($C_S$) | Standard Sample Taker | 1.0 |
| | Cases in which inner tube used | 1.1 – 1.3 |

Youd et al., (2001) stated that CRR increases with increase in fines content ratio (<0.075mm) in liquefaction analysis and offered a new correction about proportion of Corrected SPT blow number ($(N_1)_{60}$) to the fine content ratio that the soil contains. This correction is ($(N_1)_{60cs}$); namely, corrected blow number according to fines content ratio for liquefaction analysis.

$(N_1)_{60cs} = \alpha + \beta . (N_1)_{60}$ (3.15)

α and β are the coefficients calculated in the following formulas.

If $FC \leq \%5$ $\alpha = 0$, $\beta=1.0$ (3.16)

If $\%5 < FC < \%35$ $\alpha = \exp(1.76 - (190 / FC^2))$, $\beta=(0.99 + (FC^{1.5} / 1000))$ (3.17)

If $FC \geq \%35$ $\alpha = 5$, $\beta=1.2$

(3.18)

Using the corrected SPT blow numbers, cyclic resistance ratio (CRR) of the soil is calculated by using relation 3.19. This relation $(N_1)_{60}$ applies when the value is less than 30, in cases where $(N_1)_{60} \geq 30$, soils are very hard for liquefaction and they are considered non-liquefiable (Youd et al., 2001).

$$CRR = \frac{1}{34 - (N_1)_{60}} + \frac{(N_1)_{60}}{135} + \frac{50}{[\,10.(N_1)_{60} + 45\,]^2} - \frac{1}{200} \quad (3.19)$$

Liquefaction occurs in the depth where liquefaction resistance is overcame by the shear stresses that occur during an earthquake. This situation is expressed with the factor of safety against liquefaction by Seed and Idriss (Seed and Idriss, 1971).

$$FS = \frac{CRR}{CSR} \quad (3.20)$$

The calculated FS values are evaluated according to the following ranges;

$FS \leq 1$ There is a liquefaction risk.

$FS > 1$ There is no liquefaction risk.

CRR 7.5 values calculated for an earthquake greater than 7.5 magnitude should be corrected according to the estimated earthquake magnitude in the region studied. For this correction, a size scaling (correction) factor (MSF) revised by Youd et al., (2001) is proposed (Şen, 2004).

$$MSF = \frac{10^{2.24}}{M_W{}^{2.56}} \quad (3.21)$$

Here; Mw is the earthquake magnitude in terms of expected moment magnitude in the study area. The factor of safety against liquefaction (FS) is calculated in the following expression (3.22) (Şen, 2004).

$$FS = \left(\frac{CRR}{CSR}\right) * MSF \quad (3.22)$$

### 3.5. Shear Wave Velocity

The shear wave velocity, the soils provide information about the rigidity. It is used in the analyzes to determine soil behavior. It is determined by measuring, it in situ or calculated (depend on SPT-N). However, in some soil classification systems and earthquake hazard analyzes, 30 m of average shear wave velocity information of the soil is used (Kurnaz, 2011).

Within the scope of measurement made in the field, surface fracture method is used. It is used to determine the parameters of the soil of the study area. This method, the propagation of the waves coming from the interfaces with fraction and waves coming directly are recorded. As a seismic energy source, 8 kg weight sledgehammer is used. The energy in the S wave (shear wave) is obtained by hitting the plate placed perpendicular to the pit with 30-40 cm deep. S wave records are created. Geodetic geophones (detectors) are used in the transverse wave records. Seismograph with signal accumulation is used for precise measurement of S velocities. Vs is obtained by this method in the field (Kurnaz, 2011).

In situ measurement of the shear wave velocity can be disadvantageous in some cases, thus, shear wave velocities are often estimated from correlations associated with SPT-N numbers (Kurnaz, 2011). These correlations are given in Table 3.2.

**Table 3.2.** The empirical correlation based on SPT-N and Vs (Akın et al, 2011)

| Researchers | $V_s$ (m/s) (All type of soils) |
|---|---|
| Ohba and Trauma(1970) | $Vs= 84*N^{0.31}$ |
| Seed and Idriss(1981) | $Vs= 61*N^{0.5}$ |
| Imai and Yoshimura (1970) | $Vs=76*N^{0.33}$ |
| Iyisan (1996) | $Vs=51.5*N^{0.516}$ |
| Hasancelebi and Ulusay(2007) | $Vs=90*N^{0.309}$ |
| Tsiambos and Sabatakakis (2011) | $Vs=105.7*N^{0.327}$ |
| Vs: Shear wave velocity, N: Uncorrected SPT blow number | |

### 3.6. Soil Classification by NEHRP

National Earthquake Hazard Reduction Program (NEHRP); it is aimed to increase the expected performances of important buildings during or after an earthquake in the United States of America. The soil class according to NEHRP is based on the average of the S-wave velocity up to 30 m depth, and these classes are given in Table 3.3 (Güzel,2009).

**Table 3.3.** Soil classification criteria according to NEHRP (Güzel, 2009)

| Soil | Description | Properties |
|---|---|---|
| A | Hard rock | Vs>1500 |
| B | Rock | 760 < Vs ≤ 1500 |
| C | Very dense soil/ soft rock | 360 < Vs ≤ 760 |
| D | Stiff soil | 180 < Vs ≤ 360 |
| E | Soft soil | Vs<180 |

### 3.7. Earthquake Hazard by Soil Amplification

Soil amplification is the increase in amplitude of seismic waves as they pass through soil layers closed to the surface. The reason for this is the low density, that the soil layers have. During the earthquake, in loose soils the earthquake waves grow at a considerable rate. These soils are known to have a huge role in damages caused by the earthquake (Kurnaz, 2011). Soil amplification was calculated from the following Midorikawa (1987) formula.

$$A=68V_1^{-0.6} \quad (V_1<1100 \text{ m/s}) \tag{3.23}$$

$$A=1 \quad (V_1>1100 \text{ m/s}) \tag{3.24}$$

Here;

A : Relative amplification coefficient

$V_1$ : Shear wave velocity for depth of 30 meters

Earthquake hazard level according to calculated soil amplification; for the amplification value of 0,0-2,0, hazard level C (low hazard), for the amplification

value 2.0-4.0, hazard level B (medium hazard), for the amplification value of 4.0-6.5, hazard level A (high hazard) (Kurnaz, 2011).

### 3.8. Local soil classes by Soil Dominant Vibration Period (To)

The dominant vibration period is represents the natural vibration properties as a whole of the ground layers on the bedrock (Kanai, 1983). The following formula is used to calculate the dominant vibration period.

$$To = \sum 4H / Vs \quad (3.25)$$

Here;

To : Dominant vibration period

H : Layer thickness (m)

Vs : Shear wave velocity (m/s)

According to Turkish earthquake regulations, the dominant vibration period depending on local soil classes is given in Table 3.4. (Z1: Very dense, Z2: Stiff, Z3: Medium stiff, Z4: Loose, soft)

**Table 3.4.** The Turkish earthquake regulations, the soil dominant period (To) (Güzel, 2009)

| Soil Type | | To Soil Dominant Period (sec) | To Mean (sec) | (TA - TB) (sec) |
|---|---|---|---|---|
| **Z1** | a | 0.20 | 0.25 | 0.10 - 0.30 |
| | b | 0.25 | | |
| | c | 0.30 | | |
| **Z2** | a | 0.35 | 0.42 | 0.15 - 0.40 |
| | b | 0.40 | | |
| | c | 0.50 | | |
| **Z3** | a | 0.55 | 0.6 | 0.15 - 0.60 |
| | b | 0.60 | | |
| | c | 0.65 | | |
| **Z4** | a | 0.70 | 0.8 | 0.20 - 0.90 |
| | b | 0.80 | | |
| | c | 0.90 | | |

### 3.9. Water in the Study Area

Earthquakes cause sudden and very short movements in the soil. When the ground water is close to the surface, during earthquakes, ıt remove the contact forces holding

the soil grains together and loses soil strength. Under these conditions the soil behaves like a liquid instead of the solid material behavior (Kurnaz, 2011). Therefore, Groundwater directly influences the plan of engineering constructions and the mechanical properties of the soils (IMO, 2016).

In soil behavior and modeling, the water content in the soil has an important role. The water content is determined on the basis of the principles set out in TS 1900-1 (2006) or ASTM D 2216 (2010) (IMO, 2016)

### 3.10. Soil Classification by Eurocode 8

The Eurocode series are European Regulations relating to constructions. "Eurocode8: Design of structures for earthquake resistance" This regulation explains how constructions in earthquake zones should be designed. This regulation has been approved by the European Standards Committee. Eurocode 8 is used for the design and construction of civil engineering buildings and other works in earthquake hazard regions (Halaç, 2016).

Its aim is that human lives are protected, potantial damage during an earthquake is limited. Also, it is expected that buildings, which carry importance for civil protection, can be safe for use after earthquakes. The soil class according to Eurocode8 is based on the average velocity ($Vs_{30}$) of the S-wave velocity up to 30 m depth, and these classes are given in Table 3.5

**Table 3.5.** Soil classification criteria according to Eurocode8 (Güzel,2009)

| Soil | Description | Properties |
|---|---|---|
| A | Rock or other rock-like geological formation | Vs > 800 |
| B | Very dense sand or gravel or very stiff clay | 360 < Vs ≤ 800 |
| C | Dense sand or gravel or stiff clay | 180 < Vs ≤ 360 |
| D | Loose to medium cohesionless soil or soft to firm cohesive soil | Vs < 180 |

# CHAPTER 4

# RESULTS AND DISCUSSION

## 4.1. SPT-N Maps

SPT is a widely used field test and data used in this study have been obtained from 192 bore points within the study area. In a SPT test, the necessary blow numbers for 15cm increments into soil up to providing 45 cm penetration is determined with a split spoon sampler fitted with boring rods and this test is done by dropping a tilt hammer weighting 63.5 kg over the rod from a 760 mm height. The first 15 cm increment is ignored because of possible soil disturbance, and the total of the number of drops in the last two sets is regarded as the number of SPT-N in the soil.

The maps presented in this study are created for depths of 1.5 m, 3 m, 4.5 m, 7.5, 15 m to give the distribution of SPT values up to a depth of 15 m from the surface and its change with depth increase. The maps are generated by using the ArcGis program and with the IDW method.

Throughout the study area, it is determined that 33% of the SPT-N data obtained from 192 borehole points at 1.5 m depth are between 1-20, 8% between 21-30, and 59% between 31-50. The map prepared in this context is presented in Figure 4.1. In the northwestern part of the study area around the City Cemetery, in the Southeastern part around Üzümlü and between Orduzu pond and Çamurlu, the local value of SPT-N is under 20, the values of the local region between Karaköy that is from the east of the study area and Çamurlu are between 20 and 30, in Karakavak, Aşağıbağlar, Çöşnük, Hançukuru, Saray which is in south-west of the study area and in the area to the east of Inonu University SPT-N values are observed as 31-50.

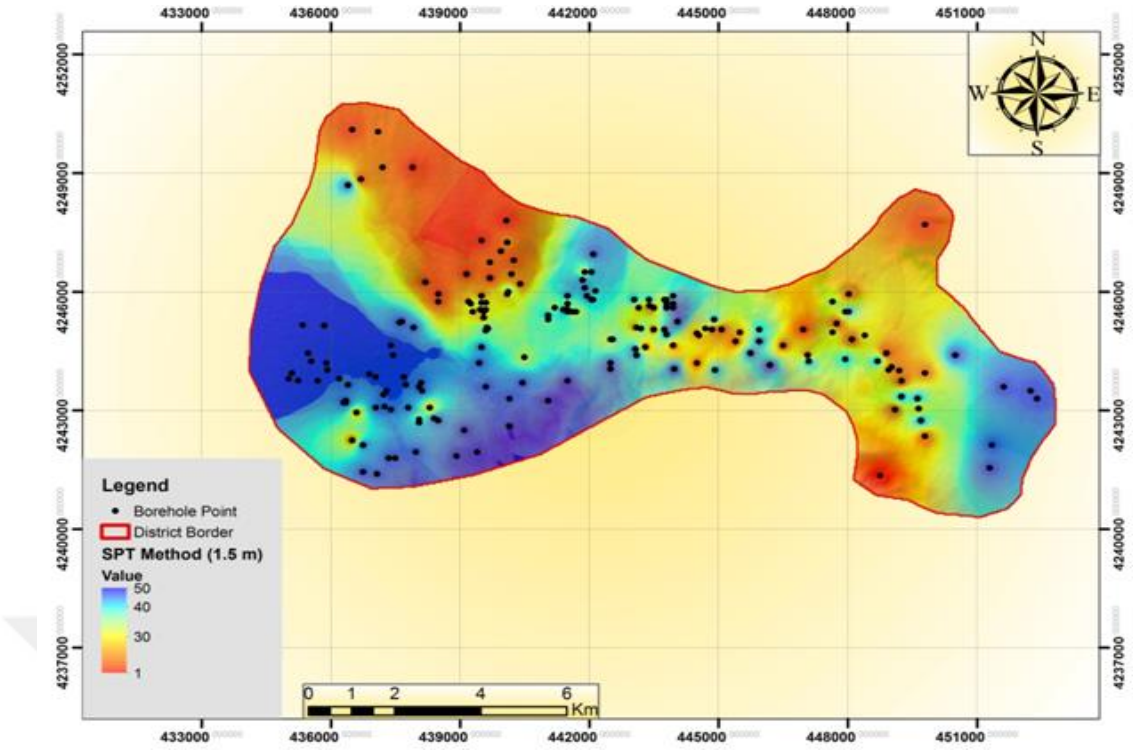


**Figure 4.1.** SPT-N map of the study area according to 1.5 m depth

Figure 4.2 presents the SPT-N values at 3m depth. The values at this depth indicate that 13% of the SPT-N data obtained from 192 borehole points are between 1-20, 7% between 21-30, and 80% between 31-50. Similarly, Figure 4.3 presents the SPT-N data at 4.5 m where they are 12% between 1-20, 5% between 21-30, and 83% between 31-50; Figure 4.4 demonstrates SPT-N blow counts at 7.5m as 8% between 1-20, 3% between 21-30, and 89% between 31-50; Figure 4.5 presents the deepest data level at 15m as 2% between 1-20, 2% between 21-30, and 92% between 31-50. If it is compared to the SPT-N blow counts at 1.5 m, the northwestern part of the study area around the City Cemetery, the Southeastern part the where the local value of SPT-N is under 20 are observed as in a smaller region. Consistently, the regions with SPT-N values ranging from 31 to 50 now spread out a larger region as expected. Figure 4.6 summarizes these findings as a percentage comparison chart consisting of data obtained from 192 borings which indicate that SPT-N values between 31 and 50 are common in the study area. The comparison of SPT-N values is important for the assessment of bearing capacity and liquefaction analysis as they strictly depend on SPT-N blow counts.

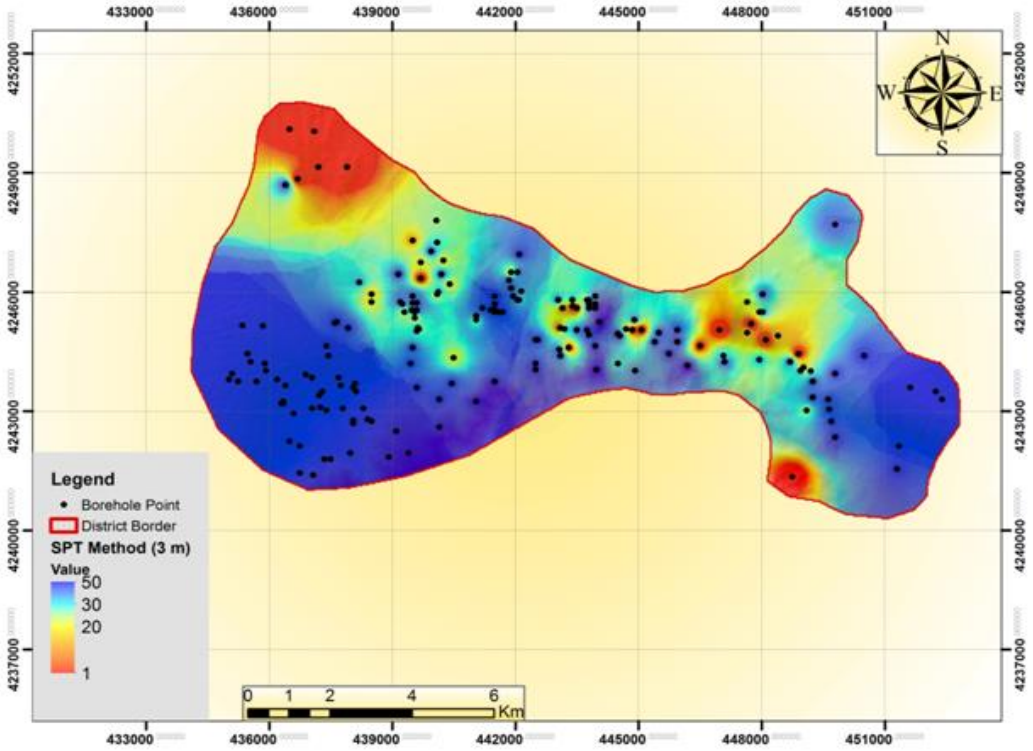


**Figure 4.2.** SPT-N map of the study area according to 3 m depth

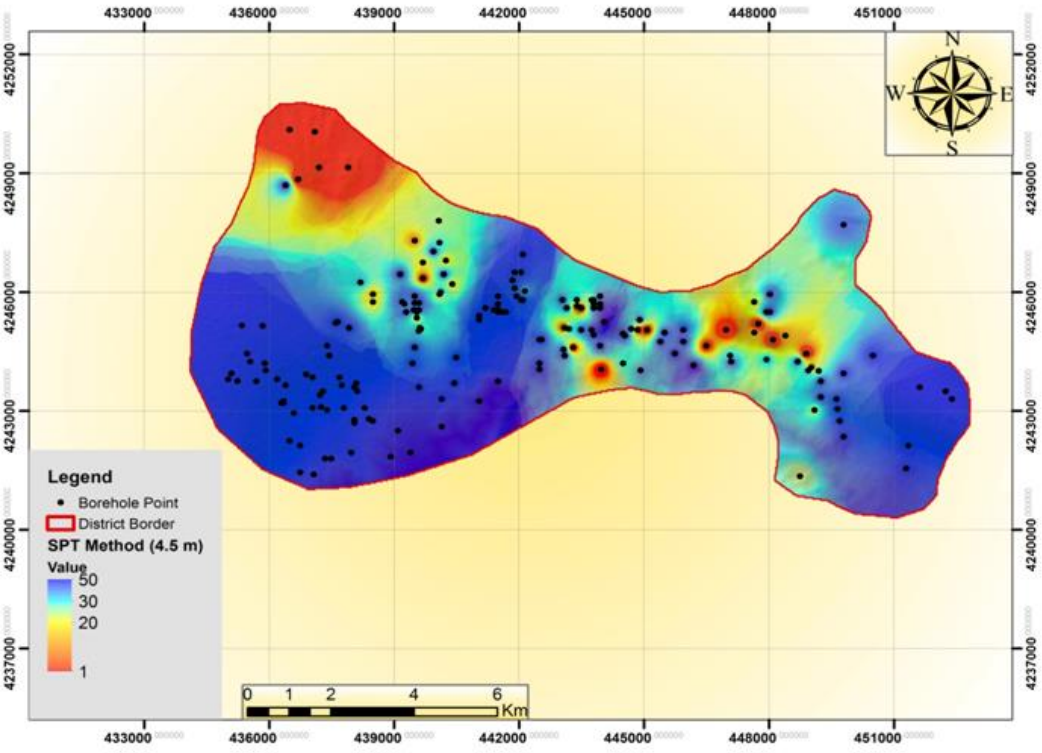


**Figure 4.3.** SPT-N map of the study area according to 4.5 m depth

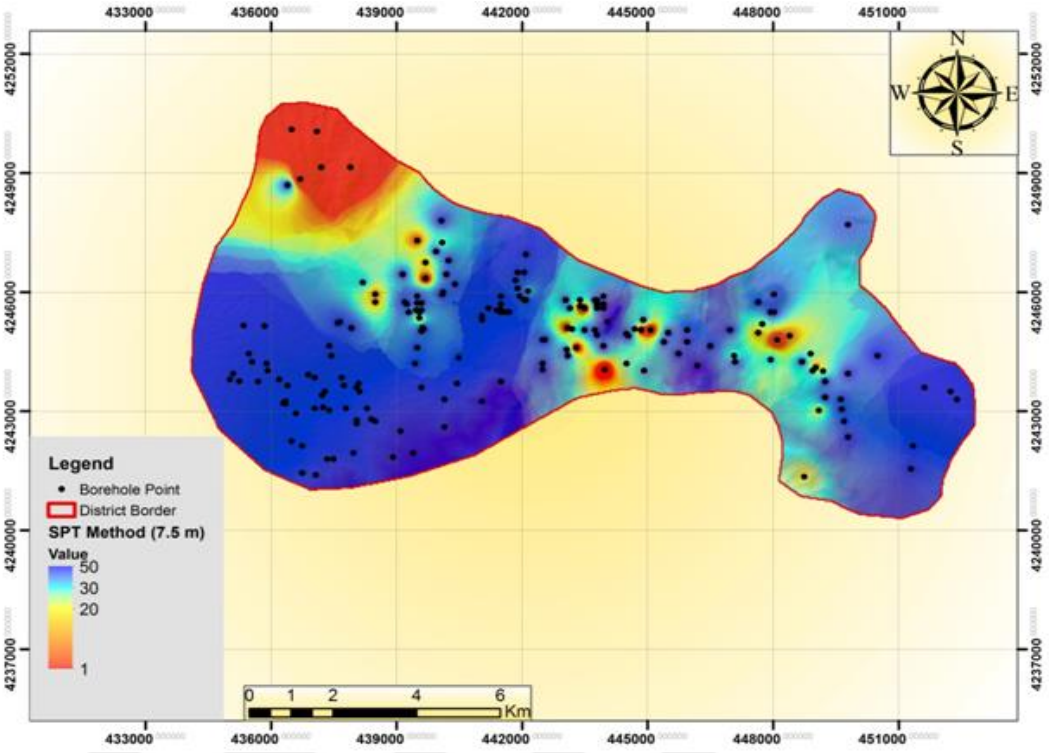


**Figure 4.4.** SPT-N map of the study area according to 7.5 m depth

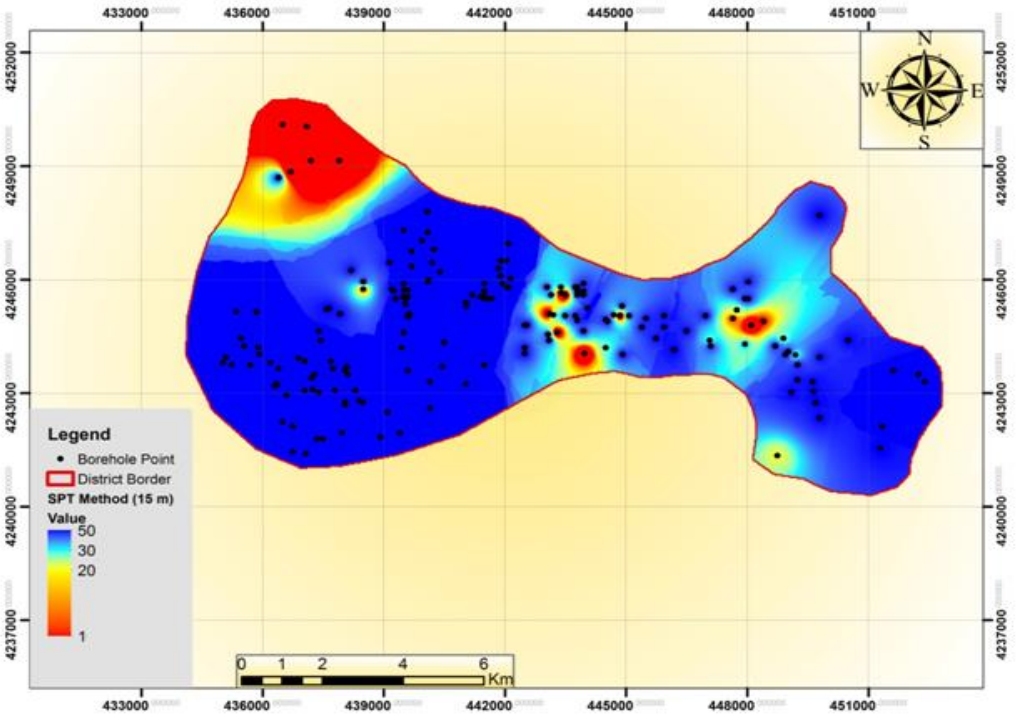


**Figure 4.5.** SPT-N map of the study area according to 15 m depth

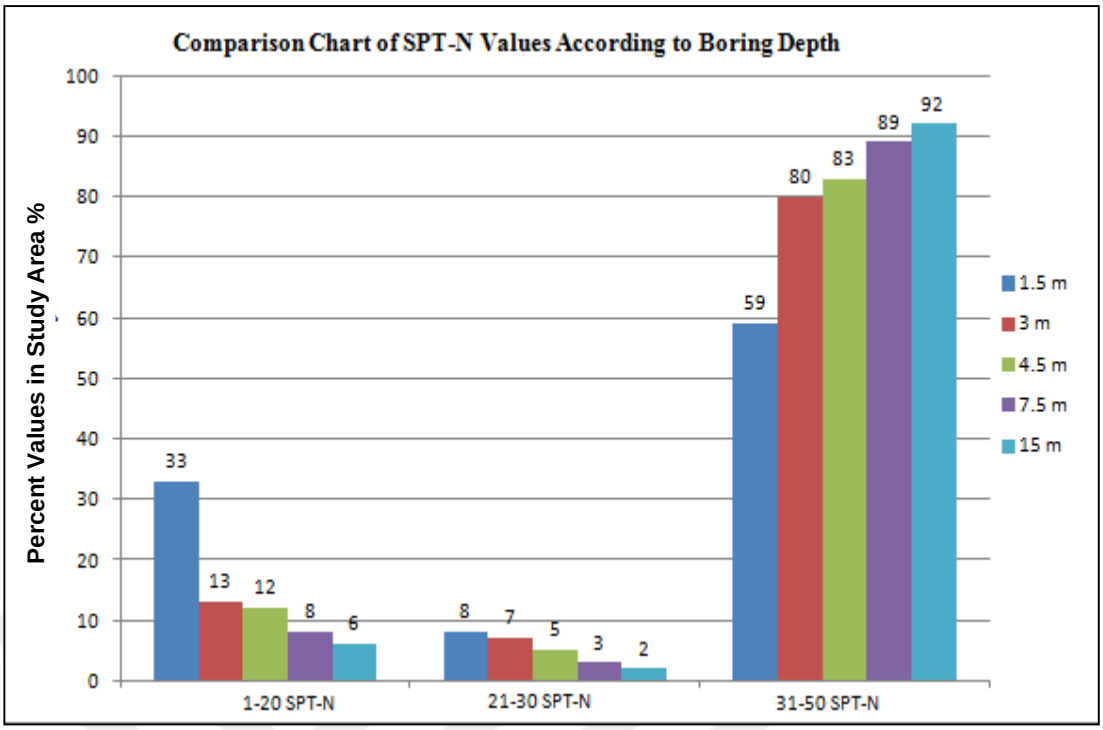


**Figure 4.6.** Comparison chart of SPT-N values according to boring depths

### 4.2. Bearing Capacity Analysis

This section presents the bearing capacity analysis of the region based on different approaches available in the literature. The field test data together with the common soil mechanics formulations employed to determine the bearing capacity of soils provide us with the opportunity to compare the bearing capacity values obtained from these methods for the region of our interest. Terzaghi and Peck method as well as Meyerhof method, which are very common methods in soil mechanics for determining the bearing capacity of soils, are employed. The results of these methods are then compared to those of two geophysical methods, which are Tezcan et al. (2010) and Keceli (1990). Geophysical methods are based on wave velocity obtained from the field tests in the region.

The Terzaghi and Peck method and the Meyerhof method are used in general for bearing capacity determination with date from field tests. The SPT-N data obtained from 192 boring points are used in the calculations. In this context, a bearing capacity map prepared by the Meyerhof method for a depth of 4.5 m is shown in Figure 4.7, and the bearing capacity map prepared by the Terzaghi and Peck method is shown in Figure 4.8. While the Terzaghi and Peck method showed the maximum

bearing capacity in the region as 488 kN / $m^2$, the Meyerhof method gave us the maximum bearing capacity value of 646 kN / $m^2$.

In the area from the northwestern part of the study area of the City Cemetery to Kiltepe has been found as the region with the lowest bearing capacity by both the Terzaghi and Peck method and the Meyerhof method. The area surrounded with Orduzu Pond, Çamurlu, and Karaköy is found to have bearing capacity values between 300-400 kN / $m^2$ by the Terzaghi ve Peck method while the Meyerhof method gives a range 450-600 kN / $m^2$ for the same region. But for the most part of the area, the bearing capacity value is around 488 kN / $m^2$ obtained by the Terzaghi and Peck method and it is around 646 kN / $m^2$ by the Meyerhof method.

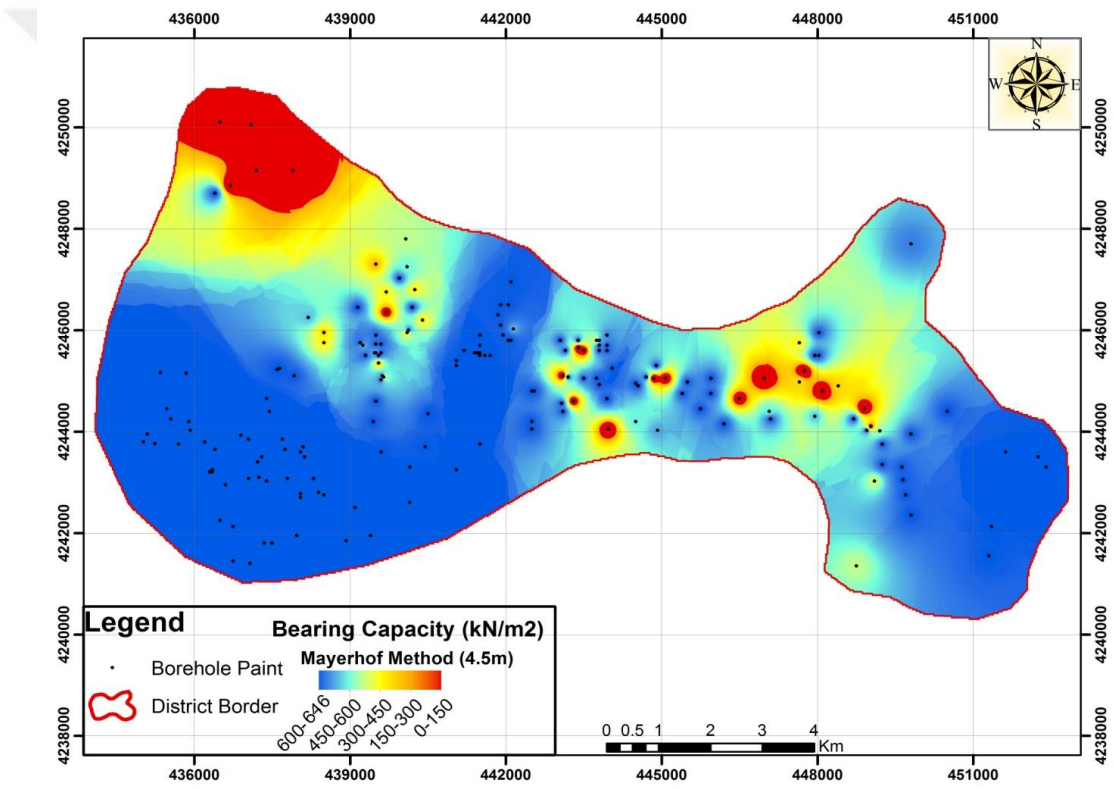


**Figure 4.7.** Bearing capacity map according to Meyerhof (1974) method (4.5 m)

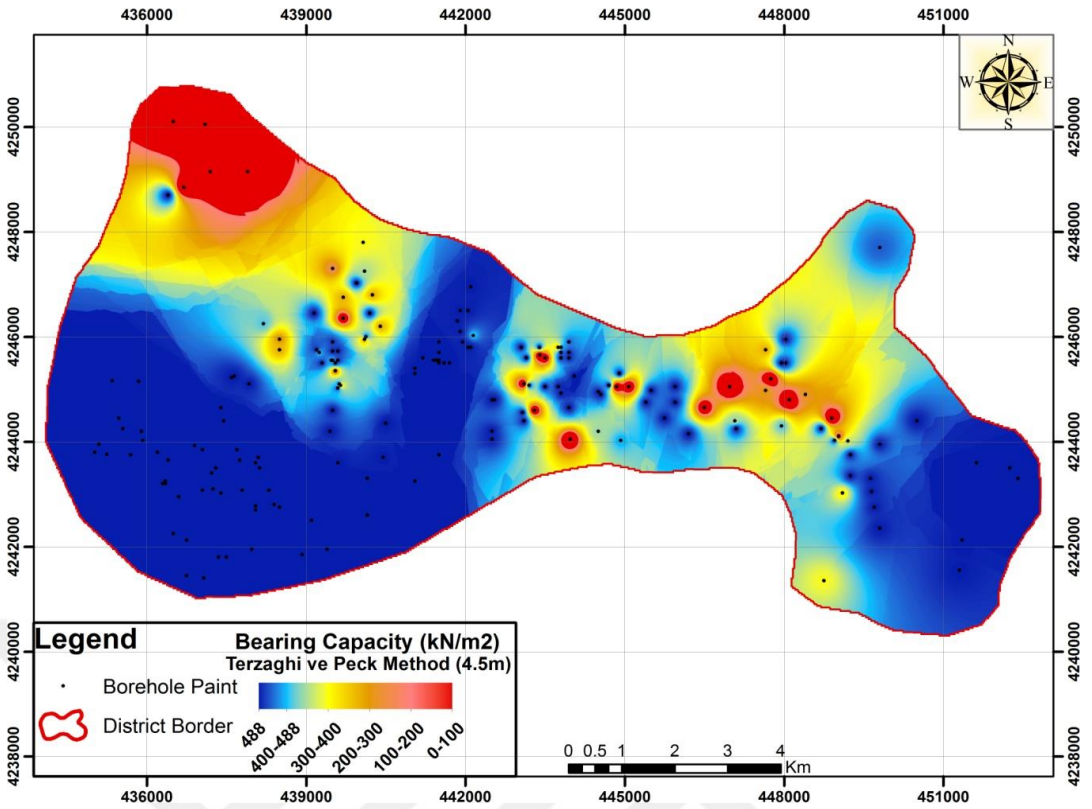


**Figure 4.8.** Bearing capacity map according to Terzaghi-Peck (1967) method (4.5 m)

The geophysical methods by Keçeli (1990) and Tezcan et al. (2010 ) to determine bearing capacity are used in. The values of density P (compression) wave velocity, S (shear) wave velocity, the dominant vibration period ($T_o$) which are obtained from the study area are used in the calculations. In this context, for a depth of 4.5 m, bearing capacity map prepared by Keçeli (1990) is shown in Figure 4.9, the bearing capacity map prepared by Tezcan et al. (2010 ) is shown in Figure 4.10. According to Keçeli (1990) values go up to 758 kN / $m^2$ and the method by Tezcan et al. (2010 ) gives up to 2460 kN / m2.

In the western part of the study area, according to the model proposed by Keçeli (1990), values of 150-450 kN / $m^2$ are found in most part of the study area while Tezcan et al. (2010) gives values of 100-1000 kN / $m^2$ for the study area.

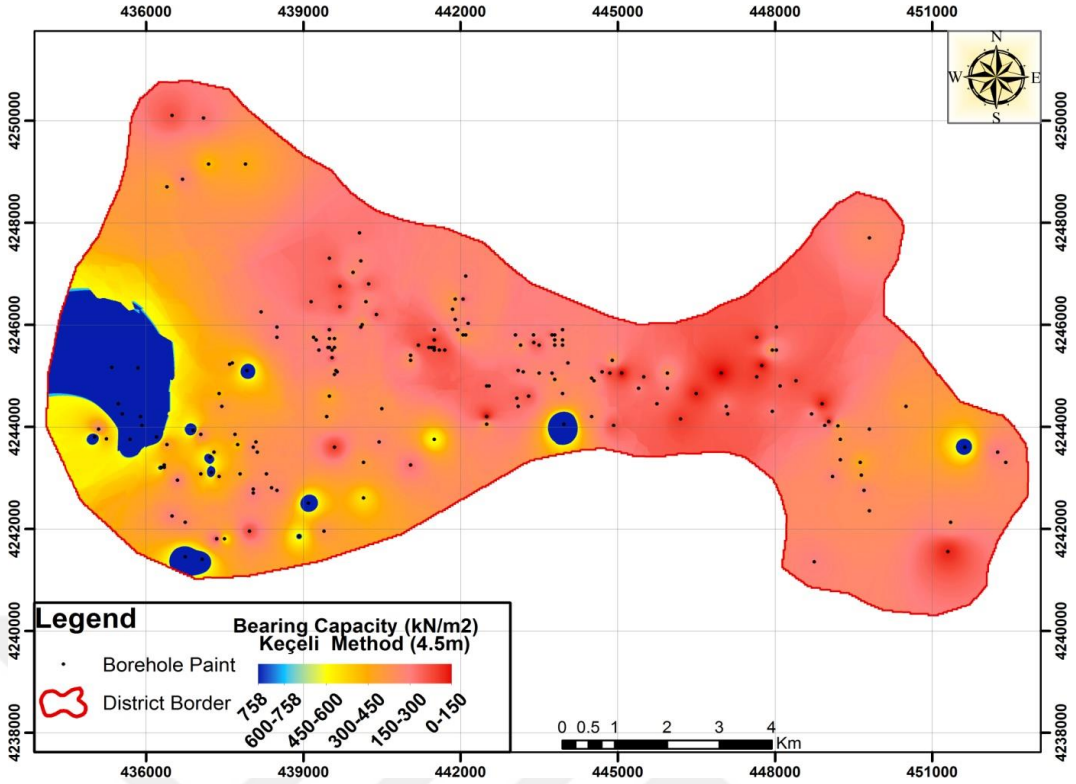


**Figure 4.9.** Bearing capacity map according to Keçeli (1990) method (4.5 m)

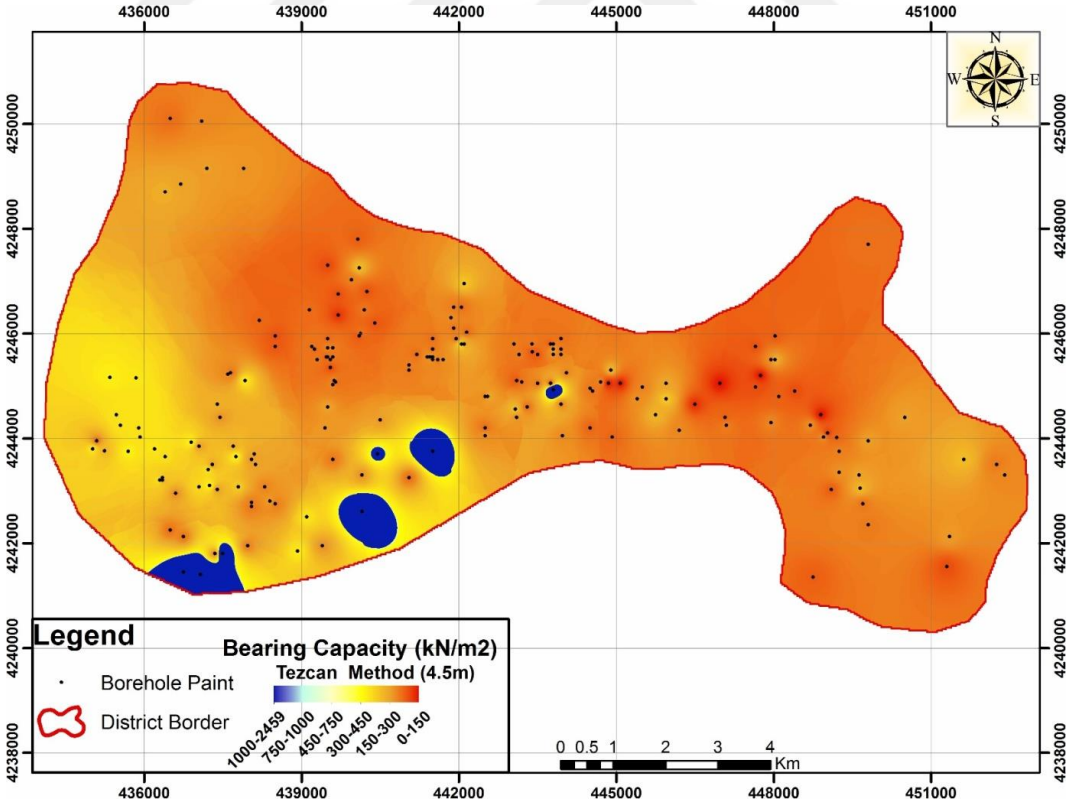


**Figure 4.10.** Bearing capacity map according to Tezcan et al (2010) method (4.5 m)

The bearing capacity values obtained by Terzaghi and Peck and Meyerhof methods show similar values at all of the depths of 1.5 m, 3 m, 4.5 m, 7.5 m, and 15 m. The calculated values are close to each other. However, it is observed that the bearing capacity values by the Meyerhof method are greater than those of the Terzaghi and Peck method when SPT-N values increase by depth. Although these two empirical soil mechanics methods present similar values, the comparison of these bearing capacity values with geophysical method results present that geophysical methods used in this study generate bearing capacity values far from the Terzaghi and Peck method or the Meyerhof method. Based on the results obtained in this study, it may be concluded that the geophysical methods should not be the primary method to determine the bearing capacity values of the soil sites.

### 4.3. Water Level and Water Content Analysis

Groundwater table and water contents at 192 have also been determined. The maps are created for 1.5 m, 3 m, 4.5 m, 7.5 m, and 15 m. The maps are again generated by using the ArcGis program and with the IDW method.

In the study area, it is found that the groundwater table exists between 3.5 m and 15 m at 29 boring points. The maps prepared in this context is presented in Figure 4.11. It is determined that the groundwater is observed between the vicinity of the City Cemetery, Orduzu Pond and Çamurlu, between Upper Çöşnük and Tandoğan, and around Kiltepe.

Water contents in the region at 1.5m, 3m, 4.5m, 7.5m, and 15 m have been determined and presented in Figures 4.12-16, respectively. Throughout the study area at 1.5 m, the water contents have been observed that 14% of the study area has between 0-10, 37% has between 11-20, 34% has between 21-30, and 15% has between %31-37. When we compare these values at 15m, we found 35% of the study area has between 0-10, 39% has between 11-20, 22% has between 21-30, 4% has between %31-37. The comparison of the maps presents light changes overall in the region.

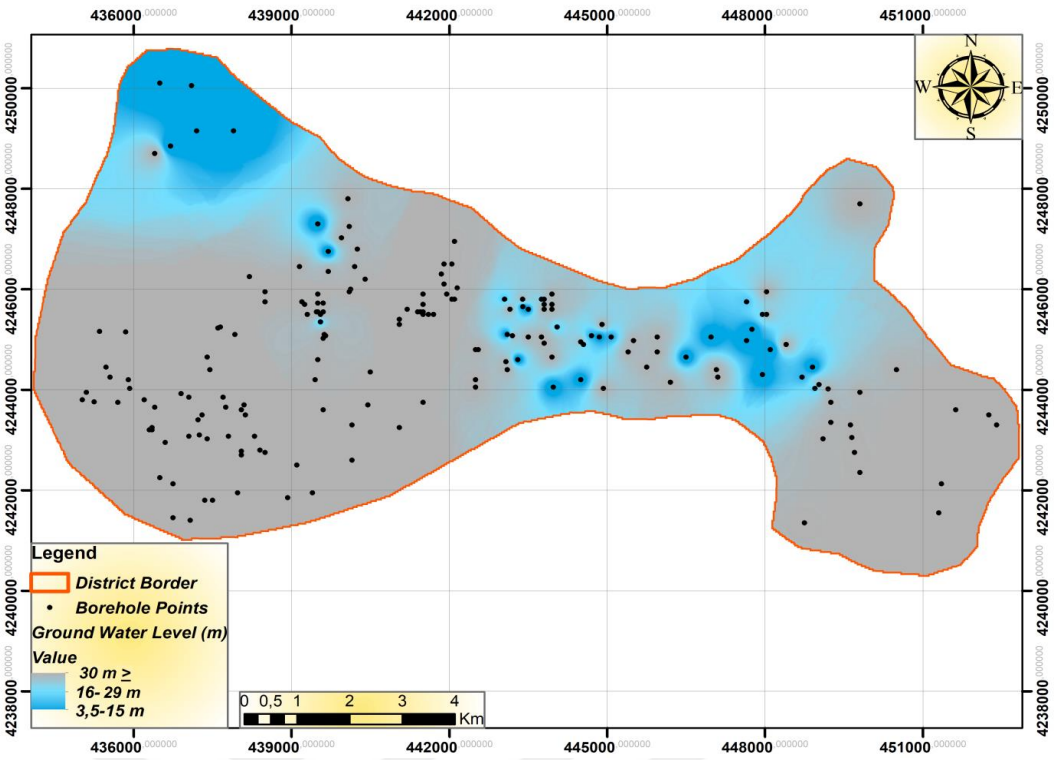


**Figure 4.11.** Map of ground water level

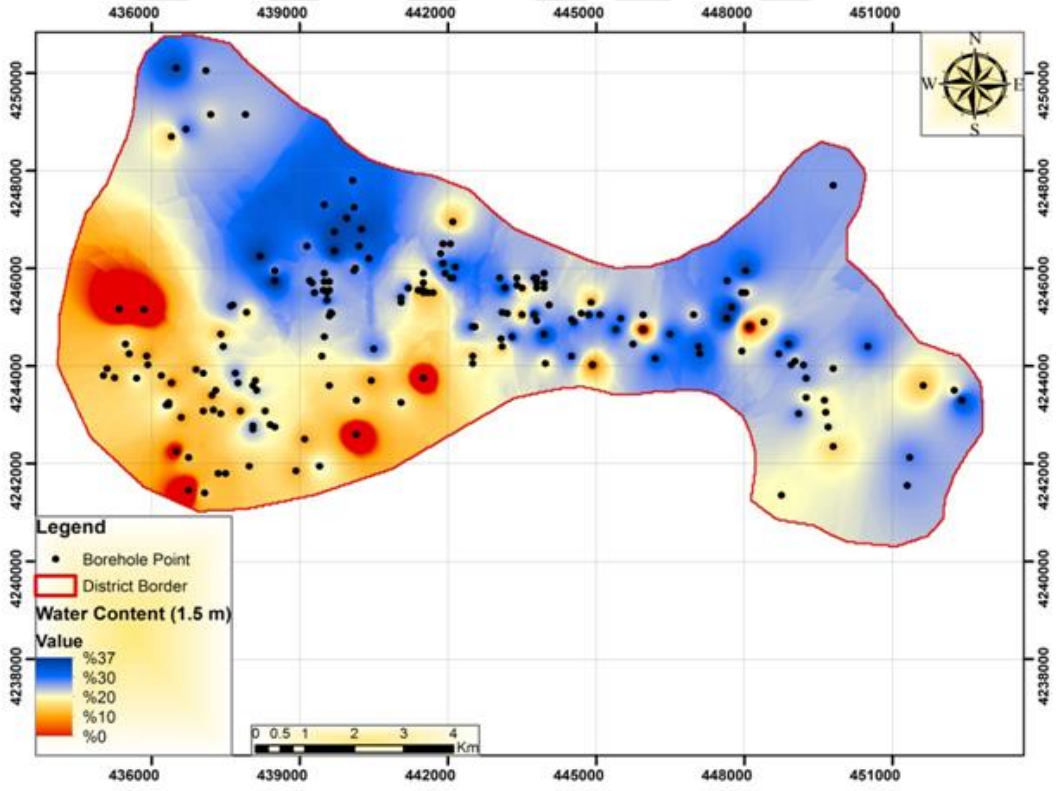


**Figure 4.12.** Water content map according to 1.5 m depth

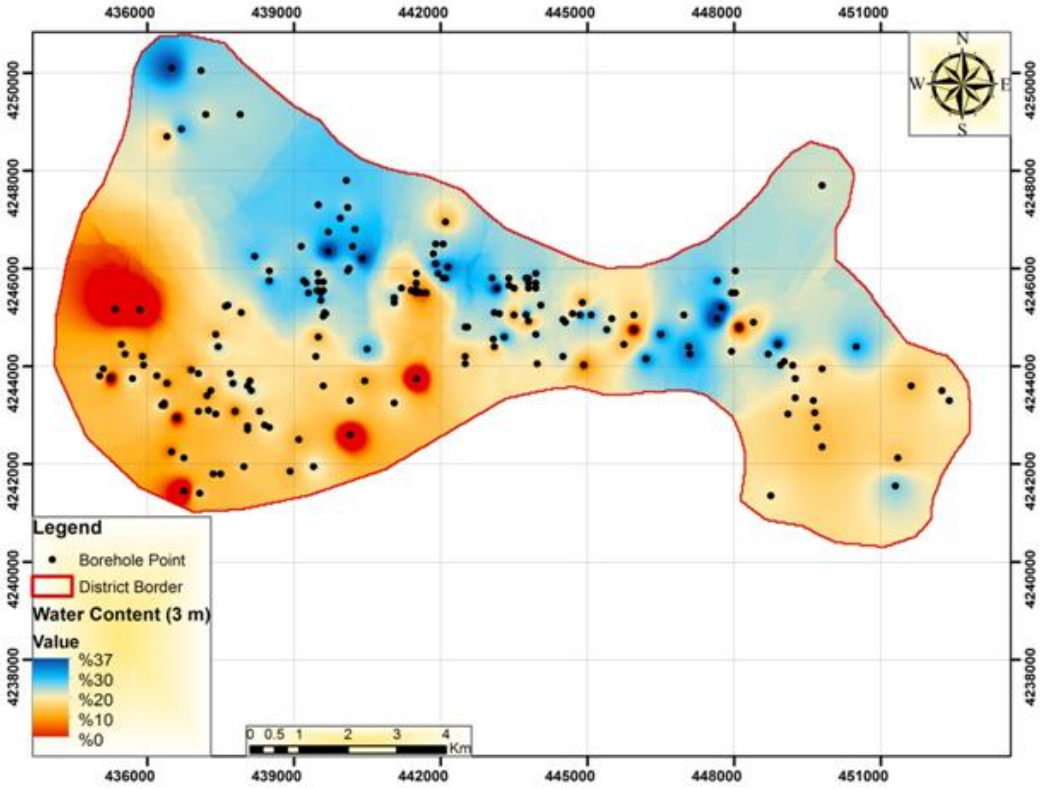


**Figure 4.13.** Water content map according to 3 m depth

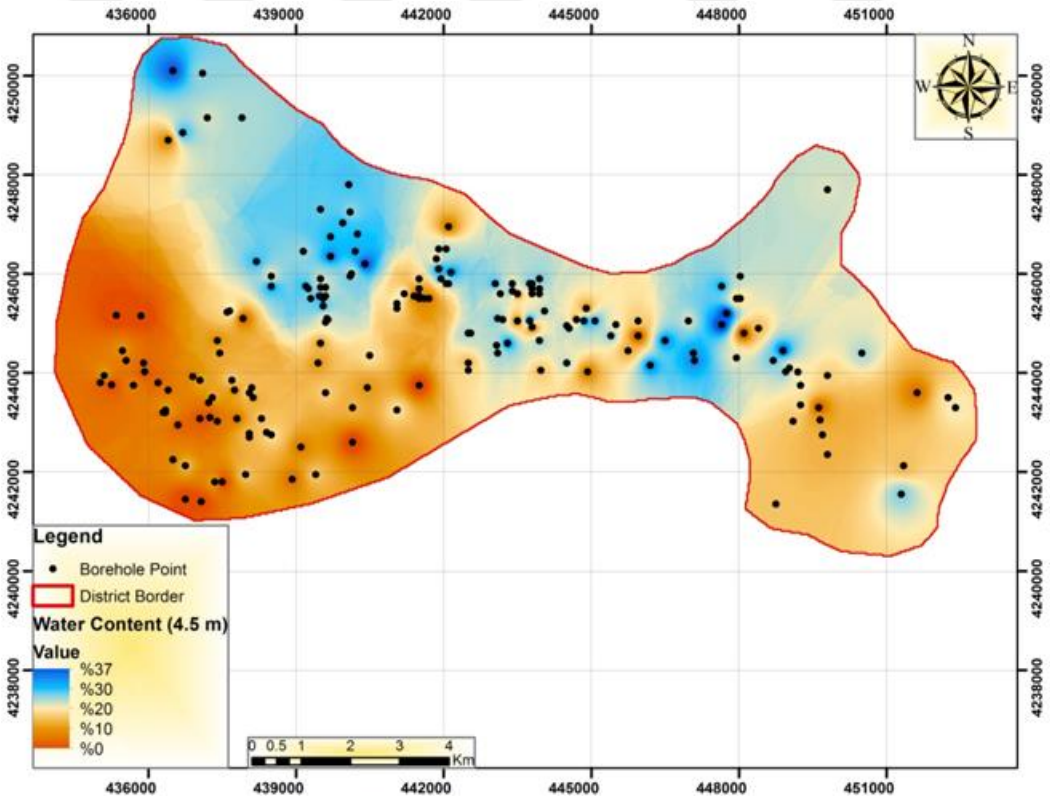


**Figure 4.14.** Water content map according to 4.5 m depth

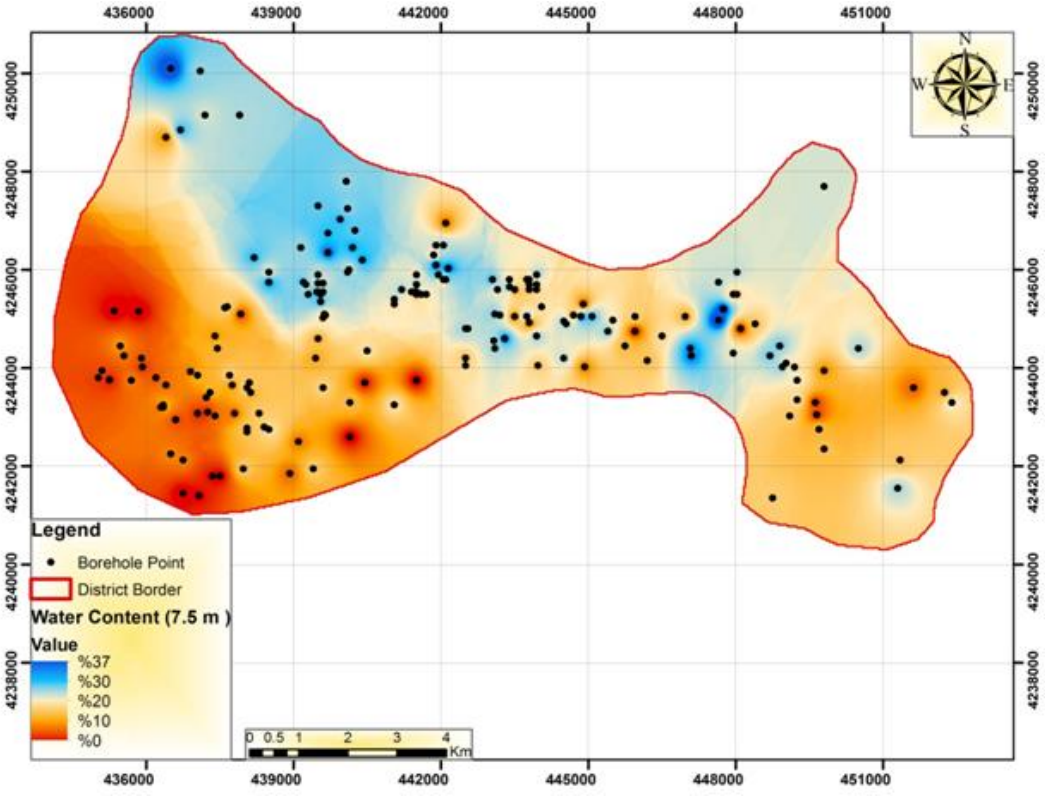


**Figure 4.15.** Water content map according to 7.5 m depth

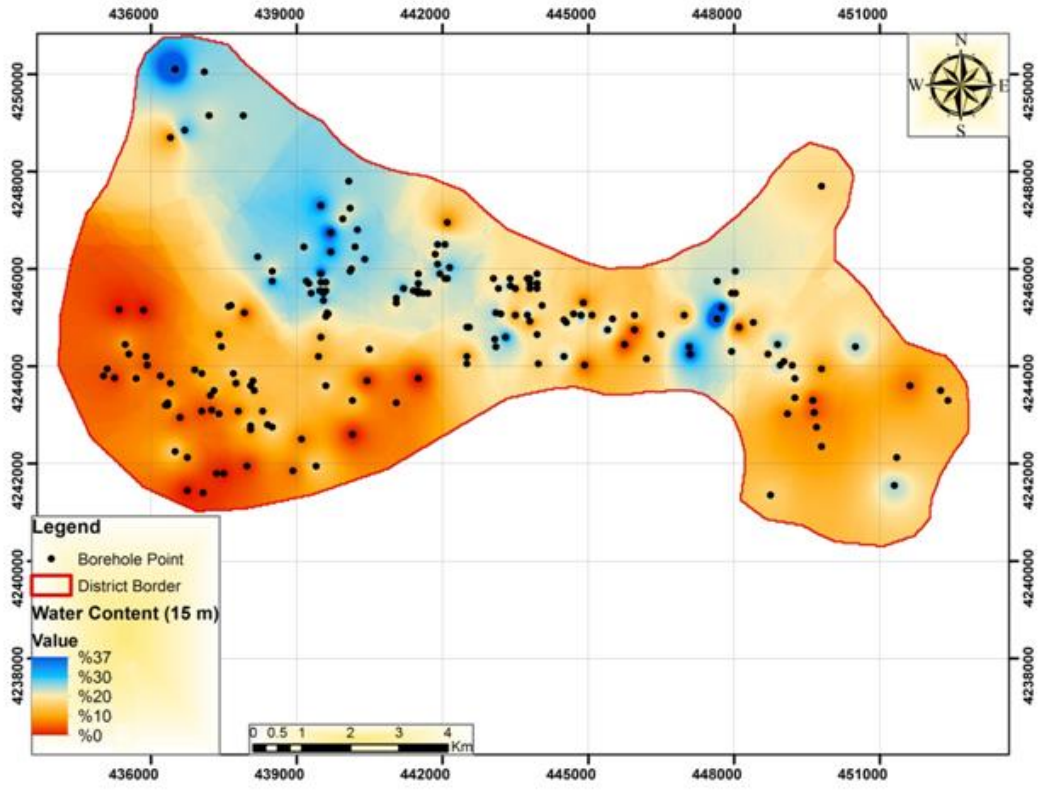


**Figure 4.16.** Water content map according to 15 m depth

Figure 4.17 presents the water contents distribution at 1.5m, 3m, 4.5m, 7.5m, and 15m depths as a comparison plot. The water content values are classified as % 0-10, % 11-20, % 21-30, % 31-37. It is seen that 11-20% value is dominant in the study area.

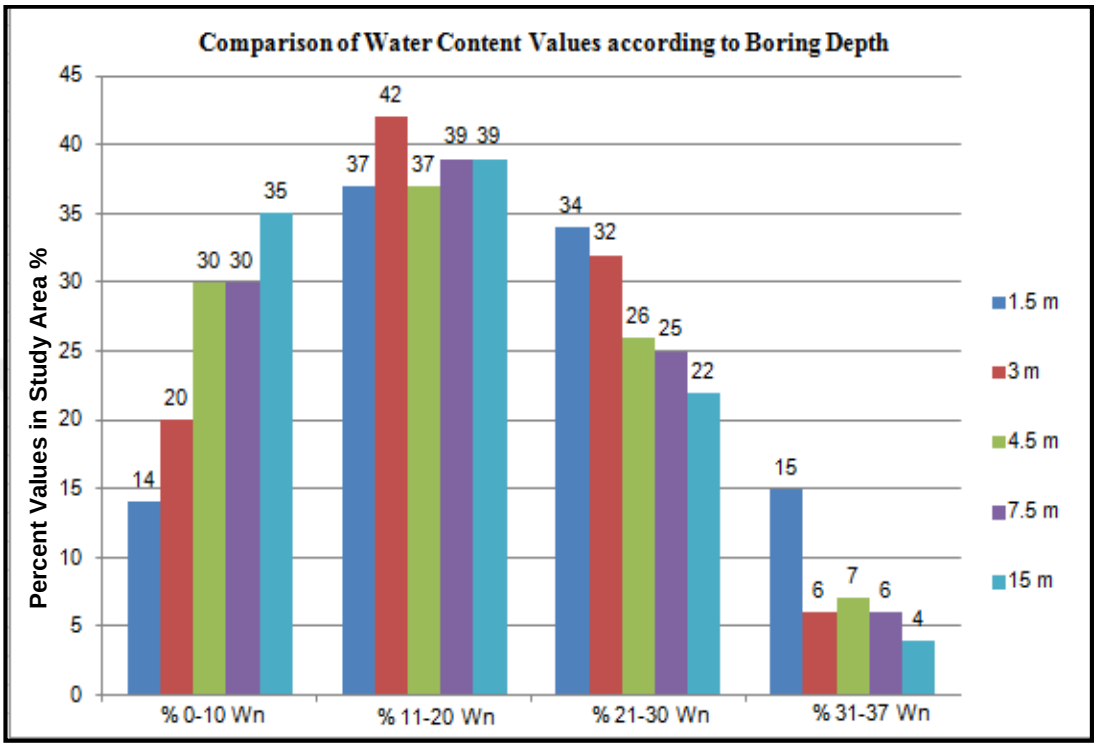


**Figure 4.17.** Comparison of water content values according to boring depths

### 4.4. Liquefaction Analysis

Various methods of analysis related to field and laboratory tests are available in the literature for determining liquefaction sensitivity. Field tests are widely used in researching the potential for liquefaction because lab-based tests are long-running and costly. The methods based on the Standard Penetration Test (SPT) are the most common of these field tests and widely used for liquefaction analysis (Şen, 2004).

The SPT blow numbers presented above obtained from 192 boring points in the field are used to determine liquefaction sensitivity. In the study area, the maps are created for depths of 1.5m, 3m, 4.5m, 7.5m, and 15m to see the distribution of liquefaction potential up to 15 m from the surface and its change with depth. Liquefaction risk maps in this study basically are based on the factor of safety (FS) against liquefaction analysis given in the method proposed by Youd and Idriss (2001). In the maps, if FS is found equal and lower than one (FS $\leq$1), it means that there is a liquefaction

risk. However, if the FS is found bigger than one ( FS> 1), it expresses the region without liquefaction risk.

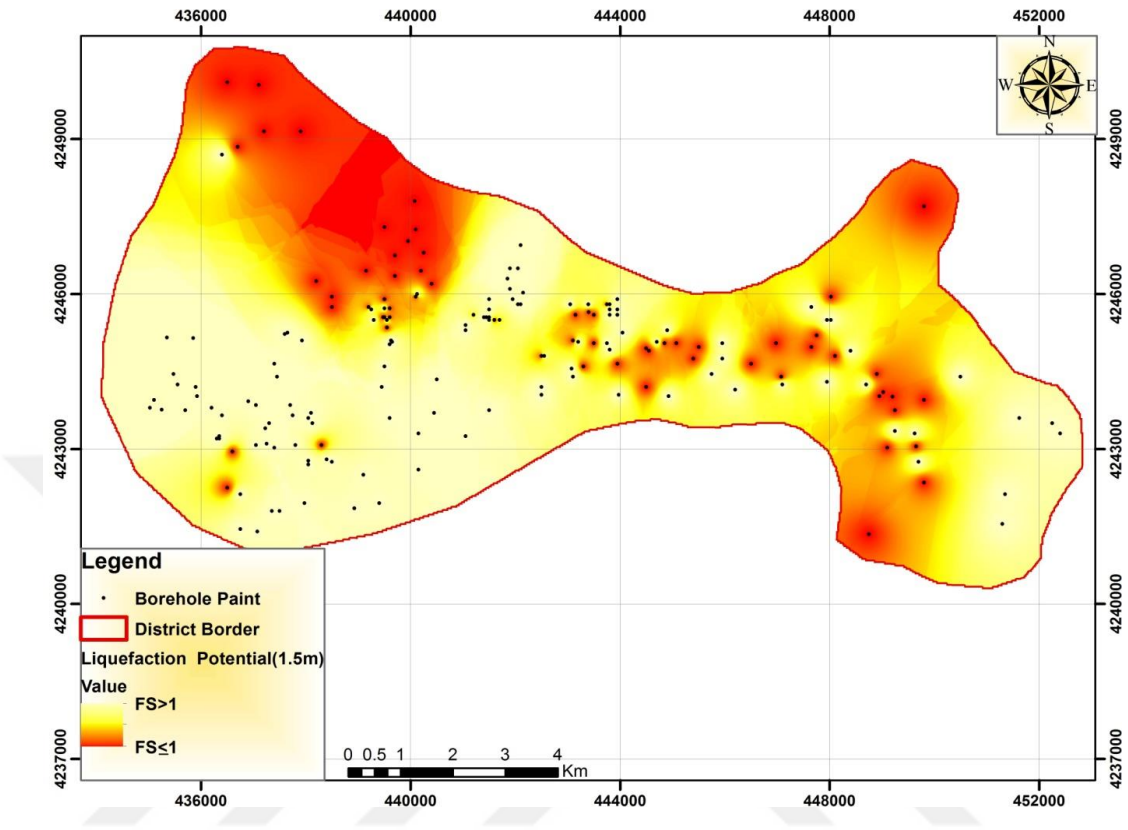


**Figure 4.18.** Liquefaction potential map according to 1.5 m depth

The method proposed by Youd and Idriss (2001) used in this study considers site conditions such as the fine content and water level. Therefore, the local site conditions are taken into account in this study. The liquefaction susceptibility maps are present for the same depths as before which are 1.5 m, 3 m, 4.5 m, 7.5 m, and 15m and, respectively, given in Figures 4.18-22. For the depth of 1.5m, 33% of the study area is found to be under liquefaction risk ( FS $\leq$1 ). The region located in the northwestern part of the study area and confined with the city Cemetery to Yeşiltepe, Kiltepe and Melekbaba as well as around Karaköy and Üzümlü in the southeast and also the region between Orduzu Pond, Çöşnük, and İnönü University are determined as liquefaction susceptible regions (Fig. 4.18). The southwest of the study area, around Yeşiltepe, Karakavak, Aşağıbağlar, Hançukuru and the area in the east of Inonu University are found as liquefaction risk free at this depth, except a few local points.

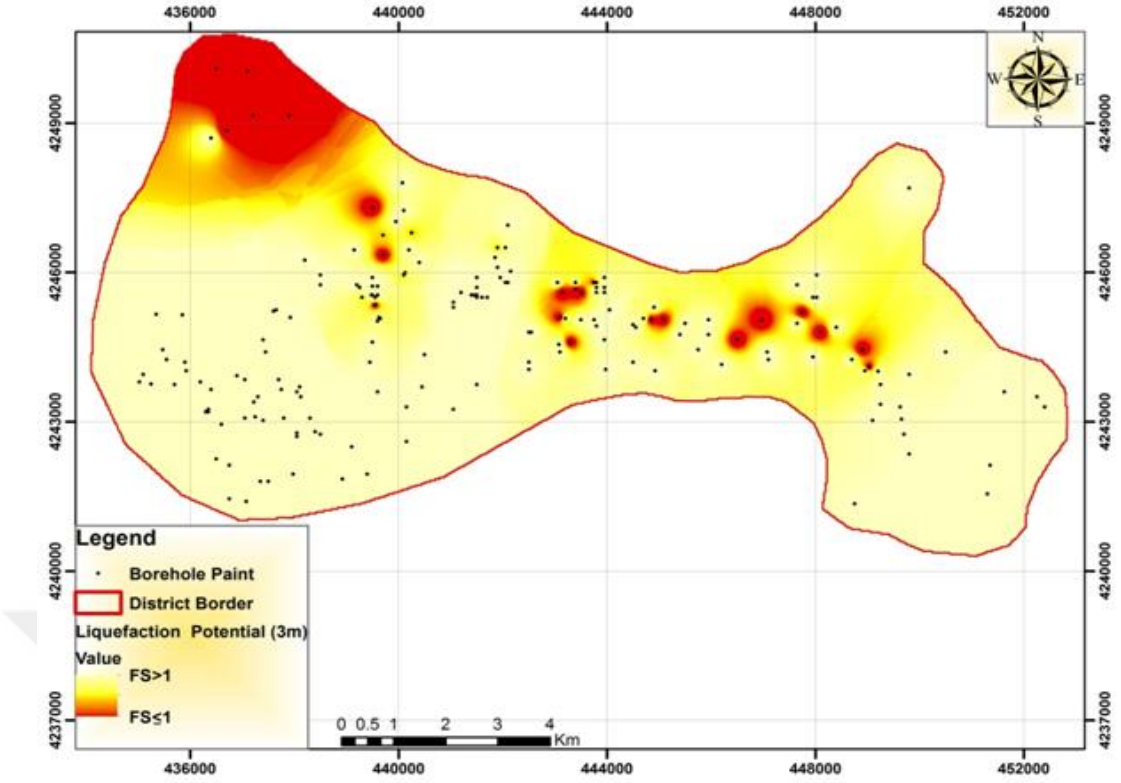


**Figure 4.19.** Liquefaction potential map according to 3 m depth

When we look at 3m, the total areas of liquefaction susceptible regions seems to decrease. Overall, 12% of the study area is a found under liquefaction risk. The region with liquefaction riskconfined by the City Cemetery, Kiltepe Tandoğan, Orduzu Pond, and Üzumlu provicences in the northwestern part of the study area is smaller. The southwest of the study area, Yeşiltepe, Karakavak, Aşağıbağlar, Hançukuru and in the area in the east of Inonu University is now totally free of liquefaction risk.

The same regions at rest of the depths with some local point all over the region are found to have liquefaction risk. Overall risk of the region can be summarized as 13% of the study area at 4.5m, 15% at 7.5m and 9% at 15m are under liquefaction risk.

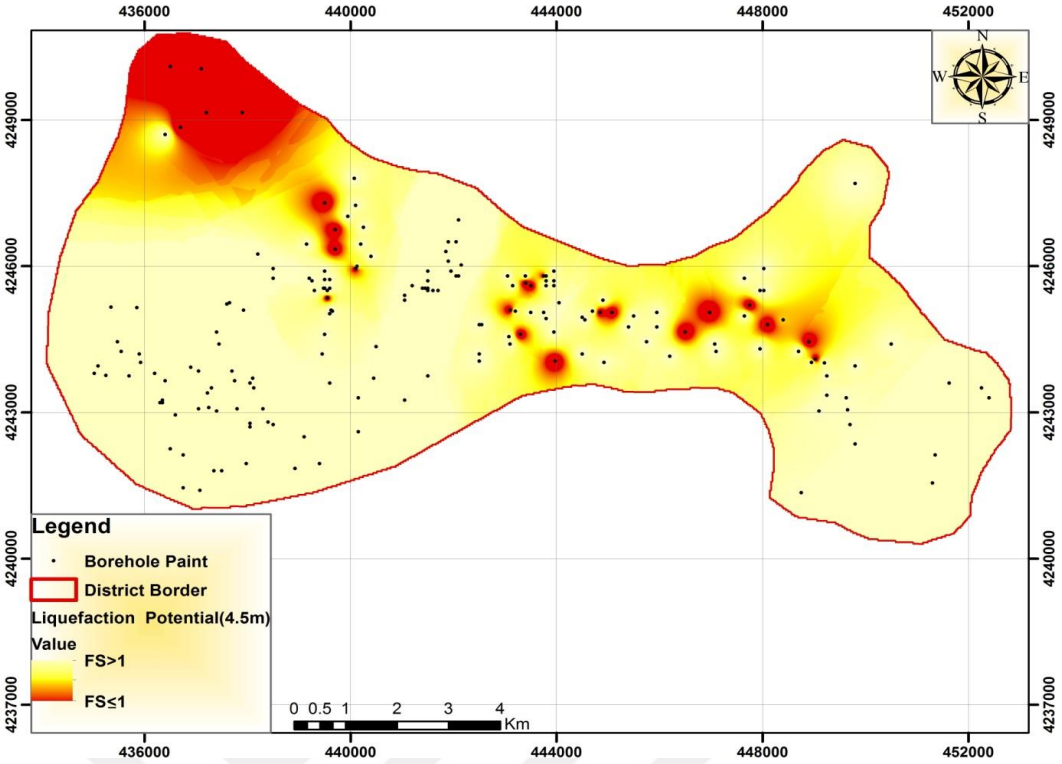


**Figure 4.20.** Liquefaction potential map according to 4.5 m depth

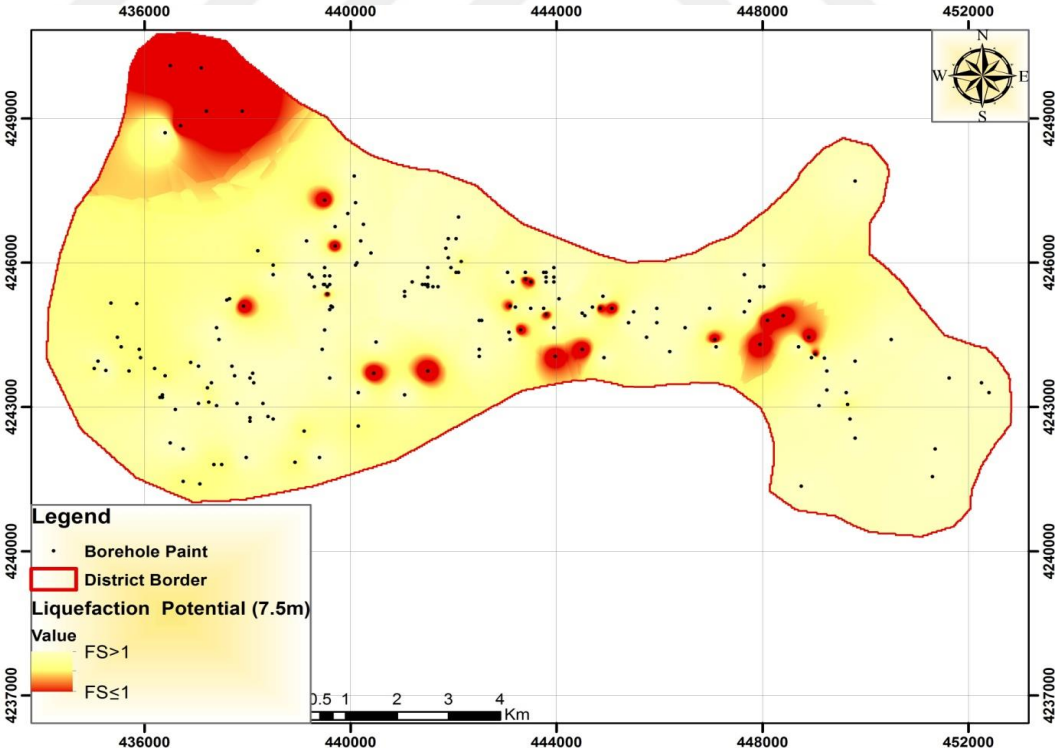


**Figure 4.21.** Liquefaction potential map according to 7.5 m depth

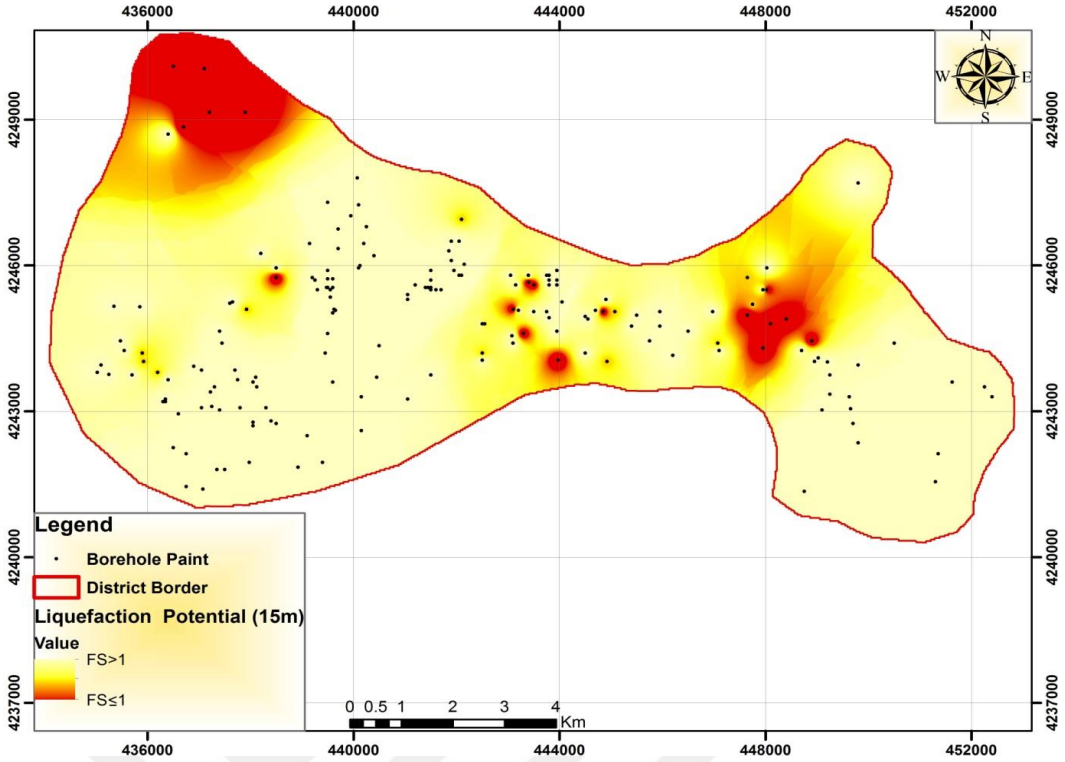


**Figure 4.22.** Liquefaction potential map according to 15 m depth

When the liquefaction risk maps are compared to the groundwater table, SPT, and bearing capacity maps, it can be easily said that they point out the approximately same locations in the region, which can be also considered as a cross-check of the results and the data obtained from boring holes. The model earthquake used in the analyses has a magnitude of 7.5 M with 0.4 peak ground acceleration is used since the region is located in the first-degree seismic zone by the Turkish seismic code. The liquefaction susceptibility of the entire region has been investigated in this study at different depths up to 15m from the top soil surface. If we ignore the first 1.5m layer thickness of the soil profile, thinking that any construction will place the foundation below this depth (frost line) or at least this level, we can consider the highest percentage of the liquefaction risk as the risk of the region. The main reasoning behind this is that once liquefaction occurs, independent of the dept, we can classify that site as liquefied.

Within the scope of the conducted study, a comparison chart showing the distribution of FS> 1 (There is no liquefaction risk) and FS $\leq$1 (There is a liquefaction risk) in the study area as a percentage for liquefaction risk at 1.5m, 3m, 4.5m, 7.5m, and 15m is presented in Figure 4.23.

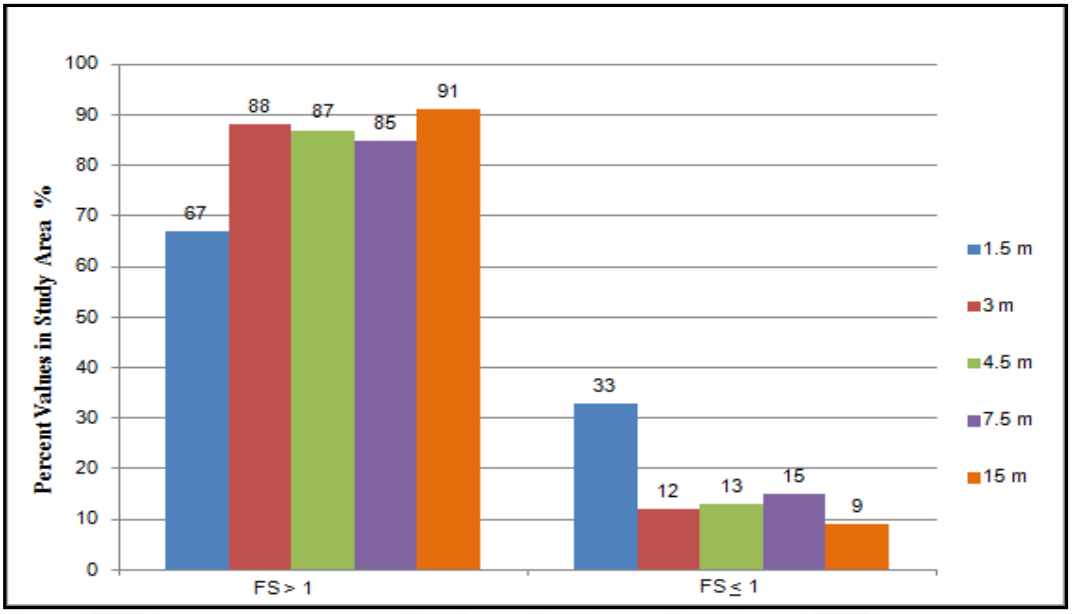


**Figure 4.23.** Comparison of liquefaction values according to boring depth

### 4.5. Shear Wave Velocity Calculation Analysis

The shear wave velocity is an important indicator for the soil stiffness when investigating the dynamic behavior of the soils. It is determined by in-situ experiments or calculated depending on other parameters such as SPT-N number. In this study, the shear wave velocities obtained from the in-situ tests are compared with the calculated values based on SPT-N field tests for depths of 1.5m, 3m, 4.5m, 7.5m, and 15 m. Moreover, a map of average shear wave velocity in the top 30 m soil is obtained. This data is used in some soil classification systems and also zoning in earthquake hazard maps.

The shear wave velocity values based on SPT-N values and obtained by Ohba and Trauma (1970), Seed and Idriss (1981), Imai and Yoshimura (1970), Iyisan (1996), Hasancelebi and Ulusay (2007), Tsiambos and Sabatakakis (2011) are compared and presented in Figs 4.24,4.26, 4.28, 4.30, and 4.32. These methods are compared with the seismic measurements in Figs 4.25, 4.27, 4.29, 4.31, and 4.33.

Based on the comparisons for the range of SPT-N values from 0 to 20, the best matches are obtained in order by Imai and Yoshimura (1970), Ohba and Trauma (1970), Hasancelebi and Ulusay (2007), Iyisan (1996), Seed and Idriss (1981), Tsiambos and Sabatakakis (2011). However, when it is based on the SPT-N values of 21-50, the order will be Imai and Yoshimura (1970), Ohba and Trauma (1970),

Hasancelebi and Ulusay (2007), Iyisan (1996), Tsiambos and Sabatakakis (2011), Seed and Idriss (1981).

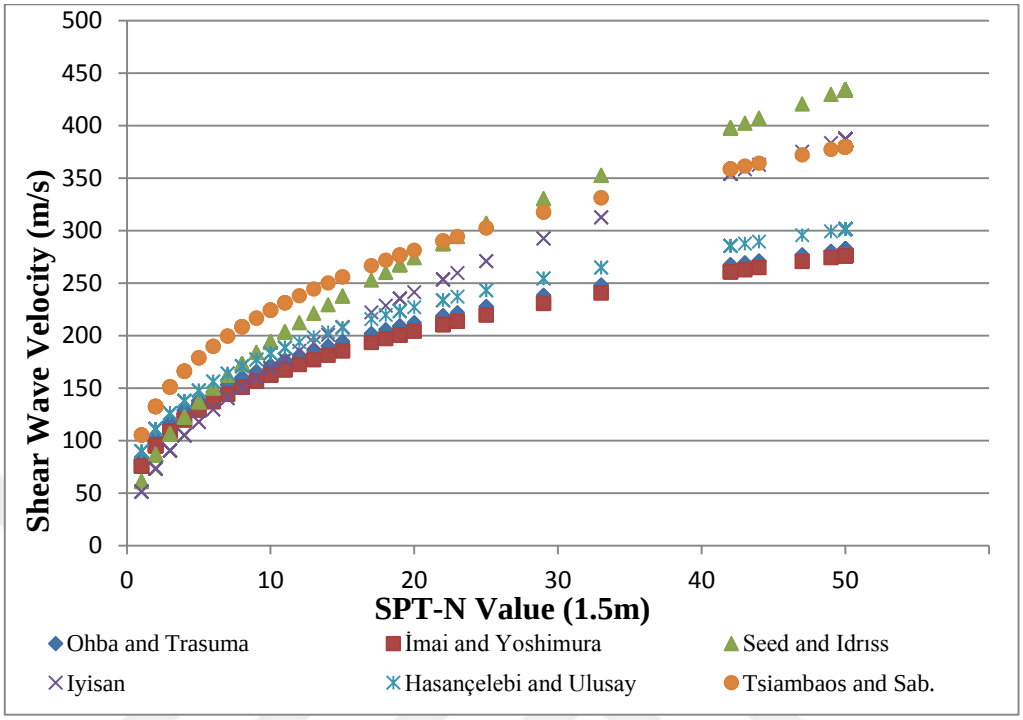


**Figure 4.24.** Comparison comparison graph of shear wave velocity calculated results according to SPT-N value 1.5 m depth

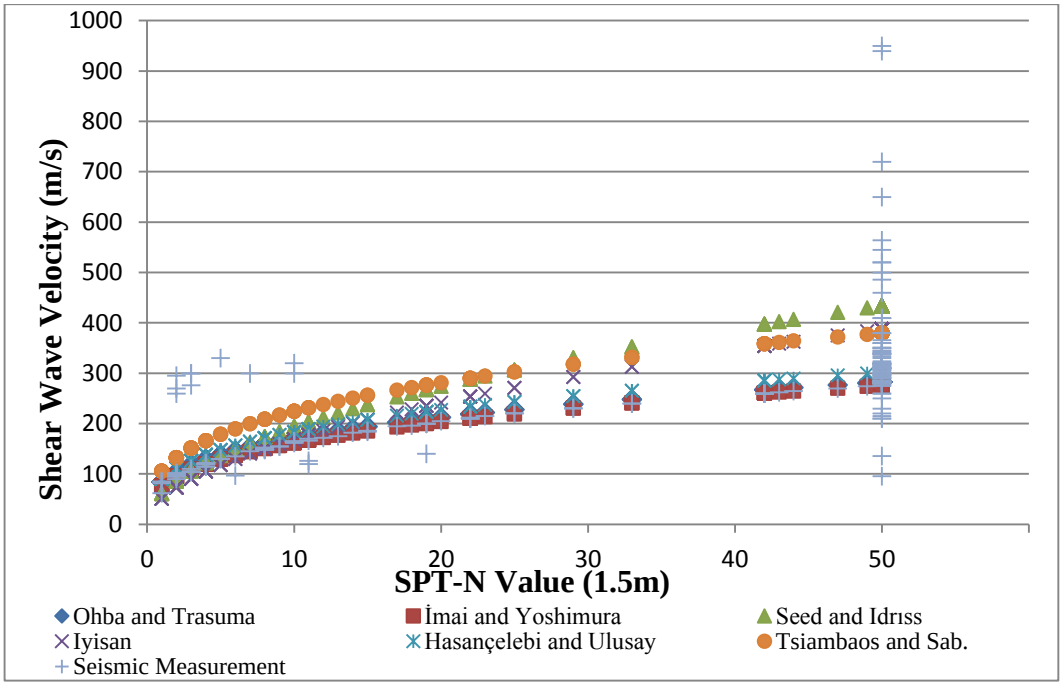


**Figure 4.25.** Comparison graph of shear wave velocity according to seismic measurements and SPT-N value 1.5m depth

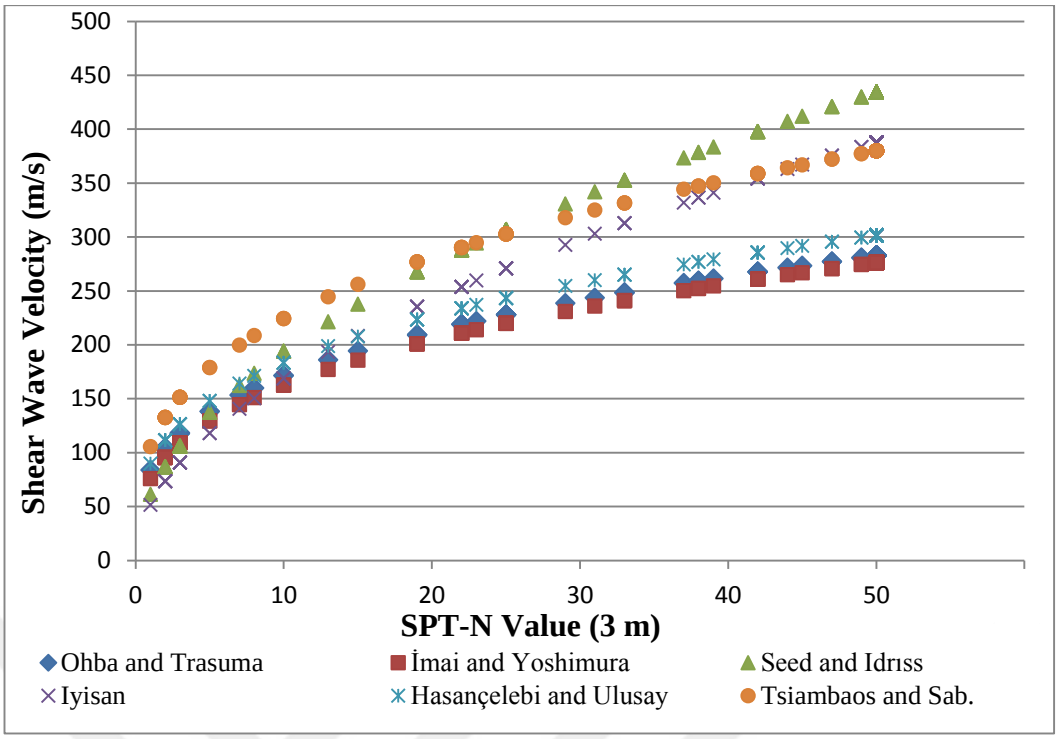


**Figure 4.26.** Comparison comparison graph of shear wave velocity calculated results according to SPT-N value 3 m depth

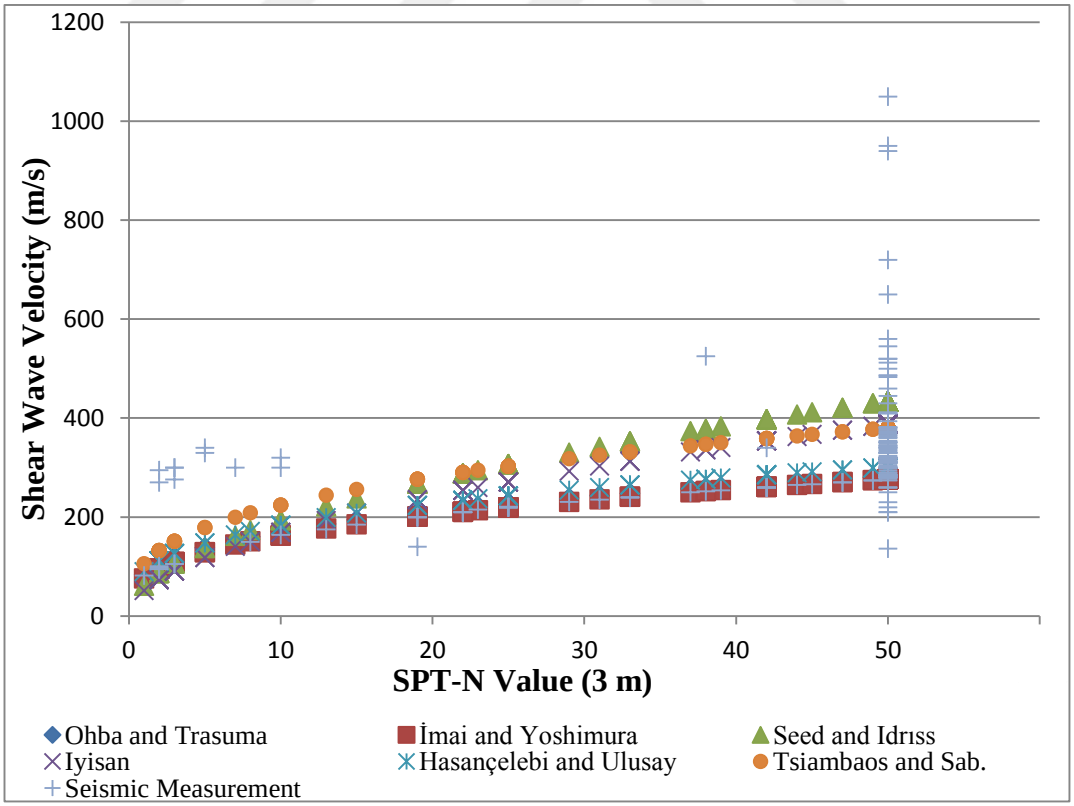


**Figure 4.27.** Comparison graph of shear wave velocity according to seismic measurements and SPT-N value 3 m depth

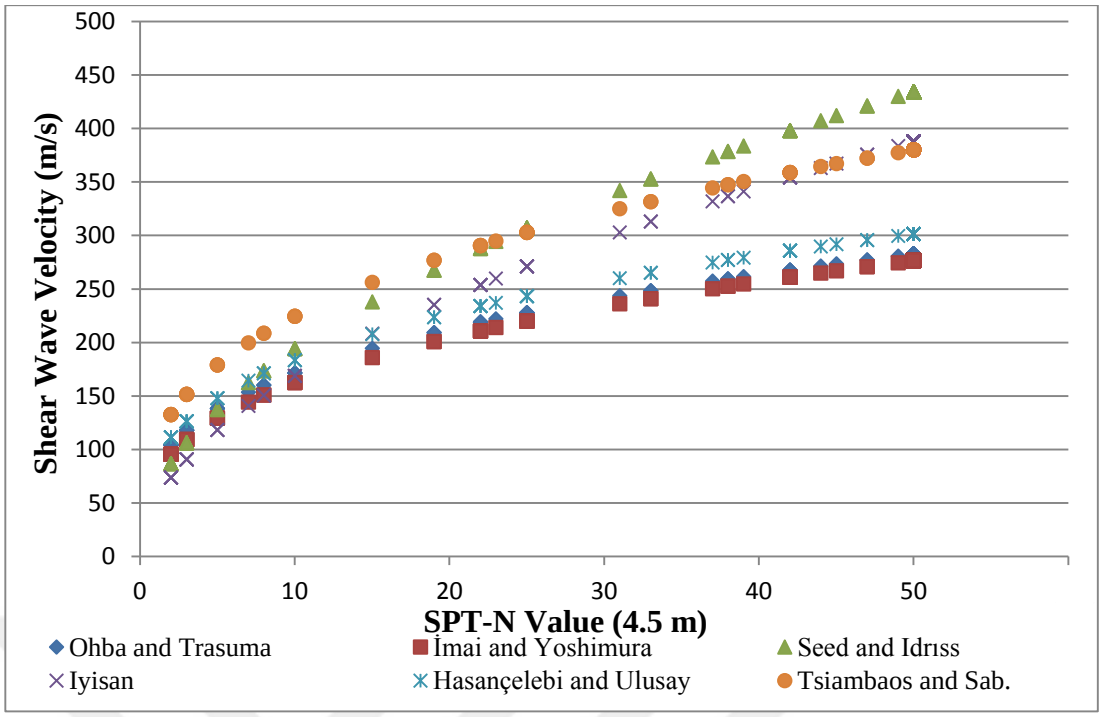


**Figure 4.28.** Comparison graph of shear wave velocity calculated results according to SPT-N value 4.5 m depth

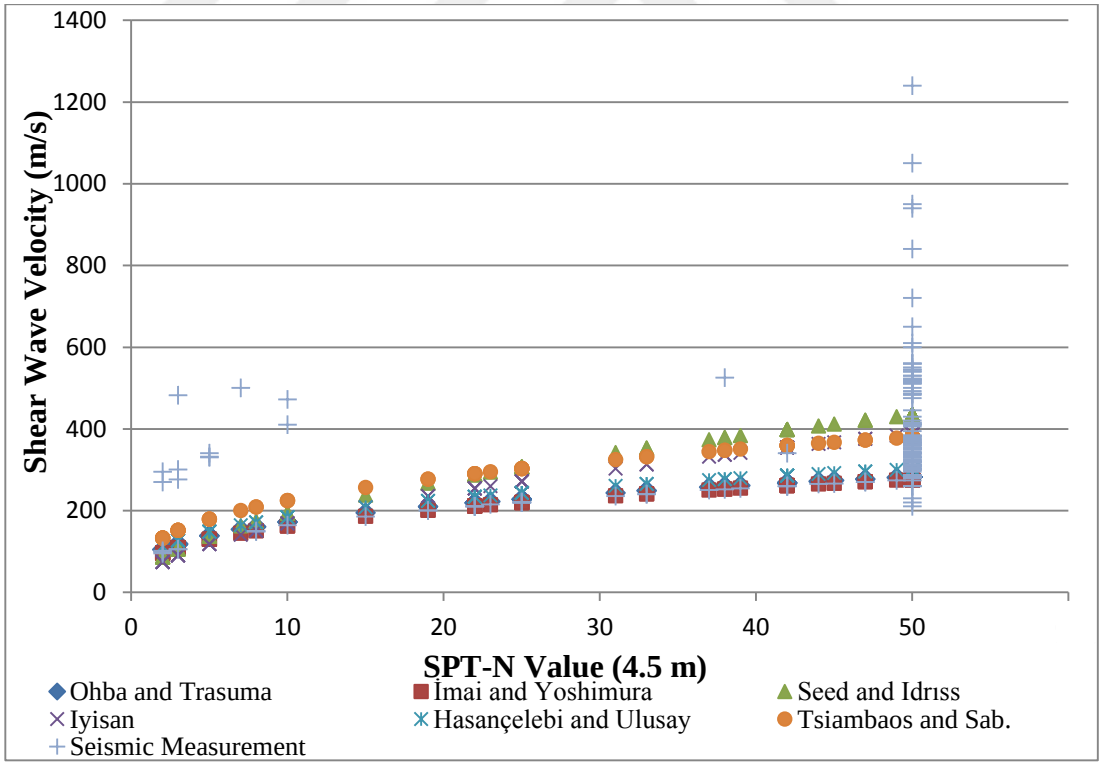


**Figure 4.29.** Comparison graph of shear wave velocity according to seismic measurements and SPT-N value 4.5m depth

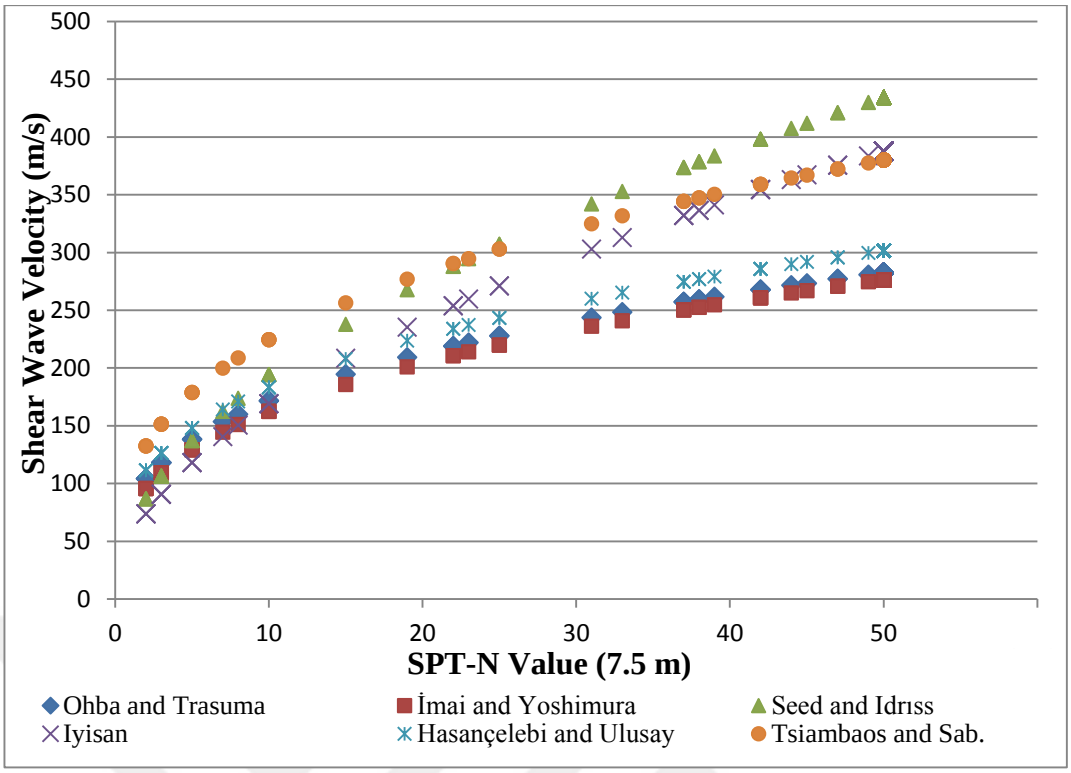


**Figure 4.30.** Comparison graph of shear wave velocity calculated results according to SPT-N value 7.5 m depth

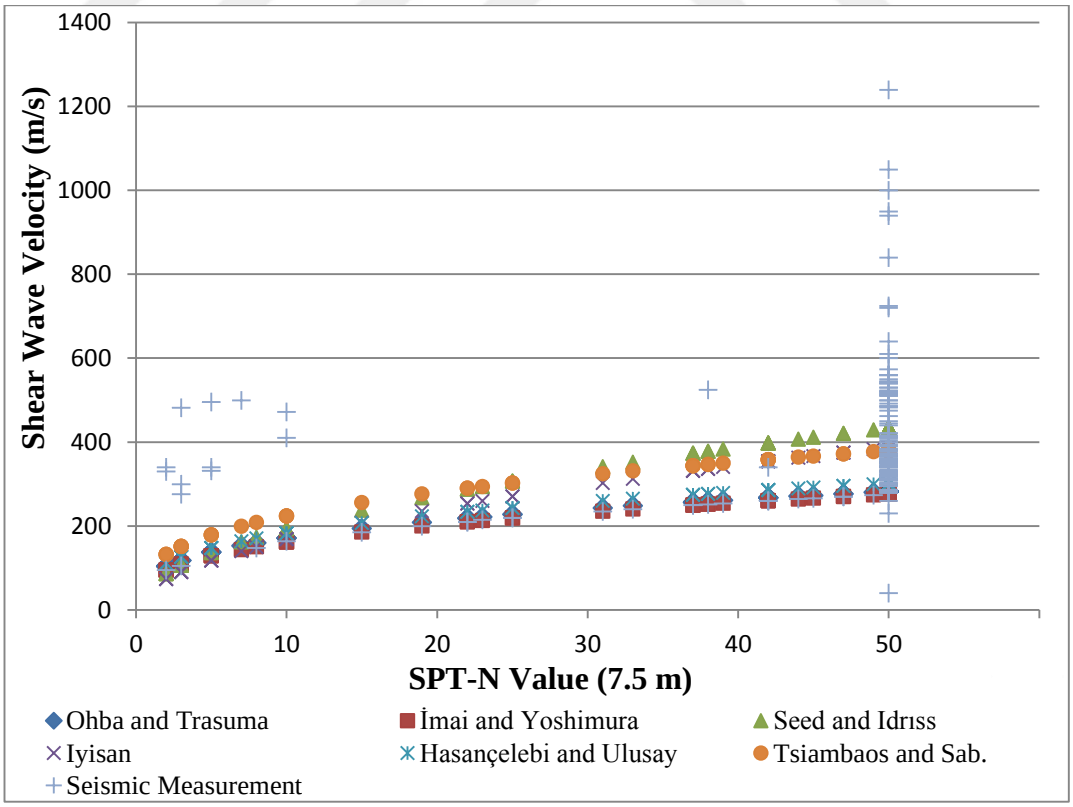


**Figure 4.31.** Comparison graph of shear wave velocity according to seismic measurements and SPT-N value 7.5m depth

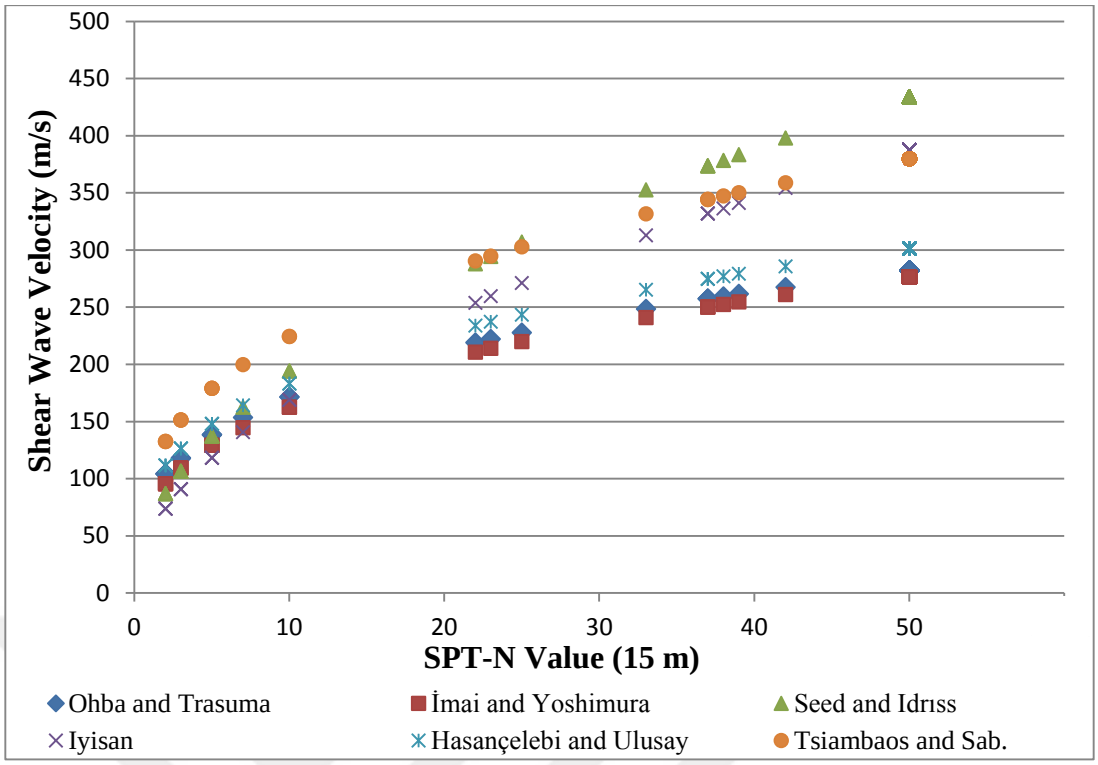


**Figure 4.32.** Comparison graph of shear wave velocity calculated results according to SPT-N value 15 m depth

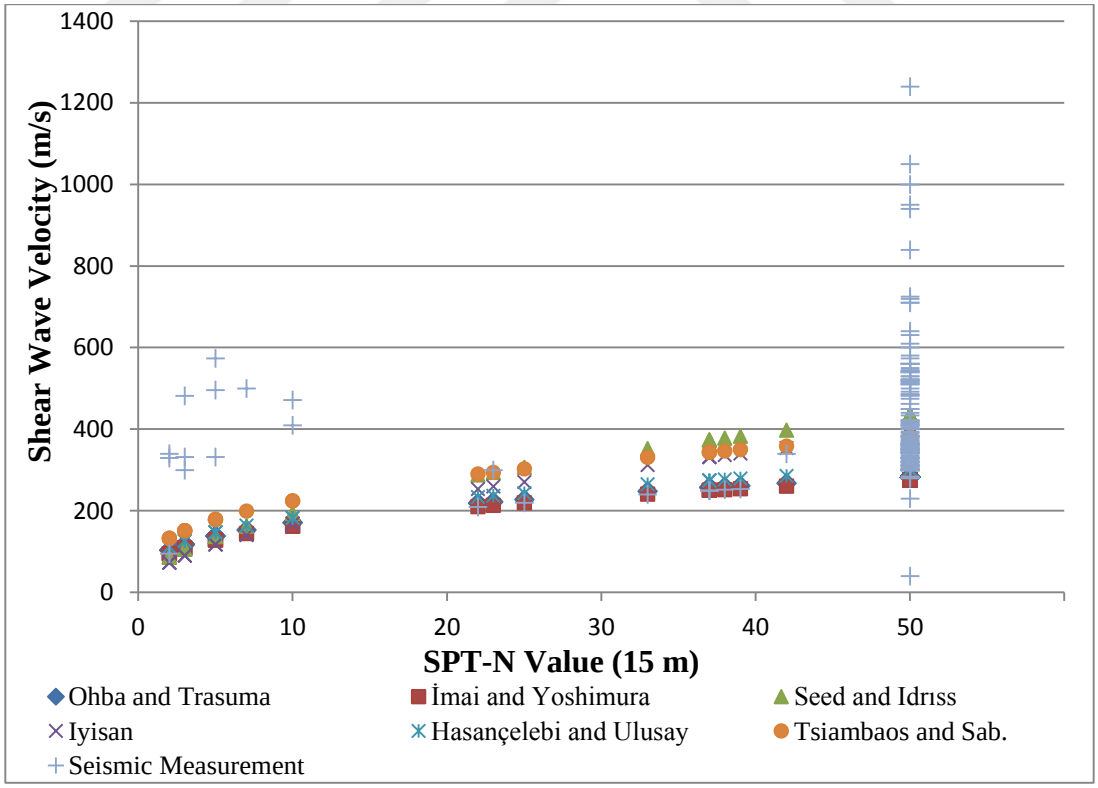


**Figure 4.33.** Comparison graph of shear wave velocity according to seismic measurements and SPT-N value 15m depth

The figures present the differences between the seismic method results and SPT-N based methods, especially when we consider the SPT-N range between 0-10. The SPT-N values 50 and higher is not expected to match with the seismic method results since when the blow count N is equal or greater than 50, this is recorded as N=50 and bigger N values are ignored in the practice. When we consider SPT-N range 10-50, it is observed that the seismic method results match with the results of the SPT-N based methods.

### 4.5.1. Analysis of Shear Wave Velocity Calculation of the Top 30 m

The average shear wave velocity of the top 30 m soil is employed in some soil classification systems and earthquake hazard analysis works. This study makes use of the data obtained by field measurements (Seismic Methods) to generate the average shear wave velocity map of the region. Maps are generated by using the ArcGis program and with the IDW method. A range of shear wave velocities changing from 104 m / s to 1950 m / s has been obtained in the analysis.

Based on the seismic method, the average shear wave velocity obtained for the upper 30 m throughout the study area is found as 1% of the study area value Vs>1500 m/s, 3% of study area value 760< Vs < 1500 m/s, 52% of study area value 360< Vs < 760 m/s, 43% of study area value 180< Vs < 360 m/s, 1% of study area value Vs< 180 m/s is determined. The map prepared in this context is presented in Figure 4.34.

In the northwestern part of the study area, Kiltepe, Çavuşoğlu, Melekbaba, Orduzu ponds, Karaköy, and Üzümlü and Çöşnük, the average shear wave velocity of the upper 30 m has been found between 180< Vs < 360 m/s which corresponds to 43% of the study area. The values between 360< Vs < 760 m/s is observed in 52% of the study area. A comparison chart of the values in the study area is also presented in Figure 4.35.

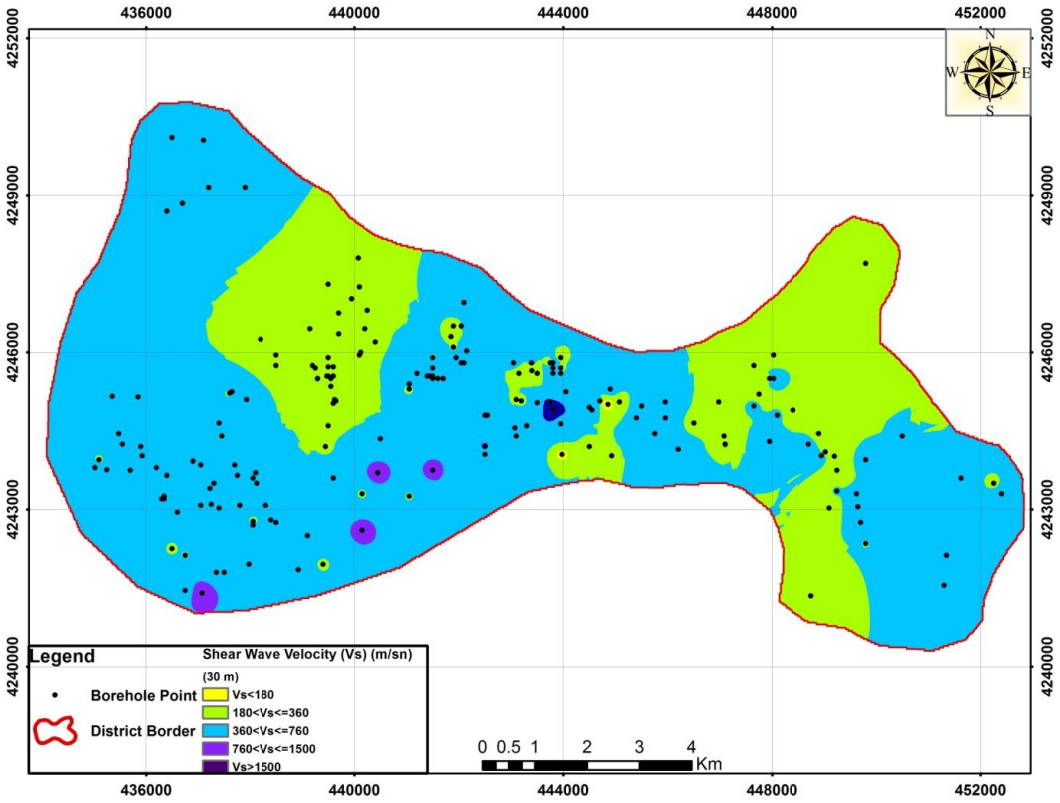


**Figure 4.34.** Shear wave velocity map of the study area according to 30 m depth

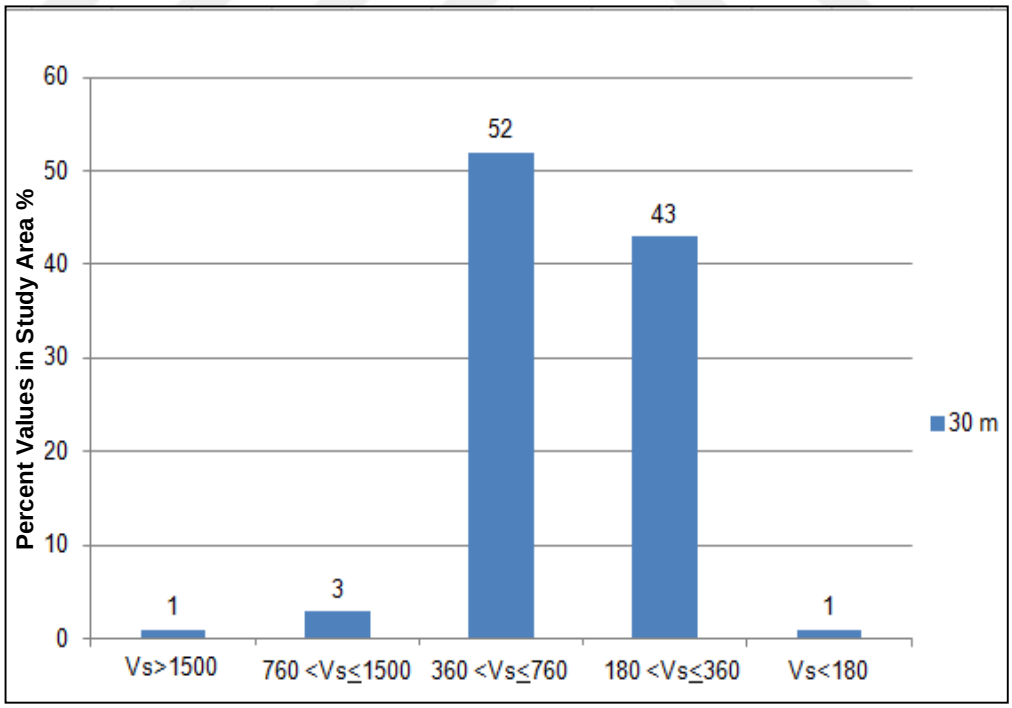


**Figure 4.35.** Distribution of Vs (30m) values in the study area

### 4.6. Soil Classification Analysis According to NEHRP Earthquake Regulation

The soil classification according to NEHRP is based on the average shear wave velocity ($Vs_{30}$) of the upper 30 m soil. The soil classification map of the region based on NEHRP has been prepared and soil classes A, B, C, D, and E throughout the region have been determined.

It is determined that 1% of the study area is A, 3% is B, 52% is C, 43% is D, and 1% is E based on the measurements made in the field. The map prepared in this context is presented in Figure 4.36.

According to the NEHRP soil classification, the northwestern part of the study area, some areas of Kiltepe, Çavuşoğlu, Melekbaba and Orduzu ponds, Karaköy, and Üzümlü and Çöşnük, are classified as the type D soil and it covers 43% of the study area. The soil class C covers 52% of the study area and dominant soil class throughout the region. A, B, E soil classes have been observed in various areas throughout the study area. A comparison chart of the values in the study area is also presented in Figure 4.37.

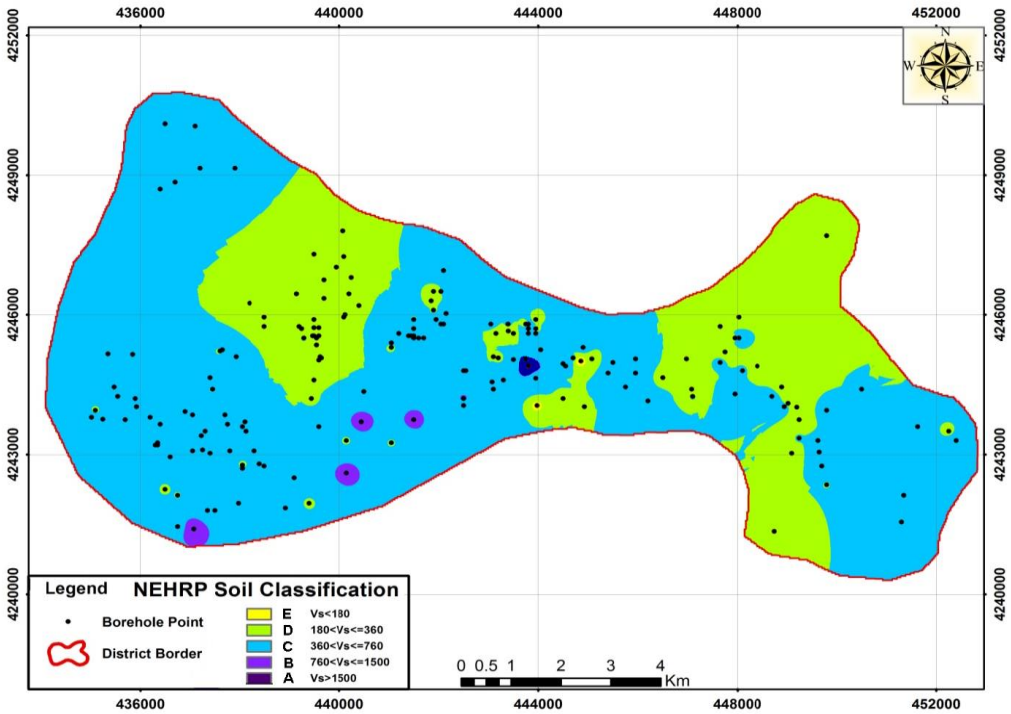


**Figure 4.36.** Soil classification map according to NEHRP

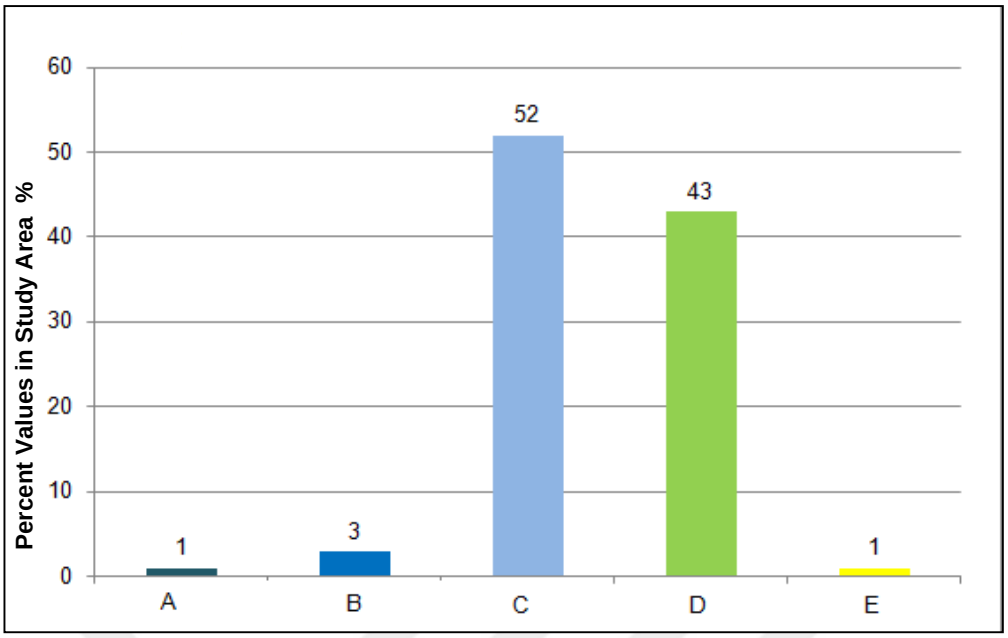


**Figure 4.37.** Distribution of soil classification values in the study area according to NEHRP

## 4.7. Analysis of the Earthquake Hazard Level According to the Soil Amplification Calculation

When planning the urbanization and city expansion in the region, determination of the earthquake effects amplified by the local site conditions is very important to design earthquake resistant structures. The average shear wave velocity of the upper 30 m has been utilized to determine the local soil effect in the study area. Here, we applied the calculations using the relationship proposed by Midorikawa (1987).

The data necessary to determine the soil amplification values are obtained from the 192 boring points in the study area. In the of the study area, the regions are classified as A (high hazard), B (medium hazard), and C (low hazard). In the region, it is determined that 1% of the study area is classified as A (high hazard), 33% B (medium hazard), and 66% C (low hazard). The map prepared in this context is presented in Figure 4.38.

The northwestern part of the study area, some areas of Kiltepe, Çavuşoğlu, Melekbaba and Orduzu ponds, Karaköy, Üzümlü and Çöşnük provinces have been classified as the B (medium hazard) region which corresponds to 33% of the study area. Overall, the region can be classified as mostly C (Low hazard) region which

consists of 66% of the study area. A (high hazard) regions are observed in some areas throughout the study area. A comparison chart of the study area is presented in Figure 4.39.

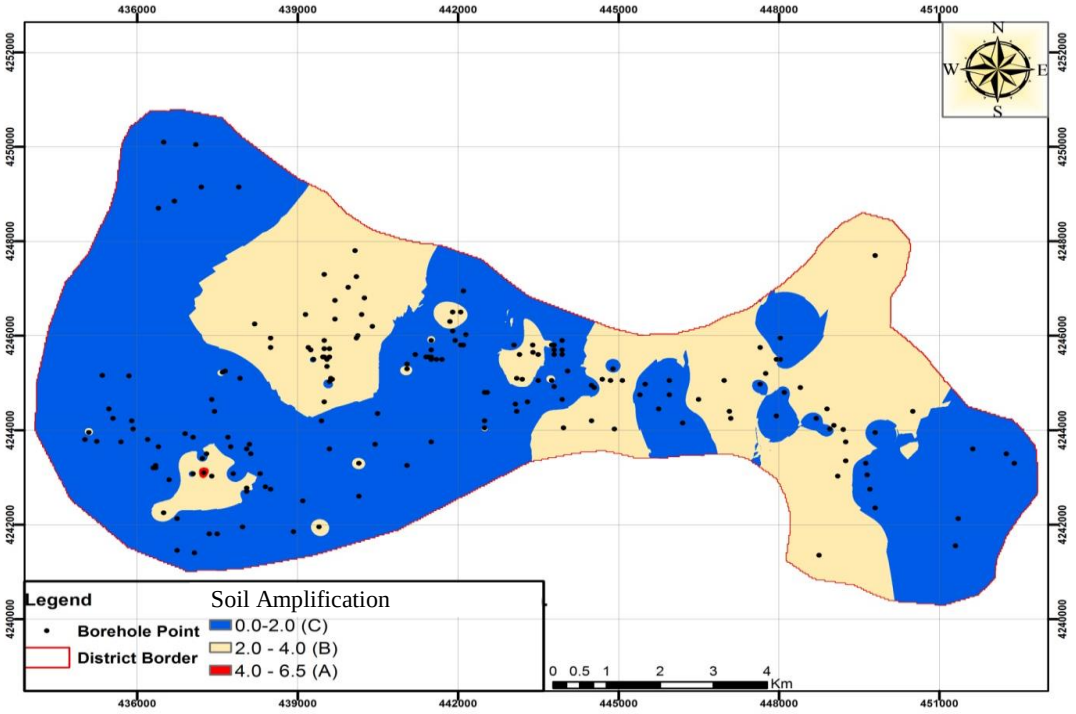


**Figure 4.38.** Hazard map according to soil amplification results

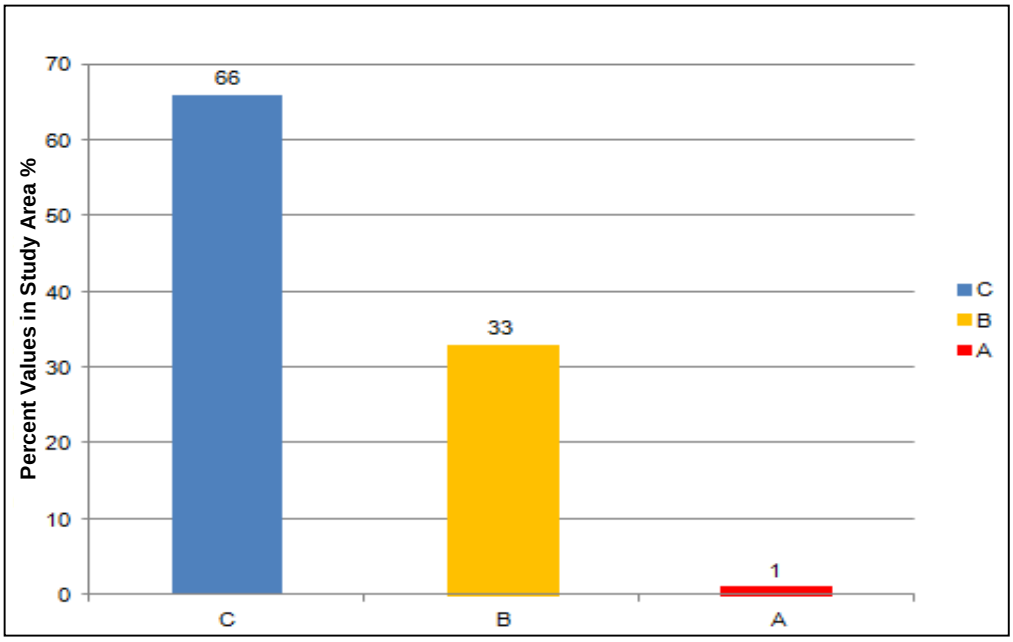


**Figure 4.39.** Distribution of hazard values in the study area according to soil amplification criteria

### 4.8. Local Soil Class Analysis According to Dominant Vibration Period (To)

According to the Turkish Earthquake Code, the soil sites can be classified based on their dominant period. The local soil classes according to the dominant period are Z1: Very dense, Z2: Stiff hard, Z3: Medium stiff, Z4: Loose, soft. The dominant period of the soils have been determined between 0.2 sec and 0,9 sec. This map of the study area is created based on Z1, Z2, Z3, Z4 local soil classes. Our calculations revealed that 13% of the study area is Z1 soil class, 47% is Z2, 26% is Z3, and %14 is Z4. The map prepared in this context is presented in Figure 4.40.

Kiltepe, Çavuşoğlu, Melekbaba and Orduzu ponds, Karaköy, and Üzümlü and Çöşnük, have Z3 and Z4 soil classes which correspond to 40% of the study area, however, Z1 and Z2 soil classes, 60% of the study area, are dominant in the region. A comparison chart according to Z1, Z2, Z3, Z4 local soil class for the study area is also presented in Figure 4.41

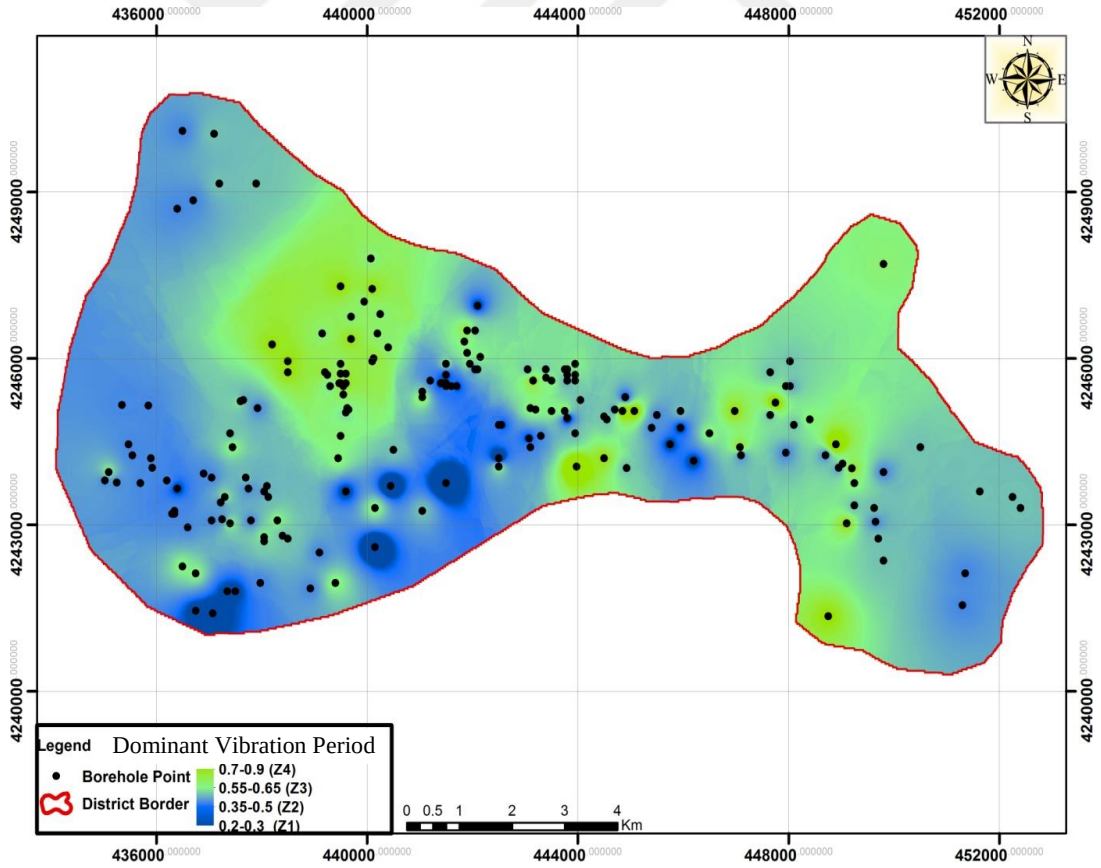


**Figure 4.40.** Soil classes map according to dominant vibration period

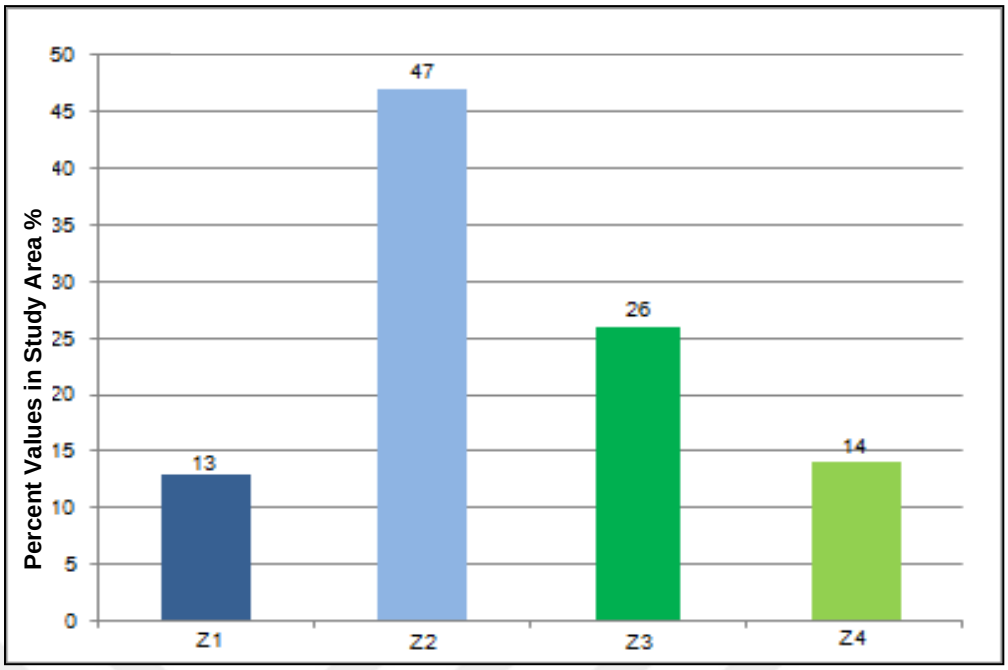


**Figure 4.41.** Distribution of soil classes according to dominant vibration period

### 4.9. Soil Classifications Analysis According to Eurocode 8

In this study, we used the average velocity ($Vs_{30}$) of the shear wave velocity given in Eurocode 8 and ignored other conditions for the comparison purpose. The soil classification consists of A, B, C, and D soil classes. It is determined that 4% of the study area is A, 52% is B, 43% is C, 1% is D soil class. The map prepared in this context is presented in Figure 4.42. A comparison chart of the values in the study area is also presented in Figure 4.43. If we compare the Eurocode8 soil classification based on the ($Vs_{30}$) with NERPH and maps based on the dominant period as well as soil amplification, we observe that they are close to each other.

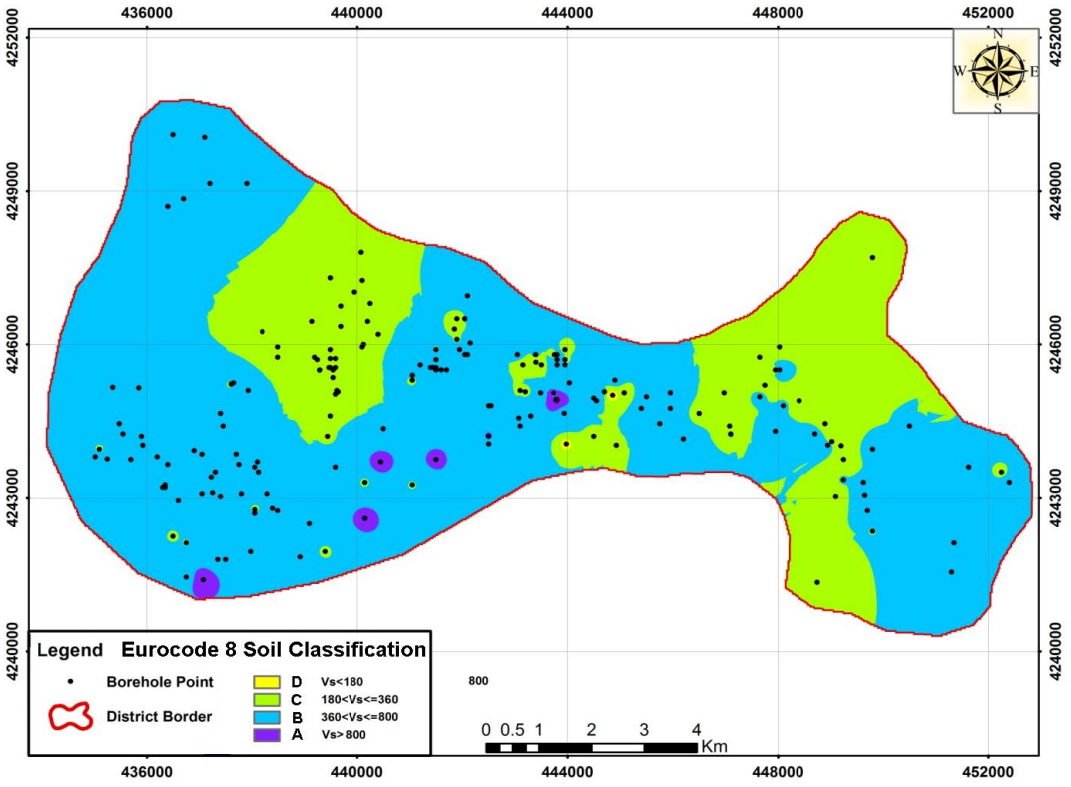


**Figure 4.42.** Soil classification map according to Eurocode 8

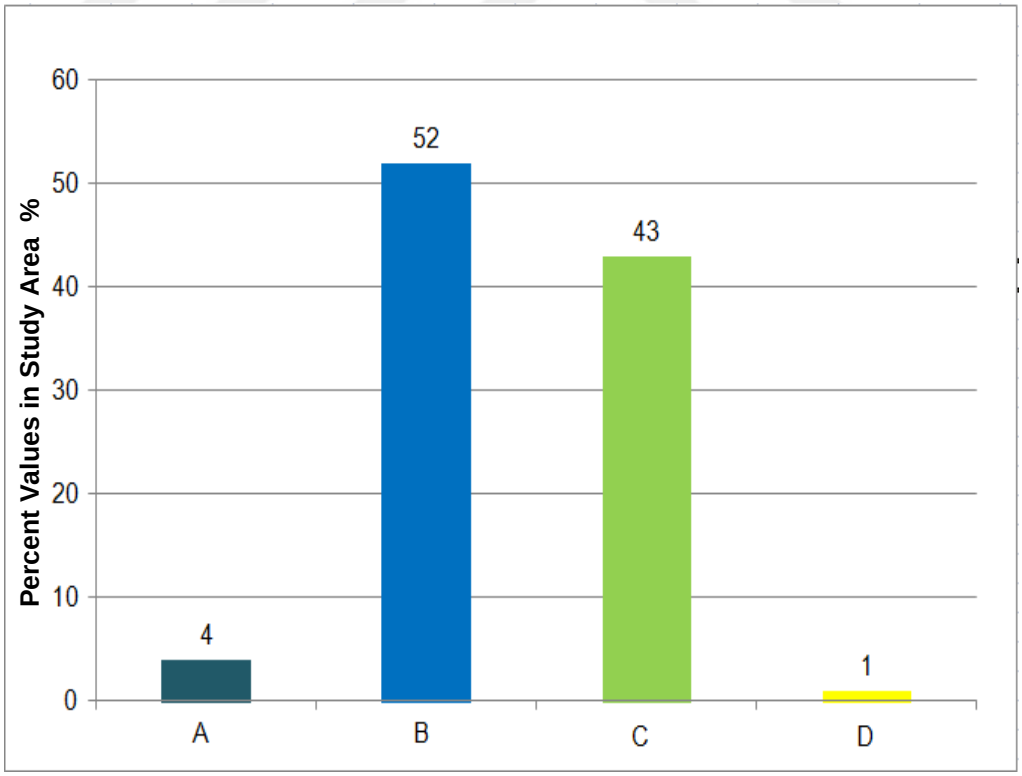


**Figure 4.43.** Distribution of soil classification values in the study area according to Eurocode 8

# CHAPTER 5

# CONCLUSIONS AND RECOMMENDATIONS

In this study, the database is created by using the values obtained from field and laboratory test results in the soil investigation reports in the Malatya Municipality archives. Maps for various depths of the study area within the borders of the Malatya municipality by using the geotechnical data in the database, with GIS-based ArcGis program and about SPT, bearing capacity, liquefaction, shear wave velocity, NEHRP Soil Class, Soil Amplification Risk Factor, Soil Dominant Vibration Period, local soil class, water content, and soil water level are created. These maps allow the geotechnical data in the study area to be evaluated visually.

The calculations are made by the data and SPT-N values at depths of 1.5m, 3 m, 4.5m, 7.5m, 15m, in the study area for bearing capacity. The maps created according to Terzaghi and Peck and Meyerhof methods show similar results and the calculated values are close to each other. However, it is observed that Meyerhof bearing capacity values are greater than Terzaghi and Peck results when blow value and depth increase.

It is noted that the bearing capacity values found by Keceli (1990) and Tezcan et. al. (2010) Method do not match with to Terzaghi and Peck (1967) and Meyerhof (1974) methods. Therefore, one should show special attention when using the bearing capacity values obtained by geophysical methods for preliminary research.

In the study area, according to the data obtained from 192 boring points, groundwater between 3.5 m and 29 m are found at 29 boring points. It is determined that the groundwater is located between the vicinity of the City Cemetery, Orduzu Pond and Çamurlu, between Upper Çöşnük and Tandoğan, and around Kiltepe. It has been assessed that the study area is not rich in terms of groundwater.

In the scope of the study, when the distribution of the water content (Wn) values for 1.5 m, 3 m, 4.5 m, 7.5 m, 15 m, 0-10% $W_n$, 11-20% $W_n$, 21-30% $W_n$, 31-37% $W_n$ is compared, it is seen that 11-20% $W_n$ value are dominant in the study area.

In the determination of the liquefaction sensitivity, there is no liquefaction risk observed in 67% of the study area, however, there is a liquefaction risk 33% of the study area for the depth. At 3 m depth, 88% of the study area shows no liquefaction risk, while 12% of the study area there is a liquefaction risk calculated. Similarly, we observed liquefaction risk 13% of the region at 4.5 m depth, 15% at 7.5 m depth, and 9% at 15 m depth. The maps help us localize the liquefaction hazard risk in the city limits. A future study about liquefaction hazard might be related to the determination of the total population in the city limits where this study presents the liquefaction risk. When we zoom in the liquefaction susceptible areas, we observe that the bearing capacity values are low in these regions. This also confirms that the overall calculations are consistent with each other. However, the regions with liquefaction risk and low bearing capacity do match with the bearing capacity estimation with geophysical methods. This is also valid with the Eurocode8 and NEHRP soil classifications. Some liquefaction zones and low bearing capacity soil sites are not classified as soft soils based on the average shear wave velocity ranges specified in these soil classification systems.

The shear wave velocity is calculated from SPT-N values obtained from seismic methods and 192 borings at 1.5m, 3 m, 4.5 m, 7.5 m, and 15 m depths. The results obtained from various methods to calculate shear wave velocities from SPT-N values have been compared. Overall, Imai and Yoshimura (1970) work well when we compare to calculated shear wave velocity with the measured shear wave velocities in the field. In general, we may say that methods were successful to match the trend with measure velocities.

With the measurements made in the field via seismic methods, the shear wave velocity for a depth of 30 m throughout the study area was determined. The measurements showed that 1% of the study area has Vs>1500 m/s, 3% of the study area has 760< Vs < 1500 m/s, 52% of study area has 360< Vs < 760 m/s, 43% of study area has 180< Vs < 360 m/s, 1% of the study area has Vs< 180 m/s. From these result, soil classes are determined according to NEHRP. This classification

gave us that 1% of the study area is found to be hard rock, 3% part of the study area is rock, 52% part of the study area is very dense soil and soft rock, 43% part of the study area is stiff soil and 1% part of the study area is soft clay soil class. The soil class C is the dominant class and exists in 52% of the study area. A, B, E soil classes have been identified in various areas throughout the study area. Hard rock, rock, soft clay soil are found in 5% of the study area of the soil classes.

The soil class evaluations according to Eurocode 8 is also conducted. It is determined that 4% of the study area is rock or other rock-like geological formation, 52% part of the study area is very dense sand or gravel or very stiff clay, 43% part of the study area is dense sand or gravel or stiff clay, 1% part of the study area is soft clay soil class loose to medium cohesionless soil or soft to firm cohesive soil. The soil class C is observed in 43% of the study area, B soil class is found in 52% of the study area and dominant throughout the study. A and D soil classes have been identified in various areas throughout the study area.

According to soil amplification calculations, the low hazard regions C cover 66% of the study area and dominant throughout the study. A (high hazard) is identified in various areas throughout the study area.

According to dominant vibration period evaluation classifies the soil sites as Z1: Very dense; Z2: Stiff; Z3: Medium stiff; Z4: Loose, soft. We found that that 13% of the study area is Z1 soil class, 47% is Z2 soil class, 26% is Z3 soil class and 14% is Z4 soil class. Our calculations showed that Z3 and Z4 soil classes cover 40% of the study area, Z1 and Z2 soil class are also found in 60% of the study area and dominant throughout the study.

The GIS-based SPT-N, bearing capacity, liquefaction, shear wave velocity, NEHRP Soil Class, Eurocode 8 Soil Class, Soil Amplification Risk Factor, Soil Dominant Vibration Period, local soil class, water content and groundwater level maps have been created and important engineering parameters have been investigated for the purpose of planning in the residential areas by public institutions. This research will help engineerings and city planners to provide sustainable geotechnical design and city plans. The important geotechnical data which has application in geotechnical

engineering is now accessible visually so that each institution involved in such planning and design activities in the city will save a great deal of time and labor.

Also, it is considered that it is of great importance that the relevant mapping activities, which are among the objectives of the National Earthquake Strategy and Action Plan 2023, should be supported and make them widespread by the local administrations.

More studies are desired to be carried out in our region and on a national basis. With the data obtained at this point, it is always possible to develop our work under the thesis and enrich the database.

## REFERENCES


AFAD (2018), https://deprem.afad.gov.tr/depremkatalogu/deprem-bolgeleri-haritasi

Akın, M.K., Kramer, S.L. and Topal T. (2011). Empirical correlations of shear wave velocity (Vs) and penetration resistance (SPT-N) for different soils in an earthquake prone area (Erbaa-Turkey*). Engineering Geology*, 119, 1–17.

Alparslan, E., Yuce, H., Erkan, B., İnan, S., Ergintav, S. and Saatcılar, R. (2006). Analysis of landslide sensitivity between the region Buyukcekmece and Kucukcekmece Lakes with remote sensing and detailed analysis with geographical information systems. *Proceedings of the 4th GIS days in Turkey*, Fatih University, Istanbul, Turkey, 558.

Anand S.A. (2000). Recent developments toward earthquake risk reduction India. *Current Science*, 79, 1270-1277.

Aydan, Ö., Ulusay, R., Hasgür, Z. and Taşkın, B. (2000). Site investigation of Kocaeli earthquake of August 17 1999. *Turkey Earthquake Foundation*, TDV/DR 08-49, 176.

Ayday, C. (2008). *Research report of earthquake hazard mapping update and change under the boundaries of Eskisehir Tepebasi Municipality*, Eskisehir, Turkey.

Ayeni, O.O., Saka, D.N. ans Ikwuemesi, G. (2004). Developing a multimedia database for tourism industry in Nigeria, Proceedings of the XXth ISPRS Congress Commission *2*, Ed. Orhan Altan. *International Society for Photogrammetry and Remote Sensing*, İstanbul, Turkey, 873.

Baysal, G. and Tecim, V. (2006). Solid waste landfill compliance analysis application with various decision methods and applications based on geographical information system (GIS). *Proceedings of the 4th GIS days in Turkiye*, *September 13-16*, Fatih University, Istanbul, Turkey, 558.

Bowles, J. E. (1996). Foundation analysis and design 5th. The McGraw-Hill Companies Inc. New York, USA.

ÇŞB, (2011). Malatya Province Environment Status Report. *Ministry of Environment And Urbanization*, Malatya.

Demirci, A., Mcadams, M.A., Alagha, O. and Karakuyu, M. (2006). The relationship between land use change and water quality in Kucukcekmece Lake watershed. *Proceedings of the 4th GIS days in Türkiye, September 13-16,* Fatih University, Istanbul, Turkey.

Ergun, S. and Sarac, İ. (2006). The Use of GIS in Medical Geography: The Case of Local Medical Clinics in Samsun. *Proceedings of the 4th GIS days in Turkiye, September 13-16,* Fatih University, Istanbul, Turkey.

Erol, A. O. and Çekinmez, Z. (2014). Field tests in geotechnical engineering. Yüksel Proje Publications, Nu: 14-01, Ankara, Turkey.

Güzel, M. (2009). *Integrated use of geological, geophysical and geotechnical data in microzonation studys (northern Adana case)*, Department Of Geological Engineering Instıtute of Natural and Applıed Scıences Unıversıty of Çukurova, PhD.Thesis, Adana.

Halaç, B. (2016). *Review of the soil classification criteria in earthquake regulations with respect to amplification*, İstanbul Technical University Institute of Science, M.A. Thesis, İstanbul.

Hasançelebi, N., Ulusay, R., 2007. *Empirical Correlations Between Shear Wave Velocity and Penetration Resistance for Ground Shaking Assessments*. Bulletin of Engineering Geology and the Environment 66, 203–213.

IMO, (2016). Soil Investigation Manual. TMMOB Chamber of Civil Engineers, Nu: IMO/16/9, ISBN 978-605-01-09-0918-4, Ankara, Turkey.

Iyisan, R. (1996). Correlations between shear wave velocity and in-situ penetration test results, *Technical Journal of Turkish Chamber of Civil Engineers*, 7 (2), 1187-1199.

Imai, T., Yoshimura, Y., (1970). Elastic wave velocity and soil properties in soft soil. Tsuchito-Kiso 18 (1), 17–22.

Kargı, H., and Sarı, N. (2006). Determination of landsat tm images of the alteration zones, a prospecting work. *Proceedings of the 4th GIS days in Turkiye*, *September 13-16,* Fatih University, Istanbul, Turkey.

Kanai, K. (1983). Engineering seismology, University of Tokyo Press, ISBN 13: 9780860083269, Tokyo, Japan.

Keçeli, A. (1990). The determination of the dynamic permissible bearing capacity and Settlement by means of the seismic method. *Jeofizik* 4(2): 83-92.

Kıncal, C. (2006). The use of GIS in field use oriented studies. *Proceedings of the 4th GIS days in Turkiye*, *September 13-16,* Fatih University, Istanbul, Turkey.

Kurnaz, T.F. (2011). *Geotechnical microzonation of Istanbul Esenler soils based on geographical information systems*, Sakarya University Graduate School of Natural and Applied Sciences, Ph.D. Thesis, Sakarya.

Kumbur, H., Oz, Z. and Hunter, E. D., (2006). Mersin University Çiftlikköy campus analysis of noise level with GIS. *Proceedings of the 4th GIS days in Turkiye*, *September 13-16,* Fatih University, Istanbul, Turkey.

Marx, C. (1992). Applications of earthquake hazard maps to land-use planning and regulations in Seattle. *Seattle Planning Department*, 25, USA.

Malatya Municipality Development Department, MMDD (2009). Survey report on the development plan of Malatya, Malatya municipality settlement area and revised development plan. Malatya, Turkey.

McKenzie, D.P. (1972). Active tectonics of the mediterranean region. *Geophysical J. R.* Astr. Soc., 30 (2), 109-185.

Meyerhof, G.G. (1974) Ultimate Bearing Capacity of Footings on Sand Layer Overlying Clay. *Canadian Geotechnical Journal*, 11, 223-229.

Midorikawa, S. (1987). Prediction of isoseismal map in Kanto plain doe to hypothetical earthquake. *Journal of Structural Dynamics*, 33B, 43-48.

Ohba, S., and Trauma, I., (1970). Dynamic response characteristics of Osaka Plain, Proceeding Annual Meeting, A. I. J.

Seed, H.B., and Idriss, I.M., (1971), Simplified procedure for evaluation soil liquefaction potential. *Journal of the Soil Mechanics and Foundations Division ASCE*, 97, 1249-1273.

Seed, H.B., Idriss, I.M., (1981). Evaluation of liquefaction potential sand deposits based on observation of performance in previous earthquakes. *ASCE National Convention (MO)*, pp. 481–544.

Sert, S., Ozocak, A. and Ural N. (2006). Use of geographic information systems with geotechnical purposes in Adapazari. *Geographic Information Systems Forensics Days*, Fatih University, Istanbul, Turkey, 8.

Spearin, D. (2004). Innovations in GIS emergency response planning. *Public Safety and Emergency Preparedness Canada*, 28.

Şen, G. (2004). *Liquefaction analysis of Gümüşler municipality advisory area and its application in geographical information system*, Pamukkale University Institute of Science, Master Thesis, Denizli.

Terzaghi, K. and Peck, R. (1967) Soil Mechanics in Engineering Practice. 2nd Edition, John Wiley, New York.

Tezcan, S. S., Keçeli A. and Özdemir, Z. (2010). Seismic technique to determine the alloqable bearing pressure for shallow foundations in Soils and Rocks. *Tübav Science Journal*, 3 (1), 1-10.

Turoğlu, H. (2006). Yonca Hill (Van) archaeological field area and GIS and RS technologies with Paleo-LANDUS analysis for its near domestic surroundings, *Proceedings of the 4th GIS days in Turkey*, Fatih University, Istanbul, Turkey.

Tsiambaos G. and Sabatakakis N., (2011). Empirical Estimation of Shear Wave Velocity from In Situ Tests on Soil Formations in Greece, *Bulletin of Engineering Geology and the Environment*, 70,291–297.

Ulusay, R. (2000). Soil liquefaction, *Blue Planet Popular Science Magazine*, TMMOB Chamber of Geological Engineers Publication, 1, 34-45.

Ündül, O. and Gürpınar, O. (2003). Liquefaction potential of aluvial grounds in cokal valley(Gallipoli) Istanbul University, *Journal of Engineering Geology*, 16, 1, 79.

Yomralioğlu, T. (2000). *Geographical information systems basic concepts and applications*. Akademi Bookstore, ISBN 975-97369-0-X, Trabzon.

Youd, T. L., Idriss, I. M., Andrus, R. D., Arango, I., Castro, G., Christian, J. T., Dobry, R., Liam Finn, W. D., Harder Jr., L. F., Hynes, M. E., Ishihara, K., Koester, J. P., Liao, S. S. C., Marcuson III, W. F., Martin, G. R., Mitchell, J. K., Moriwaki, Y., Power, M. S., Robertson, P. K., Seed, R. B. and Stokoe II K. H. (2001). Liquefaction resistance of soils: summary report from the 1996 NCEER and 1998 NCEER/NSF workshops on evaluation of liquefaction resistance of soils, *Journal of Geotechnical and Geo-environmental Engineering ASCE*, 127, 817-832.

## APPENDIX

Appendix A Bearing Capacity Table

Appendix B  Liquefaction Risk Table

Appendix C  Shear Wave Velocity Table

Appendix D Soil Class Fıgure and Earthquake Hazard Level Table

Appendix E  Malatya Municipality Permission Certificate for Data Use

| B.N | SPT N | $\gamma_n$ (KN/m$^3$) | Vp (m/s) | (To) s) | Vs (m/s) | β | Meyerhof (1974) (kN/m$^2$) | Terzaghi ve Peck (1967) (kN/m$^2$) | Keçeli (1990) (kN/m$^2$) | Tezcan et. al. (2010) (kN/m$^2$) |
|---|---|---|---|---|---|---|---|---|---|---|
| 1 | 42 | 16,7 | 840 | 0,6 | 260 | 0,8 | 475 | 409 | 210 | 347 |
| 10 | 50 | 17,6 | 1050 | 0,4 | 320 | 0,8 | 566 | 488 | 185 | 451 |
| 18 | 50 | 17,1 | 938 | 0,5 | 305 | 0,8 | 566 | 488 | 252 | 525 |
| 28 | 50 | 18,1 | 1179 | 0,4 | 345 | 0,8 | 566 | 488 | 213 | 500 |
| 37 | 50 | 16,3 | 760 | 0,5 | 314 | 0,8 | 566 | 488 | 155 | 409 |
| 46 | 10 | 13,8 | 400 | 0,6 | 164 | 0,8 | 113 | 98 | 83 | 181 |
| 55 | 50 | 20,5 | 1931 | 0,3 | 410 | 0,8 | 566 | 488 | 297 | 672 |
| 64 | 3 | 12,4 | 255 | 0,8 | 105 | 0,8 | 34 | 29,4 | 63 | 104 |
| 73 | 50 | 17,7 | 1072 | 0,5 | 312 | 0,8 | 566 | 488 | 237 | 442 |
| 82 | 50 | 16,7 | 840 | 0,5 | 285 | 0,8 | 566 | 488 | 175 | 381 |
| 91 | 3 | 13,3 | 940 | 0,5 | 300 | 0,8 | 34 | 29,4 | 156 | 319 |
| 100 | 4 | 13,9 | 410 | 0,4 | 121 | 0,8 | 45 | 39,2 | 57 | 135 |
| 109 | 4 | 12,1 | 230 | 0,6 | 115 | 0,8 | 45 | 39,2 | 42 | 111 |
| 118 | 1 | 12,5 | 265 | 0,7 | 85 | 0,8 | 11 | 9,8 | 58 | 85 |
| 127 | 4 | 13,3 | 340 | 0,7 | 115 | 0,8 | 45 | 39,2 | 79 | 122 |
| 136 | 50 | 17,9 | 1120 | 0,4 | 344 | 0,8 | 566 | 488 | 200 | 493 |
| 145 | 50 | 17 | 910 | 1,5 | 275 | 0,8 | 566 | 488 | 580 | 374 |
| 154 | 19 | 13,9 | 610 | 0,3 | 200 | 0,8 | 215 | 185,2 | 64 | 222 |
| 162 | 50 | 17,2 | 950 | 0,5 | 285 | 0,8 | 566 | 488 | 253 | 486 |
| 172 | 50 | 17,3 | 970 | 0,4 | 318 | 0,8 | 566 | 488 | 168 | 440 |
| 181 | 50 | 17,6 | 1035 | 0,5 | 300 | 0,8 | 566 | 488 | 228 | 422 |
| 190 | 50 | 16,7 | 850 | 0,6 | 292 | 0,8 | 566 | 488 | 213 | 390 |

Appendix A.1 Bearing Capacity Table (1.5 m)

| B.N | SPT N | $\gamma_n$ (KN/m$^3$) | Vp (m/s) | (To) (s) | Vs (m/s) | β | Meyerhof (1974) (kN/m$^2$) | Terzaghi ve Peck (1967) (kN/m$^2$) | Keçeli (1990) (kN/m$^2$) | Tezcan et. al. (2010) (kN/m$^2$) |
|---|---|---|---|---|---|---|---|---|---|---|
| 2 | 50 | 17,8 | 1100 | 0,4 | 340 | 0,8 | 646 | 488 | 196 | 484 |
| 11 | 50 | 20,4 | 1878 | 0,4 | 410 | 0,8 | 646 | 488 | 383 | 669 |
| 20 | 50 | 16,2 | 748 | 0,7 | 220 | 0,8 | 646 | 488 | 212 | 285 |
| 29 | 50 | 20,1 | 1767 | 0,4 | 486 | 0,8 | 646 | 488 | 355 | 781 |
| 38 | 50 | 19,5 | 1570 | 0,4 | 430 | 0,8 | 646 | 488 | 306 | 671 |
| 47 | 50 | 18,4 | 1242 | 0,4 | 350 | 0,8 | 646 | 488 | 229 | 515 |
| 56 | 39 | 16,7 | 853 | 0,7 | 254 | 0,8 | 504 | 380,4 | 249 | 339 |
| 65 | 50 | 17,1 | 934 | 0,4 | 330 | 0,8 | 646 | 488 | 160 | 451 |
| 74 | 50 | 17,8 | 1092 | 0,5 | 310 | 0,8 | 646 | 488 | 243 | 441 |
| 83 | 3 | 13,1 | 860 | 0,6 | 276 | 0,8 | 39 | 29,4 | 169 | 289 |
| 92 | 5 | 13,8 | 1100 | 0,4 | 330 | 0,8 | 65 | 49 | 152 | 364 |
| 101 | 50 | 17 | 910 | 0,3 | 337 | 0,8 | 646 | 488 | 116 | 458 |
| 110 | 50 | 17 | 915 | 0,7 | 314 | 0,8 | 646 | 488 | 272 | 427 |
| 119 | 50 | 17 | 900 | 0,7 | 302 | 0,8 | 646 | 488 | 268 | 411 |
| 128 | 42 | 16,5 | 800 | 0,7 | 260 | 0,8 | 542 | 409,6 | 231 | 343 |
| 137 | 50 | 18,2 | 1200 | 0,4 | 380 | 0,8 | 646 | 488 | 218 | 553 |
| 146 | 50 | 17,7 | 1080 | 0,3 | 320 | 0,8 | 646 | 488 | 143 | 453 |
| 155 | 50 | 17,2 | 950 | 0,4 | 362 | 0,8 | 646 | 488 | 163 | 498 |
| 164 | 22 | 16,3 | 760 | 0,6 | 210 | 0,8 | 284 | 214,6 | 186 | 274 |
| 173 | 50 | 17,3 | 970 | 0,4 | 318 | 0,8 | 646 | 488 | 168 | 440 |
| 182 | 19 | 16,1 | 740 | 0,7 | 200 | 0,8 | 245 | 185,2 | 208 | 258 |
| 192 | 50 | 17,3 | 968 | 0,6 | 310 | 0,8 | 646 | 488 | 251 | 429 |

Appendix A.2 Bearing Capacity Table (3 m)

| B.N | SPT N | $\gamma_n$ (KN/m$^3$) | Vp (m/s) | (To) (s) | Vs (m/s) | β | Meyerhof (1974) (kN/m$^2$) | Terzaghi ve Peck (1967) kN/m$^2$) | Keçeli (1990) (kN/m$^2$) | Tezcan et. al. (2010) (kN/m$^2$) |
|---|---|---|---|---|---|---|---|---|---|---|
| 3 | 50 | 21,6 | 2380 | 0,4 | 560 | 0,8 | 646 | 488 | 514 | 968 |
| 12 | 50 | 21,8 | 2450 | 0,4 | 545 | 0,8 | 646 | 488 | 534 | 950 |
| 21 | 50 | 17,1 | 940 | 0,7 | 310 | 0,8 | 646 | 488 | 281 | 424 |
| 30 | 50 | 20,8 | 2044 | 0,3 | 520 | 0,8 | 646 | 488 | 319 | 865 |
| 39 | 50 | 17,7 | 1062 | 0,5 | 280 | 0,8 | 646 | 488 | 235 | 396 |
| 48 | 50 | 18,2 | 1208 | 0,4 | 340 | 0,8 | 646 | 488 | 220 | 495 |
| 57 | 50 | 18 | 1133 | 0,5 | 285 | 0,8 | 646 | 488 | 255 | 410 |
| 66 | 50 | 18,1 | 1160 | 0,5 | 394 | 0,8 | 646 | 488 | 262 | 571 |
| 75 | 50 | 18,2 | 1200 | 0,4 | 340 | 0,8 | 646 | 488 | 218 | 495 |
| 84 | 2 | 12,9 | 791 | 0,6 | 270 | 0,8 | 26 | 19,6 | 153 | 279 |
| 93 | 10 | 14,1 | 1095 | 0,5 | 410 | 0,8 | 129 | 98 | 193 | 462 |
| 102 | 50 | 18,5 | 1265 | 0,3 | 445 | 0,8 | 646 | 488 | 176 | 659 |
| 111 | 50 | 17 | 910 | 0,7 | 300 | 0,8 | 646 | 488 | 271 | 408 |
| 120 | 50 | 16,2 | 747 | 0,6 | 284 | 0,8 | 646 | 488 | 182 | 368 |
| 129 | 50 | 17,3 | 979 | 0,6 | 310 | 0,8 | 646 | 488 | 254 | 429 |
| 138 | 50 | 21,6 | 2350 | 0,4 | 523 | 0,8 | 646 | 488 | 508 | 904 |
| 147 | 50 | 17,8 | 1100 | 0,4 | 351 | 0,8 | 646 | 488 | 196 | 500 |
| 156 | 50 | 16,6 | 833 | 0,3 | 274 | 0,8 | 646 | 488 | 104 | 364 |
| 165 | 50 | 18,1 | 1160 | 0,6 | 351 | 0,8 | 646 | 488 | 315 | 508 |
| 174 | 50 | 17,5 | 1018 | 0,5 | 295 | 0,8 | 646 | 488 | 223 | 413 |
| 183 | 50 | 17,2 | 960 | 0,3 | 300 | 0,8 | 646 | 488 | 124 | 413 |
| 189 | 50 | 18,4 | 1260 | 0,6 | 382 | 0,8 | 646 | 488 | 348 | 562 |

Appendix A.3 Bearing Capacity Table (4.5 m)

| B.N | SPT N | $\gamma_n$ (KN/m$^3$) | Vp (m/s) | (To) (s) | Vs (m/s) | β | Meyerhof (1974) (kN/m$^2$) | Terzaghi ve Peck (1967) (kN/m$^2$) | Keçeli (1990) (kN/m$^2$) | Tezcan et. al. (2010) (kN/m$^2$) |
|---|---|---|---|---|---|---|---|---|---|---|
| 4 | 50 | 21,7 | 2410 | 0,4 | 560 | 0,8 | 646 | 488 | 523 | 972 |
| 13 | 50 | 21,4 | 2300 | 0,4 | 545 | 0,8 | 646 | 488 | 492 | 933 |
| 22 | 50 | 17,9 | 1118 | 0,6 | 355 | 0,8 | 646 | 488 | 300 | 508 |
| 31 | 22 | 15,3 | 600 | 0,6 | 210 | 0,8 | 284 | 214,6 | 138 | 257 |
| 40 | 50 | 18,1 | 1162 | 0,5 | 285 | 0,8 | 646 | 488 | 263 | 413 |
| 49 | 38 | 16 | 717 | 0,7 | 252 | 0,8 | 491 | 370,8 | 201 | 323 |
| 58 | 50 | 17,9 | 1125 | 0,5 | 280 | 0,8 | 646 | 488 | 252 | 401 |
| 67 | 47 | 16,8 | 862 | 0,6 | 270 | 0,8 | 607 | 458,6 | 217 | 363 |
| 76 | 50 | 17,5 | 623 | 0,6 | 320 | 0,8 | 646 | 488 | 164 | 448 |
| 85 | 2 | 12,1 | 1017 | 0,6 | 340 | 0,8 | 26 | 19,6 | 185 | 329 |
| 94 | 5 | 13,9 | 1100 | 0,4 | 340 | 0,8 | 65 | 49 | 153 | 378 |
| 103 | 50 | 17,8 | 800 | 0,6 | 330 | 0,8 | 646 | 488 | 214 | 470 |
| 112 | 42 | 16,3 | 767 | 0,7 | 260 | 0,8 | 542 | 409,6 | 219 | 339 |
| 121 | 50 | 17,1 | 940 | 0,7 | 320 | 0,8 | 646 | 488 | 281 | 438 |
| 130 | 38 | 16,5 | 800 | 0,7 | 525 | 0,8 | 491 | 370,8 | 231 | 693 |
| 139 | 50 | 21,5 | 2340 | 0,4 | 522 | 0,8 | 646 | 488 | 503 | 898 |
| 148 | 50 | 17,6 | 760 | 0,2 | 260 | 0,8 | 646 | 488 | 67 | 366 |
| 157 | 50 | 17,8 | 811 | 0,4 | 322 | 0,8 | 646 | 488 | 144 | 459 |
| 166 | 50 | 18 | 950 | 0,6 | 348 | 0,8 | 646 | 488 | 257 | 501 |
| 171 | 50 | 17,8 | 1100 | 0,6 | 352 | 0,8 | 646 | 488 | 368 | 628 |
| 184 | 50 | 18,4 | 1260 | 0,5 | 383 | 0,8 | 646 | 488 | 290 | 564 |
| 188 | 50 | 17,9 | 1125 | 0,6 | 354 | 0,8 | 646 | 488 | 302 | 507 |

Appendix A.4 Bearing Capacity Table (7.5 m)

| B.N | SPT N | $\gamma_n$ (KN/m$^3$) | Vp (m/s) | (To) (s) | Vs (m/s) | β | Meyerhof (1974) (kN/m$^2$) | Terzaghi ve Peck (1967) (kN/m$^2$) | Keçeli (1990) (kN/m$^2$) | Tezcan et. al. (2010) (kN/m$^2$) |
|---|---|---|---|---|---|---|---|---|---|---|
| 5 | 50 | 18,4 | 1250 | 0,4 | 360 | 0,8 | 646 | 488 | 230 | 530 |
| 14 | 50 | 18,1 | 1167 | 0,4 | 350 | 0,8 | 646 | 488 | 211 | 507 |
| 23 | 50 | 18,3 | 1210 | 0,5 | 365 | 0,8 | 646 | 488 | 277 | 534 |
| 32 | 50 | 16,7 | 844 | 0,5 | 230 | 0,8 | 646 | 488 | 176 | 307 |
| 41 | 50 | 19,5 | 1587 | 0,5 | 420 | 0,8 | 646 | 488 | 387 | 655 |
| 50 | 37 | 16,2 | 750 | 0,9 | 250 | 0,8 | 478 | 361,2 | 273 | 324 |
| 59 | 50 | 20 | 1750 | 0,5 | 410 | 0,8 | 646 | 488 | 438 | 656 |
| 68 | 50 | 18,2 | 1190 | 0,5 | 390 | 0,8 | 646 | 488 | 271 | 568 |
| 77 | 50 | 18,6 | 1302 | 0,5 | 434 | 0,8 | 646 | 488 | 303 | 646 |
| 86 | 3 | 13,3 | 1031 | 0,5 | 300 | 0,8 | 39 | 29,4 | 171 | 319 |
| 95 | 7 | 14,1 | 1670 | 0,4 | 500 | 0,8 | 90 | 68,6 | 235 | 564 |
| 104 | 50 | 17,7 | 1080 | 0,6 | 342 | 0,8 | 646 | 488 | 287 | 484 |
| 113 | 50 | 17,4 | 995 | 0,6 | 330 | 0,8 | 646 | 439 | 260 | 459 |
| 122 | 50 | 17,3 | 980 | 0,6 | 342 | 0,8 | 646 | 488 | 254 | 473 |
| 131 | 50 | 18 | 1135 | 0,6 | 330 | 0,8 | 646 | 488 | 306 | 475 |
| 140 | 50 | 19,9 | 1700 | 0,4 | 483 | 0,8 | 646 | 488 | 338 | 769 |
| 149 | 50 | 18,9 | 1390 | 0,3 | 412 | 0,8 | 646 | 488 | 197 | 623 |
| 158 | 50 | 18 | 1140 | 0,5 | 300 | 0,8 | 646 | 488 | 257 | 432 |
| 167 | 50 | 17,6 | 1051 | 0,6 | 330 | 0,8 | 646 | 488 | 277 | 465 |
| 182 | 50 | 17,6 | 1045 | 0,7 | 300 | 0,8 | 646 | 488 | 415 | 545 |
| 185 | 50 | 17,7 | 1070 | 0,6 | 334 | 0,8 | 646 | 488 | 284 | 473 |
| 187 | 50 | 19,6 | 1600 | 0,5 | 450 | 0,8 | 646 | 488 | 392 | 706 |

Appendix A.5 Bearing Capacity Table (15 m)

| B.N | $r_d$ | σv (kpa) | σv' (kpa) | $(\gamma_n)$ KN/m3 | a max | CSR | N | $C_N$ | $C_E$ | $C_B$ | $C_R$ | $C_S$ | $(N_1)_{60}$ | 200 SIEVE % | $(N_1)_{60CS}$ | CRR | FS= CRR/CSR | 1.5 M Exp. |
|---|---|---|---|---|---|---|---|---|---|---|---|---|---|---|---|---|---|---|
| 2 | 0,99 | 26,70 | 26,70 | 17,80 | 0.4g | 0,26 | 50 | 1,50 | 0,75 | 1,00 | 1,00 | 1,00 | 56,24 | (N1)60≥ 30 soils are too dense to liquefy and are classed as non-liquefiable | | | | FS>1 No Liquefaction |
| 8 | 0,99 | 21,30 | 21,30 | 14,20 | 0.4g | 0,26 | 19 | 1,56 | 0,75 | 1,00 | 1,00 | 1,00 | 22,19 | 19 | 27,20 | 0,34 | 1,34 | FS>1 No Liquefaction |
| 21 | 0,99 | 23,25 | 23,25 | 15,50 | 0.4g | 0,26 | 13 | 1,54 | 0,75 | 1,00 | 1,00 | 1,00 | 14,97 | 20 | 19,10 | 0,20 | 0,79 | FS ≤ 1 Liquefaction |
| 32 | 0,99 | 19,05 | 19,05 | 12,70 | 0.4g | 0,26 | 6 | 1,58 | 0,75 | 1,00 | 1,00 | 1,00 | 7,12 | 12 | 8,00 | 0,10 | 0,37 | FS ≤ 1 Liquefaction |
| 51 | 0,99 | 23,10 | 23,10 | 15,40 | 0.4g | 0,26 | 25 | 1,54 | 0,75 | 1,00 | 1,00 | 1,00 | 28,83 | 12 | 31,05 | 0,56 | 2,19 | FS>1 No Liquefaction |
| 71 | 0,99 | 26,40 | 26,40 | 17,60 | 0.4g | 0,26 | 50 | 1,50 | 0,75 | 1,00 | 1,00 | 1,00 | 56,35 | (N1)60≥ 30 soils are too dense to liquefy and are classed as non-liquefiable | | | | FS>1 No Liquefaction |
| 88 | 0,99 | 23,10 | 23,10 | 15,40 | 0.4g | 0,26 | 23 | 1,54 | 0,75 | 1,00 | 1,00 | 1,00 | 26,52 | 28 | 38,17 | 0,04 | 0,15 | FS ≤ 1 Liquefaction |
| 99 | 0,99 | 28,50 | 28,50 | 19,00 | 0.4g | 0,26 | 50 | 1,48 | 0,75 | 1,00 | 1,00 | 1,00 | 55,56 | (N1)60≥ 30 soils are too dense to liquefy and are classed as non-liquefiable | | | | FS>1 No Liquefaction |
| 121 | 0,99 | 23,25 | 23,25 | 15,50 | 0.4g | 0,26 | 18 | 1,54 | 0,75 | 1,00 | 1,00 | 1,00 | 20,73 | 11 | 21,97 | 0,24 | 0,94 | FS ≤ 1 Liquefaction |
| 133 | 0,99 | 25,80 | 25,80 | 17,20 | 0.4g | 0,26 | 50 | 1,51 | 0,75 | 1,00 | 1,00 | 1,00 | 56,58 | (N1)60≥ 30 soils are too dense to liquefy and are classed as non-liquefiable | | | | FS>1 No Liquefaction |
| 142 | 0,99 | 21,45 | 21,45 | 14,30 | 0.4g | 0,26 | 10 | 1,56 | 0,75 | 1,00 | 1,00 | 1,00 | 11,66 | 25 | 16,65 | 0,18 | 0,69 | FS ≤ 1 Liquefaction |
| 156 | 0,99 | 21,00 | 21,00 | 14,00 | 0.4g | 0,26 | 22 | 1,56 | 0,75 | 1,00 | 1,00 | 1,00 | 25,74 | 11 | 27,23 | 0,35 | 1,34 | FS>1 No Liquefaction |
| 161 | 0,99 | 22,35 | 22,35 | 14,90 | 0.4g | 0,26 | 11 | 1,55 | 0,75 | 1,00 | 1,00 | 1,00 | 12,75 | 12 | 13,98 | 0,15 | 0,58 | FS ≤ 1 Liquefaction |
| 192 | 0,99 | 25,95 | 25,95 | 17,30 | 0.4g | 0,26 | 50 | 1,51 | 0,75 | 1,00 | 1,00 | 1,00 | 56,53 | (N1)60≥ 30 soils are too dense to liquefy and are classed as non-liquefiable | | | | FS>1 No Liquefaction |

Appendix B.1 Liquefaction Risk Table (1.5 m)

| B.N | $r_d$ | σv (kpa) | σv' (kpa) | $(\gamma_n)$ KN/m3 | a max | CSR | N | $C_N$ | $C_E$ | $C_B$ | $C_R$ | $C_S$ | $(N_1)_{60}$ | 200 SIEVE % | $(N_1)_{60CS}$ | CRR | FS= CRR/CSR | 3 M Exp. |
|---|---|---|---|---|---|---|---|---|---|---|---|---|---|---|---|---|---|---|
| 1 | 0,98 | 50,10 | 50,10 | 16,70 | 0.4g | 0,25 | 42 | 1,29 | 0,75 | 1,00 | 1,00 | 1,00 | 40,74 | (N1)60≥ 30 soils are too dense to liquefy and are classed as non-liquefiable | | | | FS>1 No Liquefaction |
| 7 | 0,98 | 51,00 | 51,00 | 17,00 | 0.4g | 0,25 | 50 | 1,29 | 0,75 | 1,00 | 1,00 | 1,00 | 48,25 | (N1)60≥ 30 soils are too dense to liquefy and are classed as non-liquefiable | | | | FS>1 No Liquefaction |
| 23 | 0,98 | 46,50 | 46,50 | 15,50 | 0.4g | 0,25 | 25 | 1,32 | 0,75 | 1,00 | 1,00 | 1,00 | 24,77 | 12 | 26,75 | 0,33 | 1,30 | FS>1 No Liquefaction |
| 39 | 0,98 | 53,10 | 53,10 | 17,70 | 0.4g | 0,25 | 50 | 1,27 | 0,75 | 1,00 | 1,00 | 1,00 | 47,66 | (N1)60≥ 30 soils are too dense to liquefy and are classed as non-liquefiable | | | | FS>1 No Liquefaction |
| 46 | 0,98 | 41,40 | 41,40 | 13,80 | 0.4g | 0,25 | 10 | 1,36 | 0,75 | 1,00 | 1,00 | 1,00 | 10,22 | 18 | 12,95 | 0,14 | 0,55 | FS ≤ 1 Liquefaction |
| 76 | 0,98 | 46,50 | 46,50 | 15,50 | 0.4g | 0,25 | 19 | 1,32 | 0,75 | 1,00 | 1,00 | 1,00 | 18,83 | 6 | 15,46 | 0,16 | 0,65 | FS ≤ 1 Liquefaction |
| 89 | 0,98 | 50,10 | 50,10 | 16,70 | 0.4g | 0,25 | 50 | 1,29 | 0,75 | 1,00 | 1,00 | 1,00 | 48,50 | (N1)60≥ 30 soils are too dense to liquefy and are classed as non-liquefiable | | | | FS>1 No Liquefaction |
| 98 | 0,98 | 42,00 | 42,00 | 14,00 | 0.4g | 0,25 | 8 | 1,36 | 0,75 | 1,00 | 1,00 | 1,00 | 8,15 | 12 | 9,09 | 0,11 | 0,41 | FS ≤ 1 Liquefaction |
| 105 | 0,98 | 47,70 | 47,70 | 15,90 | 0.4g | 0,25 | 22 | 1,31 | 0,75 | 1,00 | 1,00 | 1,00 | 21,65 | 12 | 23,43 | 0,26 | 1,04 | FS>1 No Liquefaction |
| 121 | 0,98 | 51,30 | 51,30 | 17,10 | 0.4g | 0,25 | 50 | 1,28 | 0,75 | 1,00 | 1,00 | 1,00 | 48,16 | (N1)60≥ 30 soils are too dense to liquefy and are classed as non-liquefiable | | | | FS>1 No Liquefaction |
| 159 | 0,98 | 48,90 | 48,90 | 16,30 | 0.4g | 0,25 | 29 | 1,30 | 0,75 | 1,00 | 1,00 | 1,00 | 28,33 | 9 | 28,61 | 0,39 | 1,54 | FS>1 No Liquefaction |
| 169 | 0,98 | 51,30 | 51,30 | 17,10 | 0.4g | 0,25 | 50 | 1,28 | 0,75 | 1,00 | 1,00 | 1,00 | 48,16 | (N1)60≥ 30 soils are too dense to liquefy and are classed as non-liquefiable | | | | FS>1 No Liquefaction |
| 170 | 0,98 | 56,40 | 56,40 | 18,80 | 0.4g | 0,25 | 50 | 1,25 | 0,75 | 1,00 | 1,00 | 1,00 | 46,77 | (N1)60≥ 30 soils are too dense to liquefy and are classed as non-liquefiable | | | | FS>1 No Liquefaction |
| 182 | 0,98 | 48,30 | 48,30 | 16,10 | 0.4g | 0,25 | 19 | 1,31 | 0,75 | 1,00 | 1,00 | 1,00 | 18,63 | 21 | 23,88 | 0,27 | 1,06 | FS>1 No Liquefaction |

Appendix B.2 Liquefaction Risk Table (3 m)

| B.N | $r_d$ | σv (kpa) | σv' (kpa) | $(\gamma_n)$ KN/m3 | a max | CSR | N | $C_N$ | $C_E$ | $C_B$ | $C_R$ | $C_S$ | $(N_1)_{60}$ | 200 SIEVE % | $(N_1)_{60CS}$ | CRR | FS= CRR/CSR | 4.5 M Exp. |
|---|---|---|---|---|---|---|---|---|---|---|---|---|---|---|---|---|---|---|
| 3 | 0,97 | 97,20 | 97,20 | 21,60 | 0.4g | 0,25 | 50 | 1,01 | 0,75 | 1,00 | 1,00 | 1,00 | 37,98 | (N1)60≥ 30 soils are too dense to liquefy and are classed as non-liquefiable | | | | FS>1 No Liquefaction |
| 9 | 0,97 | 82,80 | 82,80 | 18,40 | 0.4g | 0,25 | 50 | 1,08 | 0,75 | 1,00 | 1,00 | 1,00 | 40,68 | (N1)60≥ 30 soils are too dense to liquefy and are classed as non-liquefiable | | | | FS>1 No Liquefaction |
| 20 | 0,97 | 72,90 | 72,90 | 16,20 | 0.4g | 0,25 | 50 | 1,14 | 0,75 | 1,00 | 1,00 | 1,00 | 42,77 | (N1)60≥ 30 soils are too dense to liquefy and are classed as non-liquefiable | | | | FS>1 No Liquefaction |
| 31 | 0,97 | 68,85 | 68,85 | 15,30 | 0.4g | 0,25 | 22 | 1,16 | 0,75 | 1,00 | 1,00 | 1,00 | 19,22 | 18 | 23,32 | 0,26 | 1,04 | FS>1 No Liquefaction |
| 35 | 0,97 | 80,55 | 80,55 | 17,90 | 0.4g | 0,25 | 50 | 1,10 | 0,75 | 1,00 | 1,00 | 1,00 | 41,14 | (N1)60≥ 30 soils are too dense to liquefy and are classed as non-liquefiable | | | | FS>1 No Liquefaction |
| 42 | 0,97 | 73,80 | 73,80 | 16,40 | 0.4g | 0,25 | 31 | 1,14 | 0,75 | 1,00 | 1,00 | 1,00 | 26,39 | 12 | 28,47 | 0,39 | 1,54 | FS>1 No Liquefaction |
| 83 | 0,97 | 58,95 | 58,95 | 13,10 | 0.4g | 0,25 | 3 | 1,23 | 0,75 | 1,00 | 1,00 | 1,00 | 2,77 | 19 | 4,47 | 0,07 | 0,27 | FS ≤ 1 Liquefaction |
| 90 | 0,97 | 64,80 | 59,80 | 14,40 | 0.4g | 0,27 | 10 | 1,22 | 0,75 | 1,00 | 1,00 | 1,00 | 9,18 | 13 | 10,50 | 0,12 | 0,43 | FS ≤ 1 Liquefaction |
| 100 | 0,97 | 81,00 | 81,00 | 18,00 | 0.4g | 0,25 | 50 | 1,09 | 0,75 | 1,00 | 1,00 | 1,00 | 41,04 | (N1)60≥ 30 soils are too dense to liquefy and are classed as non-liquefiable | | | | FS>1 No Liquefaction |
| 106 | 0,97 | 72,45 | 72,45 | 16,10 | 0.4g | 0,25 | 25 | 1,14 | 0,75 | 1,00 | 1,00 | 1,00 | 21,43 | 21 | 27,28 | 0,35 | 1,37 | FS>1 No Liquefaction |
| 107 | 0,97 | 79,20 | 79,20 | 17,60 | 0.4g | 0,25 | 50 | 1,10 | 0,75 | 1,00 | 1,00 | 1,00 | 41,42 | (N1)60≥ 30 soils are too dense to liquefy and are classed as non-liquefiable | | | | FS>1 No Liquefaction |
| 145 | 0,97 | 80,55 | 80,55 | 17,90 | 0.4g | 0,25 | 5 | 1,10 | 0,75 | 1,00 | 1,00 | 1,00 | 4,11 | 26 | 6,94 | 0,09 | 0,35 | FS ≤ 1 Liquefaction |
| 155 | 0,97 | 77,40 | 77,40 | 17,20 | 0.4g | 0,25 | 50 | 1,11 | 0,75 | 1,00 | 1,00 | 1,00 | 41,79 | (N1)60≥ 30 soils are too dense to liquefy and are classed as non-liquefiable | | | | FS>1 No Liquefaction |
| 164 | 0,97 | 73,35 | 73,35 | 16,30 | 0.4g | 0,25 | 22 | 1,14 | 0,75 | 1,00 | 1,00 | 1,00 | 18,77 | 27 | 26,93 | 0,34 | 1,33 | FS>1 No Liquefaction |

Appendix B.3 Liquefaction Risk Table (4.5 m)

| B.N | $r_d$ | σv (kpa) | σv' (kpa) | $(\gamma_n)$ KN/m3 | a max | CSR | N | $C_N$ | $C_E$ | $C_B$ | $C_R$ | $C_S$ | $(N_1)_{60}$ | 200 SIEVE % | $(N_1)_{60CS}$ | CRR | FS= CRR/CSR | 7.5 M Exp. |
|---|---|---|---|---|---|---|---|---|---|---|---|---|---|---|---|---|---|---|
| 4 | 0,94 | 162,75 | 162,75 | 21,70 | 0.4g | 0,24 | 50 | 0,78 | 0,75 | 1,00 | 1,00 | 1,00 | 29,18 | 34 | 47,35 | 0,27 | 1,11 | FS>1 No Liquefaction |
| 11 | 0,94 | 153,00 | 153,00 | 20,40 | 0.4g | 0,24 | 50 | 0,81 | 0,75 | 1,00 | 1,00 | 1,00 | 30,22 | (N1)60≥ 30 soils are too dense to liquefy and are classed as non-liquefiable | | | | FS>1 No Liquefaction |
| 18 | 0,94 | 143,25 | 143,25 | 19,10 | 0.4g | 0,24 | 50 | 0,84 | 0,75 | 1,00 | 1,00 | 1,00 | 31,34 | (N1)60≥ 30 soils are too dense to liquefy and are classed as non-liquefiable | | | | FS>1 No Liquefaction |
| 31 | 0,94 | 114,75 | 114,75 | 15,30 | 0.4g | 0,24 | 22 | 0,94 | 0,75 | 1,00 | 1,00 | 1,00 | 15,46 | 23 | 20,80 | 0,23 | 0,92 | FS ≤ 1 Liquefaction |
| 32 | 0,94 | 125,25 | 125,25 | 16,70 | 0.4g | 0,24 | 50 | 0,90 | 0,75 | 1,00 | 1,00 | 1,00 | 33,64 | (N1)60≥ 30 soils are too dense to liquefy and are classed as non-liquefiable | | | | FS>1 No Liquefaction |
| 49 | 0,94 | 120,00 | 120,00 | 16,00 | 0.4g | 0,24 | 38 | 0,92 | 0,75 | 1,00 | 1,00 | 1,00 | 26,13 | 32 | 40,81 | 0,15 | 0,62 | FS ≤ 1 Liquefaction |
| 57 | 0,94 | 135,00 | 135,00 | 18,00 | 0.4g | 0,24 | 50 | 0,86 | 0,75 | 1,00 | 1,00 | 1,00 | 32,35 | (N1)60≥ 30 soils are too dense to liquefy and are classed as non-liquefiable | | | | FS>1 No Liquefaction |
| 87 | 0,94 | 125,25 | 120,25 | 16,70 | 0.4g | 0,25 | 42 | 0,92 | 0,75 | 1,00 | 1,00 | 1,00 | 28,84 | 27 | 40,57 | 0,14 | 0,56 | FS ≤ 1 Liquefaction |
| 96 | 0,94 | 102,75 | 102,75 | 13,70 | 0.4g | 0,24 | 50 | 0,99 | 0,75 | 1,00 | 1,00 | 1,00 | 37,04 | (N1)60≥ 30 soils are too dense to liquefy and are classed as non-liquefiable | | | | FS>1 No Liquefaction |
| 107 | 0,94 | 132,00 | 132,00 | 17,60 | 0.4g | 0,24 | 50 | 0,87 | 0,75 | 1,00 | 1,00 | 1,00 | 32,74 | (N1)60≥ 30 soils are too dense to liquefy and are classed as non-liquefiable | | | | FS>1 No Liquefaction |
| 116 | 0,94 | 114,75 | 114,75 | 15,30 | 0.4g | 0,24 | 8 | 0,94 | 0,75 | 1,00 | 1,00 | 1,00 | 5,62 | 19 | 7,82 | 0,09 | 0,39 | FS ≤ 1 Liquefaction |
| 123 | 0,94 | 162,00 | 162,00 | 21,60 | 0.4g | 0,24 | 50 | 0,78 | 0,75 | 1,00 | 1,00 | 1,00 | 29,26 | 29 | 42,80 | 0,20 | 0,81 | FS ≤ 1 Liquefaction |
| 150 | 0,94 | 148,50 | 148,50 | 19,80 | 0.4g | 0,24 | 50 | 0,82 | 0,75 | 1,00 | 1,00 | 1,00 | 30,73 | (N1)60≥ 30 soils are too dense to liquefy and are classed as non-liquefiable | | | | FS>1 No Liquefaction |
| 186 | 0,94 | 180,75 | 180,75 | 24,10 | 0.4g | 0,24 | 50 | 0,73 | 0,75 | 1,00 | 1,00 | 1,00 | 27,43 | 27 | 38,66 | 0,07 | 0,27 | FS ≤ 1 Liquefaction |

Appendix B.4 Liquefaction Risk Table (7.5 m)

| B.N | $r_d$ | σv (kpa) | σv' (kpa) | $(\gamma_n)$ KN/m3 | a max | CSR | N | $C_N$ | $C_E$ | $C_B$ | $C_R$ | $C_S$ | $(N_1)_{60}$ | 200 SIEVE % | $(N_1)_{60CS}$ | CRR | $FS=\frac{CRR}{CSR}$ | 15 M Exp. |
|---|---|---|---|---|---|---|---|---|---|---|---|---|---|---|---|---|---|---|
| 6 | 0,77 | 291,00 | 291,00 | 19,40 | 0.4g | 0,20 | 50 | 0,54 | 0,75 | 1,00 | 1,00 | 1,00 | 20,07 | 12 | 21,76 | 0,24 | 1,19 | FS>1 No Liquefaction |
| 16 | 0,77 | 288,00 | 288,00 | 19,20 | 0.4g | 0,20 | 50 | 0,54 | 0,75 | 1,00 | 1,00 | 1,00 | 20,22 | 28 | 29,46 | 0,43 | 2,17 | FS>1 No Liquefaction |
| 25 | 0,77 | 291,00 | 291,00 | 19,40 | 0.4g | 0,20 | 50 | 0,54 | 0,75 | 1,00 | 1,00 | 1,00 | 20,07 | 18 | 24,30 | 0,28 | 1,39 | FS>1 No Liquefaction |
| 41 | 0,77 | 292,50 | 292,50 | 19,50 | 0.4g | 0,20 | 50 | 0,53 | 0,75 | 1,00 | 1,00 | 1,00 | 20,00 | 21 | 25,54 | 0,30 | 1,51 | FS>1 No Liquefaction |
| 45 | 0,77 | 265,50 | 265,50 | 17,70 | 0.4g | 0,20 | 37 | 0,57 | 0,75 | 1,00 | 1,00 | 1,00 | 15,84 | 26 | 22,51 | 0,25 | 1,25 | FS>1 No Liquefaction |
| 63 | 0,77 | 283,50 | 283,50 | 18,90 | 0.4g | 0,20 | 50 | 0,55 | 0,75 | 1,00 | 1,00 | 1,00 | 20,45 | 11 | 21,67 | 0,24 | 1,19 | FS>1 No Liquefaction |
| 88 | 0,77 | 231,00 | 131,00 | 15,40 | 0.4g | 0,35 | 23 | 0,88 | 0,75 | 1,00 | 1,00 | 1,00 | 15,12 | 33 | 24,79 | 0,29 | 0,82 | FS ≤ 1 Liquefaction |
| 99 | 0,77 | 315,00 | 315,00 | 21,00 | 0.4g | 0,20 | 50 | 0,51 | 0,75 | 1,00 | 1,00 | 1,00 | 18,97 | 33 | 30,69 | 0,52 | 2,62 | FS>1 No Liquefaction |
| 107 | 0,77 | 264,00 | 264,00 | 17,60 | 0.4g | 0,20 | 50 | 0,57 | 0,75 | 1,00 | 1,00 | 1,00 | 21,48 | 17 | 25,48 | 0,30 | 1,51 | FS>1 No Liquefaction |
| 127 | 0,77 | 244,50 | 244,50 | 16,30 | 0.4g | 0,20 | 25 | 0,60 | 0,75 | 1,00 | 1,00 | 1,00 | 11,32 | 19 | 14,48 | 0,15 | 0,77 | FS ≤ 1 Liquefaction |
| 139 | 0,77 | 322,50 | 322,50 | 21,50 | 0.4g | 0,20 | 50 | 0,50 | 0,75 | 1,00 | 1,00 | 1,00 | 18,64 | 24 | 25,26 | 0,30 | 1,48 | FS>1 No Liquefaction |
| 149 | 0,77 | 283,50 | 283,50 | 18,90 | 0.4g | 0,20 | 50 | 0,55 | 0,75 | 1,00 | 1,00 | 1,00 | 20,45 | 11 | 21,67 | 0,24 | 1,19 | FS>1 No Liquefaction |
| 159 | 0,77 | 256,50 | 256,50 | 17,10 | 0.4g | 0,20 | 50 | 0,58 | 0,75 | 1,00 | 1,00 | 1,00 | 21,91 | 15 | 25,07 | 0,29 | 1,47 | FS>1 No Liquefaction |
| 178 | 0,77 | 372,00 | 372,00 | 24,80 | 0.4g | 0,20 | 50 | 0,45 | 0,75 | 1,00 | 1,00 | 1,00 | 16,77 | 33 | 27,32 | 0,35 | 1,74 | FS>1 No Liquefaction |

Appendix B.5 Liquefaction Risk Table (15 m)

| B.N. | Seismic (Vs) (m/s) | SPT-N | Ohba and Trauma (1970) (Vs) (m/s) | Seed and Idriss (1981) (Vs) (m/s) | Imai and Yoshimura (1970) (Vs) (m/s) | Iyisan (1996) (Vs) (m/s) | Hasancelebi and Ulusay (2007) (Vs) (m/s) | Tsiambos and Sabatakakis (2011) (Vs) (m/s) |
|---|---|---|---|---|---|---|---|---|
| 1 | 260 | 42 | 268 | 398 | 261 | 354 | 286 | 359 |
| 11 | 230 | 50 | 282 | 434 | 276 | 388 | 301 | 380 |
| 22 | 250 | 50 | 282 | 434 | 276 | 388 | 301 | 380 |
| 33 | 274 | 49 | 281 | 430 | 275 | 384 | 300 | 377 |
| 44 | 120 | 4 | 129 | 123 | 120 | 105 | 138 | 166 |
| 55 | 410 | 50 | 282 | 434 | 276 | 388 | 301 | 380 |
| 66 | 260 | 42 | 268 | 398 | 261 | 354 | 286 | 359 |
| 77 | 310 | 50 | 282 | 434 | 276 | 388 | 301 | 380 |
| 88 | 215 | 23 | 222 | 294 | 214 | 260 | 237 | 295 |
| 99 | 500 | 50 | 282 | 434 | 276 | 388 | 301 | 380 |
| 110 | 200 | 19 | 209 | 268 | 201 | 235 | 224 | 277 |
| 121 | 196 | 18 | 206 | 260 | 197 | 229 | 220 | 272 |
| 132 | 98 | 2 | 104 | 87 | 96 | 74 | 111 | 133 |
| 143 | 333 | 50 | 282 | 434 | 276 | 388 | 301 | 380 |
| 155 | 300 | 50 | 282 | 434 | 276 | 388 | 301 | 380 |
| 166 | 284 | 50 | 282 | 434 | 276 | 388 | 301 | 380 |
| 177 | 310 | 50 | 282 | 434 | 276 | 388 | 301 | 380 |
| 188 | 285 | 50 | 282 | 434 | 276 | 388 | 301 | 380 |

Appendix C.1 Shear Wave Velocity Table (1.5 m)

| B.N. | Seismic (Vs) (m/s) | SPT-N | Ohba and Trauma (1970) (Vs) (m/s) | Seed and Idriss (1981) (Vs) (m/s) | Imai and Yoshimura (1970) (Vs) (m/s) | Iyisan (1996) (Vs) (m/s) | Hasancelebi and Ulusay (2007) (Vs) (m/s) | Tsiambos and Sabatakakis (2011) (Vs) (m/s) |
|---|---|---|---|---|---|---|---|---|
| 3 | 310 | 50 | 282 | 434 | 276 | 388 | 301 | 380 |
| 14 | 210 | 50 | 282 | 434 | 276 | 388 | 301 | 380 |
| 25 | 290 | 50 | 282 | 434 | 276 | 388 | 301 | 380 |
| 36 | 365 | 50 | 282 | 434 | 276 | 388 | 301 | 380 |
| 47 | 350 | 50 | 282 | 434 | 276 | 388 | 301 | 380 |
| 58 | 280 | 50 | 282 | 434 | 276 | 388 | 301 | 380 |
| 69 | 285 | 50 | 282 | 434 | 276 | 388 | 301 | 380 |
| 80 | 282 | 50 | 282 | 434 | 276 | 388 | 301 | 380 |
| 91 | 300 | 3 | 118 | 106 | 109 | 91 | 126 | 151 |
| 102 | 445 | 50 | 282 | 434 | 276 | 388 | 301 | 380 |
| 113 | 266 | 45 | 273 | 412 | 267 | 367 | 292 | 367 |
| 124 | 282 | 50 | 282 | 434 | 276 | 388 | 301 | 380 |
| 135 | 280 | 50 | 282 | 434 | 276 | 388 | 301 | 380 |
| 146 | 320 | 50 | 282 | 434 | 276 | 388 | 301 | 380 |
| 157 | 260 | 50 | 282 | 434 | 276 | 388 | 301 | 380 |
| 168 | 287 | 50 | 282 | 434 | 276 | 388 | 301 | 380 |
| 179 | 720 | 50 | 282 | 434 | 276 | 388 | 301 | 380 |
| 190 | 352 | 50 | 282 | 434 | 276 | 388 | 301 | 380 |

Appendix C.2 Shear Wave Velocity Table (3 m)

| B.N. | Seismic (Vs) (m/s) | SPT-N | Ohba and Trauma (1970) (Vs) (m/s) | Seed and Idriss (1981) (Vs) (m/s) | Imai and Yoshimura (1970) (Vs) (m/s) | Iyisan (1996) (Vs) (m/s) | Hasancelebi and Ulusay (2007) (Vs) (m/s) | Tsiambos and Sabatakakis (2011) (Vs) (m/s) |
|---|---|---|---|---|---|---|---|---|
| 5 | 360 | 50 | 282 | 434 | 276 | 388 | 301 | 380 |
| 16 | 330 | 50 | 282 | 434 | 276 | 388 | 301 | 380 |
| 27 | 410 | 50 | 282 | 434 | 276 | 388 | 301 | 380 |
| 31 | 210 | 22 | 219 | 288 | 211 | 254 | 234 | 290 |
| 43 | 240 | 33 | 248 | 353 | 241 | 313 | 265 | 332 |
| 56 | 254 | 39 | 262 | 383 | 255 | 341 | 279 | 350 |
| 63 | 265 | 44 | 271 | 407 | 265 | 363 | 290 | 364 |
| 76 | 200 | 19 | 209 | 268 | 201 | 235 | 224 | 277 |
| 87 | 340 | 42 | 268 | 398 | 261 | 354 | 286 | 359 |
| 97 | 318 | 50 | 282 | 434 | 276 | 388 | 301 | 380 |
| 108 | 286 | 50 | 282 | 434 | 276 | 388 | 301 | 380 |
| 118 | 200 | 19 | 209 | 268 | 201 | 235 | 224 | 277 |
| 129 | 310 | 50 | 282 | 434 | 276 | 388 | 301 | 380 |
| 140 | 483 | 50 | 282 | 434 | 276 | 388 | 301 | 380 |
| 151 | 381 | 50 | 282 | 434 | 276 | 388 | 301 | 380 |
| 160 | 286 | 50 | 282 | 434 | 276 | 388 | 301 | 380 |
| 170 | 515 | 50 | 282 | 434 | 276 | 388 | 301 | 380 |
| 180 | 384 | 50 | 282 | 434 | 276 | 388 | 301 | 380 |

Appendix C.3 Shear Wave Velocity Table (4.5 m)

| B.N. | Seismic (Vs) (m/s) | SPT-N | Ohba and Trauma (1970) (Vs) (m/s) | Seed and Idriss (1981) (Vs) (m/s) | Imai and Yoshimura (1970) (Vs) (m/s) | Iyisan (1996) (Vs) (m/s) | Hasancelebi and Ulusay (2007) (Vs) (m/s) | Tsiambos and Sabatakakis (2011) (Vs) (m/s) |
|---|---|---|---|---|---|---|---|---|
| 7 | 350 | 50 | 282 | 434 | 276 | 388 | 301 | 380 |
| 18 | 400 | 50 | 282 | 434 | 276 | 388 | 301 | 380 |
| 28 | 600 | 50 | 282 | 434 | 276 | 388 | 301 | 380 |
| 39 | 280 | 50 | 282 | 434 | 276 | 388 | 301 | 380 |
| 42 | 235 | 31 | 244 | 342 | 236 | 303 | 260 | 325 |
| 45 | 250 | 37 | 257 | 373 | 250 | 332 | 275 | 344 |
| 46 | 164 | 10 | 172 | 194 | 162 | 169 | 183 | 224 |
| 67 | 270 | 47 | 277 | 421 | 271 | 375 | 296 | 372 |
| 75 | 462 | 50 | 282 | 434 | 276 | 388 | 301 | 380 |
| 90 | 472 | 10 | 172 | 194 | 162 | 169 | 183 | 224 |
| 103 | 330 | 50 | 282 | 434 | 276 | 388 | 301 | 380 |
| 112 | 260 | 42 | 268 | 398 | 261 | 354 | 286 | 359 |
| 123 | 530 | 50 | 282 | 434 | 276 | 388 | 301 | 380 |
| 138 | 523 | 50 | 282 | 434 | 276 | 388 | 301 | 380 |
| 148 | 260 | 50 | 282 | 434 | 276 | 388 | 301 | 380 |
| 159 | 304 | 50 | 282 | 434 | 276 | 388 | 301 | 380 |
| 171 | 352 | 50 | 282 | 434 | 276 | 388 | 301 | 380 |
| 192 | 360 | 50 | 282 | 434 | 276 | 388 | 301 | 380 |

Appendix C.4 Shear Wave Velocity Table (7.5 m)

| B.N. | Seismic (Vs) (m/s) | SPT-N | Ohba and Trauma (1970) (Vs) (m/s) | Seed and Idriss (1981) (Vs) (m/s) | Imai and Yoshimura (1970) (Vs) (m/s) | Iyisan (1996) (Vs) (m/s) | Hasancelebi and Ulusay (2007) (Vs) (m/s) | Tsiambos and Sabatakakis (2011) (Vs) (m/s) |
|---|---|---|---|---|---|---|---|---|
| 9 | 360 | 50 | 282 | 434 | 276 | 388 | 301 | 380 |
| 19 | 520 | 50 | 282 | 434 | 276 | 388 | 301 | 380 |
| 29 | 486 | 50 | 282 | 434 | 276 | 388 | 301 | 380 |
| 41 | 420 | 50 | 282 | 434 | 276 | 388 | 301 | 380 |
| 50 | 250 | 37 | 257 | 373 | 250 | 332 | 275 | 344 |
| 53 | 250 | 37 | 257 | 373 | 250 | 332 | 275 | 344 |
| 65 | 540 | 50 | 282 | 434 | 276 | 388 | 301 | 380 |
| 93 | 410 | 10 | 172 | 194 | 162 | 169 | 183 | 224 |
| 111 | 300 | 50 | 282 | 434 | 276 | 388 | 301 | 380 |
| 122 | 342 | 50 | 282 | 434 | 276 | 388 | 301 | 380 |
| 131 | 330 | 50 | 282 | 434 | 276 | 388 | 301 | 380 |
| 141 | 373 | 50 | 282 | 434 | 276 | 388 | 301 | 380 |
| 152 | 450 | 50 | 282 | 434 | 276 | 388 | 301 | 380 |
| 163 | 1000 | 50 | 282 | 434 | 276 | 388 | 301 | 380 |
| 174 | 385 | 50 | 282 | 434 | 276 | 388 | 301 | 380 |
| 186 | 940 | 50 | 282 | 434 | 276 | 388 | 301 | 380 |
| 187 | 450 | 50 | 282 | 434 | 276 | 388 | 301 | 380 |
| 188 | 354 | 50 | 282 | 434 | 276 | 388 | 301 | 380 |

Appendix C.5 Shear Wave Velocity Table (15 m)

| B. N. | Vs (30m) (m/sec) | NEHRP Soil Class | Eurocode 8 Soil Class | Dominant Vibration Period (To) (sec) | Local Soil Class | Soil Amplification | Earthquake Hazard Level |
|---|---|---|---|---|---|---|---|
| 1 | 330 | D | C | 0.6 | Z3 | 2.10 | B |
| 10 | 481 | C | B | 0.4 | Z2 | 1.67 | C |
| 20 | 275 | D | C | 0.7 | Z4 | 2.34 | B |
| 30 | 555 | C | B | 0.3 | Z1 | 1.59 | C |
| 40 | 359 | D | C | 0.5 | Z2 | 1.99 | C |
| 50 | 184 | D | C | 0.9 | Z4 | 2.98 | B |
| 60 | 520 | C | B | 0.4 | Z2 | 1.60 | C |
| 70 | 366 | C | B | 0.5 | Z2 | 1.97 | C |
| 80 | 345 | D | C | 0.6 | Z3 | 2.04 | B |
| 90 | 424 | C | B | 0.5 | Z2 | 1.80 | C |
| 100 | 404 | C | B | 0.4 | Z2 | 1.86 | C |
| 110 | 284 | D | C | 0.7 | Z4 | 2.29 | B |
| 120 | 340 | D | C | 0.6 | Z3 | 2.06 | B |
| 130 | 303 | D | C | 0.7 | Z4 | 2.21 | B |
| 140 | 463 | C | B | 0.4 | Z2 | 1.71 | C |
| 150 | 690 | C | B | 0.3 | Z1 | 1.35 | C |
| 160 | 362 | C | B | 0.6 | Z3 | 1.98 | C |
| 170 | 478 | C | B | 0.4 | Z2 | 1.68 | C |
| 180 | 356 | D | C | 0.5 | Z2 | 2.03 | B |
| 190 | 330 | D | C | 0.6 | Z3 | 2.10 | B |

Appendix D Soil Class Figure and Earthquake Hazard Level Table

T.C.
MALATYA BÜYÜKŞEHİR BELEDİYE BAŞKANLIĞI
İmar ve Şehircilik Dairesi Başkanlığı

Sayı : 12754253-622.03
Konu : Talebiniz Hk.

Sayın BAHADIR KARABAŞ
Battalgazi/MALATYA

İlgi : BAHADIR KARABAŞ'IN 08.02.2017 tarihli başvurusu.

Büyükşehir Belediyemizce Malatya ili Malatya yerleşim alanın imar planına ve revize imar planına esas jeolojik-jeoteknik ve jeofizik etüd raporu 2009 yılında onaylanmış olup,bahse konu yazınızda bu çalışmayı yüksek lisans tezinde faydalanmak için Malatya Büyükşehir Belediyemizden izin istemektesiniz.

İlgili çalışmadan faydalanmanızda Başkanlığımızca herhangi bir sakınca görülmemiş olup, çalışma ile ilgili dökümanları Daire Başkanlığımız teknik elemanlarından temin edebilirsiniz.

Bilgilerinize rica olunur.

e-imzalıdır
Memiş AVUNDUK
Daire Başkanı a.
İmar ve Şehircilik Daire Bşk.V.

Bu Belge 5070 Sayılı Elektronik İmza Kanunu Gereği Elektronik İmza İle İmzalanmıştır
9./2./2017

MALATYA BÜYÜKŞEHİR BELEDİYESİ
e-posta:kemaleddinyucetas@malatya.bel.tr
Telefon:3771516

Ayrıntılı bilgi için:KEMALEDDİN YÜCETAŞ
Elektronik Ağ: www.malatya.bel.tr

1 / 1

Evrakın elektronik imzalı suretine http://ebelge.malatya.bel.tr adresinden 2900bba1-d427-4b7e-a13e-974dafa9a15c kodu ile erişebilirsiniz.
Bu belge 5070 sayılı elektronik imza kanuna göre güvenli elektronik imza ile imzalanmıştır.

Appendix E Municipality Permission Certificate